Analysing Performance of Optical and Passive Microwave Data to Infer Soil Moisture in the Upper Soil layers for the Prominent Crops in Eastern Part of Rajasthan, India

Ambika Mukund

January, 2008

Analysing Performance of Optical and Passive Microwave Data to Infer Soil Moisture in the Upper Soil layers for the Prominent Crops in Eastern Part of Rajasthan, India

by

Ambika Mukund

Thesis submitted to the International Institute for Geo-information Science and Earth Observation in partial fulfilment of the requirements for the degree of Master of Science in Geo-information Science and Earth Observation, Specialisation: (Geo- Hazards)

Thesis Assessment Board

Chairman: Dr Cess Van Westen
External Examiner: Dr R.P Singh (SAC, Ahmedabad)
IIRS Member: Dr S.K. Saha
IIRS Member: Dr N.R. Patel

Thesis supervisors

Dr. N. R. Patel, IIRS
Prof. Victor Jetten, ITC
Drs. Valentijn Venus, ITC

INTERNATIONAL INSTITUTE FOR GEO-INFORMATION SCIENCE AND EARTH OBSERVATION ENSCHEDE, THE NETHERLANDS

&

INDIAN INSTITUTE OF REMOTE SENSING, NATIONAL REMOTE SENSING AGENCY (NRSA), DEPARTMENT OF SPACE, DEHRADUN, INDIA

I certify that although I might have conferred with others in preparing for this assignment, and drawn upon a range of sources cited in this work, the content of this thesis work is my original work.

Signed……

Disclaimer

This document describes work undertaken as part of a programme of study at the International Institute for Geo-information Science and Earth Observation. All views and opinions expressed therein remain the sole responsibility of the author, and do not necessarily represent those of the institute.

Dedicated to amma, acha and ammoma….

Abstract

Soil Moisture is a key state variable of the energy and water cycle on earth surface. For areas like Rajasthan in India, which remain under constant threat of drought, comprehensive information on soil moisture variability can help in early drought prediction, drought monitoring and evaluation of drought impact on agricultural production. Limitations of acquiring adequate in-situ measurements and the high demand of data exhibited by models make remote sensing a highly viable option for extraction of knowledge about soil moisture variation at the root-zone. With the advent of optical remote sensed data with high spatial resolution and passive microwave data with high temporal resolution, it is desirable to use them to obtain soil moisture measurements for agricultural drought assessment. This study assesses the ability of Vegetation Temperature condition Index, developed from interpretation of NDVI –Ts space using surface reflectance and land surface temperature provided by Terra MODIS on an 8 day basis, to estimate soil moisture status at a spatial resolution of 1km. VTCI was attempted to be computed at 250mts by downscaling LST, and based on the agriculture land cover alone. Further estimation was done by regressing VTCI and 31 in-situ volumetric soil moisture measurements for the surface and at depths of 15cm, 30 cm and 45cm for the prominent crops in Eastern Rajasthan. The ability of passive microwave parameters, horizontally polarised brightness temperature (T_{BH}) and Polarisation Difference (PD) provided by Aqua – AMSRE on a daily basis at a coarse spatial resolution of 25 km, to assess soil moisture condition was also explored in the study. Comparison of the assessments by both VTCI and the passive microwave parameters were done with soil moisture simulated using a GIS based simple water balance model. The model adopts the equation for water balance suggested by Thornthwaite and Mather (1955). The simulation is done for 5 * 5 km grids on a weekly basis and the inputs required are effective rainfall, maximum crop evapotranspiration and maximum available water capacity.

The results for VTCI at 1km and computed for the whole image was found to be more representative of the average profile soil moisture condition than the other two versions. A strong relation of VTCI and the average profile soil moisture till 50cms depth beneath the surface was observed with a coefficient of determination of 0.63. The relationship was more relevant at the surface and at 30cm depth than 15cm and 45cm. All relationships were significant at 0.01 level for 2-tailed analysis. Estimation of average profile soil moisture from VTCI was done for 2003. The estimated volumetric soil moisture content showed high variability with different climatic region. The mean measure for semi-arid region was found to be 13.45% and 26.19% for the sub-humid region. Soil moisture estimated from VTCI and that simulated using the SWBM, was found to vary with an RMSE of 7.04% for the study area, where the mean value is 14.2%. 62% in the semi-arid area and only 44% in the sub-humid area were found to be correctly estimated. The poor relation may be due to underestimation in the simulated soil moisture by the SWBM owing to uncertainties in the conventional methods used to compute its inputs. The passive microwave parameters exhibited significant relation with simulated soil moisture at a lower frequency of 6.9GHz. The correlation was better for semi-arid region than sub-humid region due to the influence of vegetation density. The coefficient of determination was 0.78 for PD and 0.75 for T_{BH} for semi-arid region and 6.9 GHz. It is found that T_{BH} and PD can well depict the temporal variation in soil moisture but fail to represent the spatial patterns owing to the high geographical dependence of microwave data. It has been concluded from these relationships that

VTCI, T_{BH} and PD can be used to infer soil moisture beneath the surface but in semi-arid areas, or specifically in sparse or moderately vegetated region.

Keywords: Root zone Soil Moisture, VTCI, Microwave Temperature Brightness, Polarisation Difference, Terra- MODIS, Aqua- AMSRE, Simple Water Balance Model

Acknowledgements

Let me begin humbly by thanking God almighty for gifting me the phase of life spent in IIRS and ITC. Thank you lord for all that has been gained as knowledge and experience from these two academic institutions. My amma and achan are lovingly remembered in this context. Their love and encouragement were my strengths in the crucial times of the research.

I express my gratitude to IIRS and ITC for allowing me to take up the M.Sc course. Thanks are due to Dr V.K. Dadhwal, Dean, IIRS for providing all the necessary facilities required for the course and research work. His expert opinion and technical guidance have proved to be precious and valuable.

I am greatly indebted to my first supervisor, Dr N.R. Patel, the one person whose scientific thought and determination was the backbone of the research work. His in-depth knowledge in the field of soil moisture, expertise on remote sensing and natural research skills have complimented the work done in this thesis. The constant guidance provided and sincere efforts he has taken to make me understand the basics of the topic are acknowledged with utmost gratitude. Thank you, sir for your patience and perseverance.

Acknowledgement is due to Drs Valentijn Venus, especially for the creative thought put in, during the conceptualization of the thesis. Prof Victor Jetten is also extended gratitude for his critical analysis of the research components and scientific writing. The valuable feedback and guidance received from both of them have helped me formulate this research.

I cannot forget the support and encouragement received from Dr V. Hari Prasad throughout the course. A scientist second and a good human being first, he deserves my utmost respect, personally and professionally. Drs Michiel Damen is also remembered here for the fatherly love and care he showed during our short stay at ITC.

Dr. B.K .Bhattacharya, SAC, Ahmedabad is extended a word of gratitude for granting permission to use the solar radiation data. Technical advice from Dr C. Jeganathan, Scientist “SE”, Geo-informatics Division, Dr S.P. Aggarwal, Scientist “SE”, WRD, Dr Jitendra Prasad, Scientist “SG” , Dr Suresh Kumar, “Scientist “SE”, ASD and Mr Pravin Takur, Scientist “SD”,WRD have helped me a lot in the process of research work. The valuable comments provided by Dr David Rossiter at the mid-term evaluation also need to be acknowledged. I am grateful to Anil Rawat, JRF, IIRS whose programming skills in IDL proved to be a blessing to me. Dr Gopal Singh, IFS, is also thanked for the help extended for field visits in Rajasthan.

A word of thanks to my friend Chandan Nayak, for his relentless support and care. Thanks Chandu, for being there. Thanks are due to the WRD ladies, Vidya and Nidhi, for being good friends. My special acknowledgement to Chand sir, Gurdeep and Rupinder for the treasurable moments shared. I take this opportunity to show gratitude to all classmates in the MSc HRA and GID 2006 – 08 batch. The fun we had at IIRS and the 3 months in ITC can never be forgotten. Tapan, Nihar, Tushar, Hrushibhaiya, Pragnya and all others in our PGD batch are also remembered. Let me not miss Sekhar L.K, Ph.D student, ITC, but for whom I would not have joined the course.

Last but not the least; I thank the Royal Govt of Netherlands for allowing the trip to Netherlands and giving an opportunity to experience the Dutch culture and customs. The fellowship provided by NUFFIC for the stay in Netherlands is greatly appreciated.

Ambika Mukund
Dehradun,
January 2008.

Table of contents

List of figures

List of tables

1. Introduction

1.1. General Background

Life cannot exist without water, be it in a human body or a small plant. A body of human being is about 85 % water, and for a plant, the percentage is closer to 90. Plants need water for a number of purposes, transpiration being the most important. Transpiration is the process in which plants lose water to the atmosphere as a consequence of photosynthesis. During photosynthesis, when the stomatal pores in the leaves open, water vapour present is transpired to the atmosphere. If the quantity of water present in the stomatal pores is not sufficient for a prolonged time, the leaf will start wilting. To avoid this life threatening situation, the plant has to supply water from the soil to leaves, through its roots and shoots (Volkmar & Woodbury 1995). To be able to do this, water must be available in sufficient amounts in the soil layer near the roots from where it is to be absorbed. Because of this seemingly simple process, root-zone soil moisture is a crucial variable in agriculture. It is also important as an environmental variable, which has far reaching significance in meteorology, hydrology and climate change. It acts as a critical element which limits the exchanges of water and energy between the land surface and atmosphere.

Water held in the upper 1-2 m of soil, where it is within the reach of the plant roots, is generally known as available soil moisture (Verstraeten et al 2006). At a particular point of time, it is influenced by a number of factors namely the precipitation history, the texture and structure of the soil which determines the water holding capacity, the slope of the land surface, which affects runoff and infiltration and the vegetation and land cover, which influences evapo-transpiration and deep percolation (Mohanty & Skaggs 2001). Natural soils usually exhibit a variation of properties both at the surface and in depth. The soil profile is the vertical cross section of a soil layer. The soil profile is never uniform and can be made up of distinct layers varying in soil properties such as texture, organic matter and bulk density with variation in depth. With this, soil moisture along the profile can show strong variation due to soil heterogeneity and forces acting upon the water in the soil such as salinity and osmotic pressure (Van Oevelen 2000).

The thin soil layer may seem to contain a small quantity of water when compared to the total amount of water on the earth, but it is the water contained by the upper 1-2 m of the soil profile that controls the partitioning of the components of the hydrological cycle (Engman 1991). The temporal and spatial variability of soil moisture determines the partitioning of precipitation into surface and subsurface runoff, evaporation and transpiration and groundwater recharge (Mohanty & Skaggs 2001). Its variation has a strong impact on surface energy balances, regional runoff, evapotranspiration and thereby vegetation productivity (Verstraeten et al 2006). Knowledge of the state of soil moisture and its spatial and temporal dynamics is therefore essential for meteorological, climatologic, hydrological and agricultural applications.

Drought monitoring or assessment is a highly relevant application in which comprehensive information on soil moisture variability can be of significant importance. Drought, to common man, is scarcity of water for his basic needs. To the scientific community it has more than 150 debatable definitions (Boken 2005), which arouse because each drought comes with unique characteristics and effects, making it the most complex of all natural hazards. Broadly, it is classified into meteorological, hydrological, agricultural and socioeconomic. A meteorological drought is the negative deviation of seasonal or annual precipitation from its long term average. A hydrological drought is said to occur when prolonged meteorological drought causes surface water and ground water scarcity. When the soil moisture decreases, it leads to decline in crop yield which is called agricultural drought and a continued drought of severe intensity that collapses the economy and socio-political situation of a region is termed as socioeconomic drought (Boken 2005). As agriculture plays an important role from the people's day to day life to a country's overall economy, recurring agricultural drought poses a great threat to its sustainable development. So researchers have been studying drought in these four concepts with consistently improving methods and parameters. Soil moisture is one of the most effective parameters for early drought prediction, drought monitoring and evaluation of drought impact on agricultural production for management of rural subsidy schemes. Studies on early detection of drought which helps in preparing humanitarian aid to affected areas and improving food security by providing crop status information to international commodity donors has proved the need to investigate the spatial and temporal variation in soil moisture as a necessity.

Knowledge about the variation of the soil moisture content in the upper layers can be obtained from three different sources, namely in-situ soil moisture measurements, hydrological or land surface models and remote sensing. The most appropriate way to capture the temporal variation of soil moisture in a soil profile is through ground based point measurements. But in-situ point measurements are always limited samples and can never give the precise spatial variation. On a regional scale, the idea of point samples is impractical as choosing field sites depending on soil properties, topography, vegetation type and density and extrapolating them to get accurate spatial representation is difficult (Wang et al 2007b). Hydrological or Land surface models are used to simulate the water content at the root-zone. The uncertainty associated with such models is high; as with the same inputs and atmospheric forcing, different models give different results. Still people prefer and continue to model as it can give an indication of the spatial and temporal variation. Another disadvantage of models is their demand for inputs. Even simple water balance models, demand a number of meteorological and ancillary data which are at times difficult for all to obtain. The high demand for data exhibited by the models and the high costs for ground measurements make remote sensing a highly viable option.

With the speedy advance of remote sensing technology in the 21st century, their applications have also widened horizons. This thesis tries to estimate soil moisture in the upper layers of the soil profile using optical remote sensed data at the best resolution possible which can be 1 km or 250mts. It is also attempted to estimate the spatial variability of soil moisture using passive microwave remote sensed data, which has the advantage of high temporal resolution, though of coarse spatial resolution. Because of lack of historic in situ soil moisture measurements, the validation cannot be done to know if they are representative of the ground reality. The results have been compared to weekly time series soil moisture simulated by a simple water balance model which combines existing methods. The use of remote sensing to as a substitute for data demanding models, in estimating soil moisture beneath the soil surface is thus tested.

1.2. Remote Sensing and Soil Moisture

Remote Sensing is the acquisition of information without direct contact with the concerned objects. With today's advanced space technology, the science of remote sensing has been thoroughly exploited to provide spatially explicit measurements at relatively lower costs (Verstraeten et al 2006). It is an economical and promising tool to obtain spatio temporal variation of land surface parameters which is to be used as input to a variety of applications from land use planning to disaster mitigation. Soil moisture is one such important land surface parameter which is being addressed by a lot of studies in the last few decades. Sensors using a wide range of the electromagnetic spectrum namely the optical which includes visible, infrared and thermal remote sensing and microwave which is of 2 types, passive and active microwave remote sensing are being exploited for information on soil moisture. The thermal and dielectric properties of water are very different from other natural surfaces. So the presence of water in soil drastically modifies the properties measured by infrared and microwave sensors (Dadhwal & Patel 2007, Prigent et al 2005).

In the field of soil moisture detection from space, most efforts are concentrated on exploiting the potential of the microwave methods. Microwave remote sensing provides a direct measurement of the surface soil moisture for a wide range a vegetation cover conditions. An advantage of microwave sensors is that it penetrates through cloud, particularly at the frequencies < 10 GHz. In addition they are independent of solar illumination and can be made any time of the day or night. They provide information about the soil moisture at a sensing depth which is in correlation with the wavelength used (Van Oevelen 2000). Passive microwave soil moisture measurement has been the most promising technique in this area, due to its all-weather capability, its direct relationship with soil moisture through the soil's dielectric constant, and a reduced sensitivity to land surface roughness and vegetation cover. The passive microwave sensors like SSM/I (Special Satellite Microwave/Imager), AMSR (Advanced Microwave Scanning Radiometer) and TMI (Tropical Rainfall Measurement Mission Microwave Imager) give free daily soil moisture data for the whole globe but of relatively poor spatial resolution than the optical sensors. Due to the long wavelengths required for soil moisture remote sensing, space-borne passive microwave radiometers (both current and planned) have a coarse spatial resolution, being on the order of 25 to 50 km, but have a frequent temporal resolution of 1 to 2 days (Guariso & Walker 2005). Low frequency (< 6 GHz) microwave sensors give the best soil moisture information as attenuation and scattering problems associated with the atmosphere and vegetation are less significant, the instruments respond to a deeper soil layer and a higher sensitivity to soil water content is present (Jackson 2005). So for the most researches on soil moisture, the L band (1-2 GHz) is preferred. In case of active microwave remote sensing, low temporal frequency and high costs constitute major constrains for their practical applications for the time being (Smith et al 2005). Among the active microwave sensors, SAR (Synthetic Aperture Radar) offer high ground resolution suitable for providing information on a farm level but due to their high costs, researches using them haven't shot up in number. Scatterometers provide data with spatial and temporal resolutions similar to space borne radiometers and are being used a lot.

Optical remote sensing i.e. the visible and infrared wavelengths are used to develop vegetation indices like NDVI (Normalised Difference Vegetation Index) which is a tested representative of the vegetation vigour on the earth surface. Root zone soil moisture controls the surface vegetation health conditions and coverage in arid and semi arid places where water is a main factor for the vegetation growth condition (Magagi & Kerr 2001). So these vegetation indices are often used to relatively represent root

zone soil moisture if not absolute. Measurement of thermally emitted radiation from the earth surface by the thermal infrared wavelength of the electromagnetic spectrum also yield useful information about surface soil water content, but the emitted radiation originates within the top few tenths of centimetres of soil. Over vegetation, they contain a blend of energy originating over vegetation and bare soil (Carlson et al). In vegetated areas, root zone soil moisture has a strong influence on surface water balance and energy partitioning due to Evapotranspiration ((Song et al 2000),Cited (Wang et al 2007b)). So, remotely sensed Land Surface Temperature is also of significance for investigating relative soil moisture status.

1.3. Relevance of Study

Rajasthan, of which the study area is a part, is the largest state in India. Its area is 10.4% of the whole country. The state has 5% of India's population though only 1% of the total water resources (Rathore 2005). Climate regimes range from extremely arid in the west to sub humid in the east. Physiographically, it is divided into the Thar desert region in the west, the Plains in the east, Aravalli hills ranging from top to bottom of the state in the east and the plateau in the south east. As most of the agriculture is rain fed, the low and uncertain character of rainfall in Rajasthan has made it highly susceptible to drought. It experienced a five-year persistent drought from 1998-2003 (Rajalakshmi 2003). In 2002, the drought attained the status of being worst in 100 years when the average rainfall deficiency was 64%, affecting 44.8 million of 56 million population in the state (Rathore 2005).

The Indian Meteorological Department (IMD) has been monitoring drought based on the deviation from precipitation from the normal for the 35 meteorological subdivisions in India. It uses Aridity Anomaly Index based on water balance studies of Thornthwaite & Mather, 1955. After the drought of 1987, the Ministry of Agriculture and the Indian Space Research Organisation got together to found the National Agricultural Drought Assessment and Monitoring System (NADAMS). It uses the NOAA AVHRR NDVI and based on its anomaly coupled with ground information, drought is monitored. For regional monitoring, the country's own IRS WiFS (Indian Remote Sensing Satellite Wide Field Sensor) and AWiFS (Advanced Wide Field Sensor) are used. The advent of Moderate Resolution Imaging Spectro radiometer (MODIS) and the availability of its data without cost for the public provides reason enough for preferring the use of MODIS in drought monitoring.

The MODIS on the Earth Observing System (EOS) Terra Mission began to produce data in February 2000. It views the entire Earth's surface every 1 to 2 days, acquiring data in 36 spectral bands. The users can download completely calibrated, preprocessed and normalized images. In the recent years, MODIS has been used extensively; a lot of indices have been developed from the products offered for drought monitoring, with vegetation and temperature as parameters. But not many have tried to study soil moisture variability beneath the surface using these datasets, which have high potential due to their higher resolution of 1km and 250mts. As this thesis tries to estimate soil moisture beneath the surface using MODIS, it is relevant to any further study that tries to assess drought in the study area, with soil moisture beneath the surface, where the crops require it, as a parameter. Also Aqua AMSRE, the passive microwave sensor launched in 2002, provides daily data, which has been exploited to give surface soil moisture. The high temporal advantage that it provides is relevant for regional drought monitoring on a continuous fashion. So if this daily data can be used to assess soil moisture variability in the study area, it can be helpful for regional drought monitoring in further research.

1.4. Statement of Scientific Problem

Surface soil moisture represents the coupling between the energy balance and water balance of the earth surface over bare soil, but in vegetated area water at the root zone is more complicated to define (Van Oevelen 2000). In agricultural areas, it is the water available at the root zone of the crops that supplies the water required for plant transpiration. The type of rooting of the crop, .i.e. shallow or deep plays a significant role in investigating the depth at which water has to be available for efficient supply to the leaves. However deep the roots go, water availability in the top 50cms of the soil is crucial for all the crops because maximum root activity takes place within 30cms for most cereals (Peacock & Wilson 1984, Pearson 1984). But this soil moisture is very difficult to measure in a spatially and temporally continuous fashion. The cost of in situ measurements and the data demands of models inspire one to think about the use of free remote sensed data to estimate the same.

Remote sensing is capable of determining an effective water content of approximately 10cms of the top soil (Choudhury et al 1995) cited in (Van Oevelen 2000). Even a microwave sensor cannot observe soil moisture along the profile but, it gives a weighted average depending on the frequency. Passive microwave emission for frequencies greater that 1 GHz show considerable influence of the profile depth on the emission. Empirically, there is general agreement on the order of magnitude of the microwave sampling depth, i.e. it ranges from $0.2\lambda_0 - 0.25\lambda_0$ where λ_0 is the wavelength in free space (Raju et al 1995). This depth also comes within 10cms from the surface and it is debatable whether the moisture content at this depth is of significance to agricultural applications.

The advantage of spatial coverage provided by remote sensing data and the low costs they incur, encourage us to think of estimating root zone soil water content from optical remote sensing measurements itself. Studies have used vegetation indices like NDVI, which represent vegetation vigour, an effect of the situation of water availability at the root zone of the plant. NDVI is the most popularly used vegetation index, but it is found to be a rather conservative indicator of water stress as the vegetation remains green even after initial water stress (McVicar & Bierwirth 2001). So a number of approaches have been proposed for indirect evaluation of soil moisture through radiometric data, essentially based on measurements of surface temperature, evaluated in the thermal infrared region, possibly integrated by vegetation information retrieved in the visible channels. VTCI is one such indicator, which combines information on the condition of vegetation and temperature. It is calculated using the concept of plotting NDVI, an index of vegetation vigour, and LST (Land Surface Temperature)(Wang et al 2001).

MODIS provides Surface Reflectance at 250mts and Land Surface Temperature at 1km spatial resolution. VTCI can be calculated at 1 km spatial resolution using these two datasets. It is desirable to study the use of VTCI to estimate soil moisture beneath the surface which will be spatial at a relatively higher resolution of 1 km and with a temporal resolution of 8 days. As the requirements for higher temporal resolution can be solved only by using the daily brightness temperature provided by passive microwave remote sensing, that aspect also needs to be explored and so tries this study.

1.5. Research Objective

Main Objective

To assess the performance of optical and microwave satellite data to infer soil moisture status in the upper soil layers for the prominent crops in Eastern Rajasthan.

Sub-objectives

The sub-objectives which need to be fulfilled to attain the main objective are

- To estimate soil moisture in the upper root zone at the best possible resolution using Vegetation Temperature Condition Index, from optical remote sensed data given by Terra MODIS.
- To assess the spatio-temporal status of soil moisture in the root zone using parameters derived from passive microwave remote sensed data provided by Aqua AMSRE.
- To estimate root zone soil moisture using a GIS based simple water balance for comparison with optical and microwave measures of soil moisture.

1.6. Research Questions

The research questions addressed by this thesis are

- Can VTCI be computed in a better method to correlate with the in –situ soil moisture in the upper root zone?
- Can Vegetation Temperature Condition Index from optical remote sensed data be used to infer the average soil moisture in the upper root zone?
- Can parameters derived from passive microwave data be used to assess soil moisture in the root zone?

1.7. Research Hypotheses

Null Hypothesis: VTCI shows best indication of soil moisture when the whole image is considered at the resolution of LST.
Alternate Hypothesis: VTCI can show better indication of soil moisture when the agriculture pixels are considered alone or if LST is downscaled

Null Hypothesis: Optical Remote Sensed Data cannot be used to infer soil moisture at the uppere root zone
Alternate Hypothesis: Optical Remote Sensed Data can be used to infer soil moisture at the upper root zone

Null Hypothesis: Passive Microwave Remote Sensed Data cannot be used to infer soil moisture at the upper root zone
Alternate Hypothesis: Passive Microwave Remote Sensed Data can be used to infer soil moisture at the upper root zone.

1.8. Overview of Methodology

The flowchart above illustrates in brief the methodology adopted. Two approaches have been used to measure soil moisture in the upper soil layers. The Optical approach uses a statistical regression between Vegetation Temperature Condition Index and in-situ soil moisture measurements to estimate soil moisture from VTCI alone. The Microwave Approach tries to develop the regression between Brightness Temperature and Polarisation Difference (PD) with Antecedent Precipitation index (API) which is a soil moisture indicator, to assess the status of soil moisture. A third approach which uses a simple water balance model (SWBM) is followed to simulate soil moisture for comparison with the measures from other two approaches.

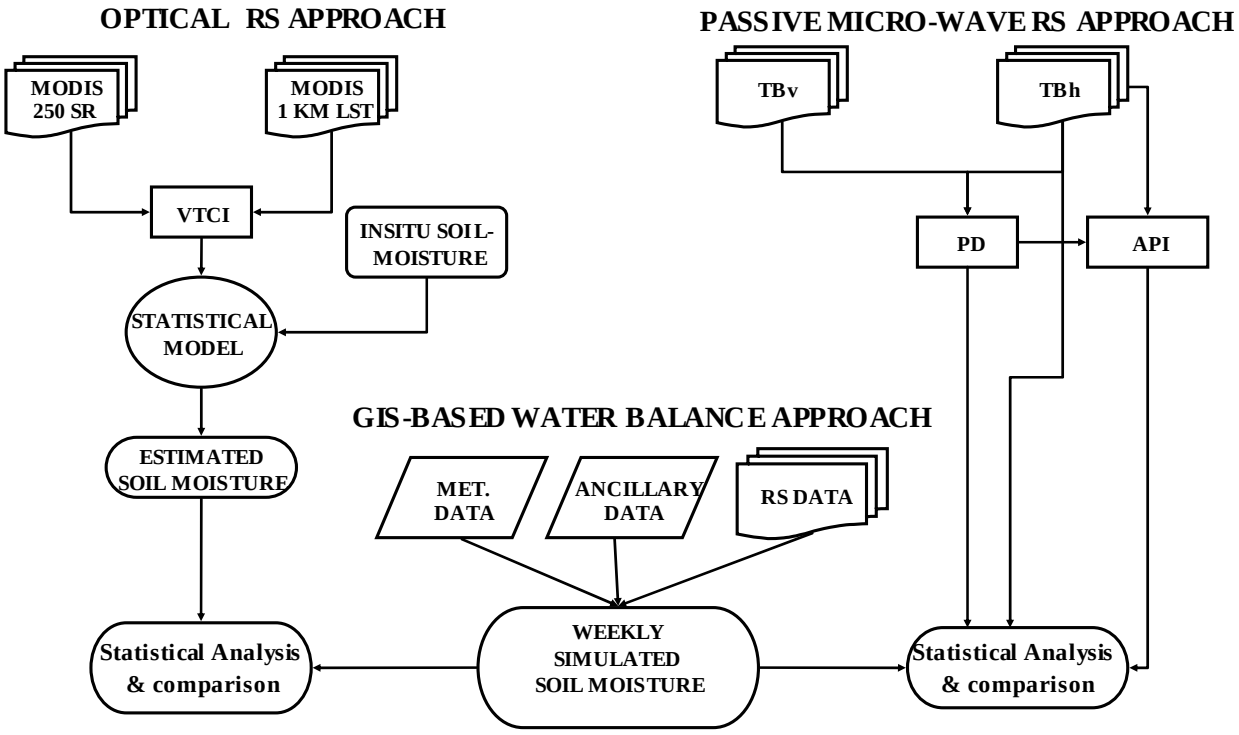

Figure 1-1: Flowchart of Methodology

1.9. Outline of Thesis

The thesis comprises of 6 chapters starting with the present one which describes its intent and usefulness. The second one gives a detailed review of the previous work done in the topic. The third chapter describes the study area and the fourth gives the elaborate methodology adopted to achieve the objectives. The results obtained and their discussions are given in Chapter 5 followed by the conclusions of the study and answers to the research questions summarized in chapter 6.

2. Literature Review

The condition of moisture in the soil can be assessed in three broad ways: measurements using resources on ground, estimation from remotely sensed data and simulation from hydrological and land-surface models. Each has its own advantages and disadvantages, none being perfect. So there is a continued demand for new and innovative ideas in this field. Many such methods are briefly reviewed in the following sections to give a broad idea to the readers, though the sections relevant to the thesis are soil moisture estimation from optical remote sensing, passive microwave remote sensing and simulation from simple water balance model.

2.1. Ground Measurement of Soil Moisture

Point measurements on ground, for soil moisture are done on soil samples of known volume or weight. The water content is expressed as grams of water per gram of oven-dry soil or grams of water per cubic centimeter of oven-dry soil (Kramer 1969). Since the bulk soil water content is variable, a considerable replication of sampling is required to give valid estimates. Depending upon the soil type, the numbers of point to show the order of variability are different. Soil moisture content can be measured through a number of other methods like Neutron Scattering, Gamma ray attenuation, Soil electrical conductivity, Tensiometers, Hygrometers etc. The choice of method used in the study depends on the objectives of the investigator. The standard method for direct measurement of soil moisture is the thermo-gravimetric method. This method consists of oven drying of the soil sample at around 105^{o} C and finding the relation between the changes in mass to the volume of the sample by

$$\theta = W_w / W_d \times \rho_b / \rho_w \qquad \textbf{Equation 2-1}$$

Where:

θ is the volumetric soil moisture content fraction,

W_w is the weight of water contained in the voids of the moist soil,

W_d is the weight of dry soil,

ρ_b is the soil bulk density (from collecting a known volume of soil), and

ρ_w is the density of water.

Although the method is inexpensive and easy, it is time consuming and repetitive measurements are not possible at the same location. This method is also prone to large errors due to sampling, transporting, handling and repeated weighing. In addition, soils with organic matter may exhibit a mass loss during oven drying due to oxidation and decomposition of the organic matter, while some types of clay will retain appreciable amounts of adsorbed water. Measurement errors may be reduced by increasing the size and number of samples (Zegelin 1996).

The soil dielectric properties also help in obtaining a measurement of the soil moisture content because of the large difference between the relative dielectric properties of liquid water (approximately 80) and dry soil (2 to 5) (Engman & Chauhan 1995, Jackson et al 1981, Schmugge 1985). This theory is put to use in measuring soil moisture using capacitance probes and TDR (Time Domain Reflectometry probes). The dielectric constant ε, indicates how polarisable a material is when subjected to an electric field (Zegelin 1996). It is usually measured relative to that of free space, and is referred to as the relative dielectric constant ε_r. The relative dielectric constant of soil is a composite of its components namely air, soil particles and water (Jackson et al 1996). The same property is used in theta probes, which is employed in this study for measurement of in-situ soil moisture. The device measures volumetric soil moisture, by responding to changes in the apparent di-electric constant of moist soil. It gives the average reading at a depth of 5cm from the surface of measurement. Figure 2.1 illustrates the instrument, Thetaprobe.

Figure 2-1: The Thetaprobe

2.2. Soil Moisture through Remote Sensing

Soil moisture measurement or estimation from remotely sensed data has come a long way due to its unique capability of monitoring large areas with long term repetitive coverage (Engman & Chauhan 1995). Remote sensing is data acquisition without direct contact with the object of interest using the different wavelengths of the electromagnetic spectrum. The reflected or emitted signals of particular wavelengths by the earth surface are captured by remote sensors and information is extracted from these signals. In the field of soil moisture, both optical and microwave remote sensing have been used. In optical, studies have used visible and thermal infrared, but a lot of efforts have gone into the microwave section, for both passive and active.

In the context of soil moisture, a necessary point, not be ignored is to affix a correct level or depth for the soil moisture estimate. This is not only for its practical applications but also for making comparisons between different techniques. Often, uncertainty arises from the lack of quantitative agreement between soil moisture estimated by differing methods, which may be because of the variation of soil moisture across the soil profile and the differing depth of measurement or estimation.

One can broadly talk about soil moisture, in two contexts, at the surface and at the root zone (Carlson et al 1995). So it is essential that the observation depths of the different remote sensing instruments be reviewed along with the work if they are to be being compared or related.

As of today, remote sensing technology is not capable of direct measurement of soil moisture. Mathematical models are used to estimate soil moisture content from the response of the sensors. The method of forward modeling which develops a mathematical relationship from model parameters like soil properties and the phenology of vegetation and the method of change detection, which minimizes the impact of all other variables at a location to enhance the difference due to change in soil moisture are two ways of extracting absolute soil moisture from remotely sensed data (Engman 1990).

2.2.1. Soil Moisture through Optical Remote Sensing

Use of Visible & Infrared Remote Sensing

Soil albedo, defined as the ratio of the reflected radiation to the incoming is measured using the visible wavelengths (0.4um to 0.8 μ m). It has a dependence on the surface soil moisture status, but is a poor indicator because soil reflectance is also influenced by the presence of organic matter, soil texture, surface roughness, angle of incidence, plant cover and colour (Engman 1991), causing wide variation in albedo even when the soil contains minimum moisture (Sadeghi et al 1984). Vegetation indices developed from optical remote sensing have been continuously used for water stress detection and vegetation vigor monitoring. As soil moisture has a direct effect on vegetation vigour, there have been studies trying to relate Normalised Difference Vegetation Index developed from visible and infrared remotely sensed data to surface and root zone soil moisture. Rao et al (Rao et al 1993) did a study on vegetated fields and found that NDVI and root zone soil moisture share a linear relationship which is crop type dependent. The NDVI relationship with surface soil moisture was then tried out by Farrar et al (Farrar et al 1994). They found that NDVI was controlled by the surface soil moisture of the concurrent month and not the present. The NDVI response to root zone soil moisture was again studied by Adegoke and Carleton (Adegoke & Carleton 2002) in the corn belt of U.S. They found that the correlation of NDVI to root zone soil moisture maximizes as NDVI lags soil moisture for 2 weeks (Wang et al 2007b).

Use of Thermal Infrared Remote Sensing

Optical remote sensing also includes thermal infrared wavelength of the electromagnetic spectrum which comes between 3 and 24 μ m. As surface soil moisture strongly influences the thermal properties of the soil which are measured by the thermal infrared sensors. A small change in soil moisture content gives considerable difference in the bulk thermal properties of the ground and it is this phenomenon that makes nights cooler than days in areas having high soil moisture content. It is found that the amplitude of diurnal cycle of Ts has a good correlation with soil moisture up to 4 cm depth (Schmugge et al 1980).The amplitude of diurnal cycle of surface skin temperature, Ts, is related to internal factors the combined effect of which is termed as thermal inertia and external factors which are meteorological conditions like relative humidity, windspeed, solar radiation, air temperature and cloudiness. When the surface is drier, the effect of the internal factors or the thermal inertia becomes dominant so that the amplitude of diurnal cycle of Ts is related to the surface soil moisture. So it is in the midday that Ts is found to be most sensitive to soil moisture(Wetzel et al 1984) .

Thermal inertia is a measure of the material resistance to temperature changes. It is an intrinsic property of every material, function of its conductibility (K), density (ρ) and specific heat capacity (**c**).

$$TI = \rho Kc \text{ (Price 1985)} \qquad \textbf{Equation 2-2}$$

Soil water has strong influence on thermal inertia because of the specific heat parameter. And for a given incoming heat flux, the soil temperature variation is inversely proportional to thermal inertia. So the diurnal cycle of Ts is used to estimate soil water content. Thermal Inertia measurements are given by remote sensing measurements but information on thermal conductivity of the surface which is not practically available is also required. A modified method by Apparent Thermal Inertia(Price 1980), an index of approximate thermal inertia with uniform solar energy and diurnal temperature range is recommended by Xue and Cracknell (Xue & Cracknell 1995).

$$ATI = (1 - A) / \Delta T \qquad \textbf{Equation 2-3}$$

Where,

$\Delta \mathbf{T}$ = the difference between the maximum (Tmax) and minimum temperature (Tmin) value that Ts assumes during the diurnal cycle.

A = Surface albedo, ratio of the reflected to incoming radiation.

The disadvantage of the thermal inertia method with remotely sensed data is the limited time sampling of Ts measurements to represent the full diurnal cycle**.**

For surface soil moisture estimation in soils with dense vegetation cover, the use of thermal infrared remotely sensed data is limited because at vegetated places the temperature measured is the leaf temperature. Leaf temperature rises only if there is substantial variation decrease in surface soil moisture because it is mainly governed by the availability of water at the root zone. This becomes an advantage if the application requires root zone soil moisture. Through the variation of leaf temperature, the plant water stress, or the soil moisture situation at the root zone can be assessed (McVicar & Jupp 1998). The possibility of inferring soil moisture content using thermal infra-red observations without using any other data was investigated by Jordan & Shih in 1993 (Jordan & DShih 1993). They used soil thermal inertia and estimated near surface soil moisture for non – transpiring surface and root zone soil moisture for transpiring surfaces. The root zone soil moisture was inferred using a relationship with evapotranspiration rate, vapour pressure deficit, vegetation type and vegetation water stress. The next year, 1994, Ottle and Vidal – Majdar (Ottle & Vidal-Madjar 1994), tried inputting thermal infrared observations namely thermal inertia, hydraulic diffusivity and evaporation into a Soil Vegetation Atmospheric Transfer Model to simulate surface fluxes, surface temperature and near surface soil moisture. The dependency of surface radiant temperature on the soil moisture content and the distribution of vegetation to assess the near surface soil moisture condition was again exploited by Gillies and Carlson in 1995 (Gillies & Carlson 1995) to determine near-surface soil moisture availability (*Mo*), using a physical relationship between NDVI and surface radiant temperature. They found the method unreliable when the vegetation id dense with a fractional cover above 80%.

Use of Surface Temperature / Normalised Difference Vegetation Index (Ts - NDVI) space

The visible, infrared and thermal infrared remotely sensed data can be combined, to use the unique spectral reflectance – emittance properties of leaves in red and infrared regions, in combination with the low thermal mass of the plant leaves relative to soil for estimation of soil moisture (Prigent et al 2005). NDVI from visible and infrared sensors and land surface temperature from the thermal infrared sensor is plotted to obtain a triangular shape as found by Carlson et al (Carlson et al 1994) or a trapezoidal shape as shown by Moran et al (Moran et al 1994). This scatter plot is called the Ts - NDVI space and is closely related to surface evapotranspiration, surface soil moisture, stomatal conductance and surface bowen ratio.

The Ts - NDVI space was used by Prince and Goward (Prince & Goward 1995) to derive surface soil moisture estimates at a global scale using the NOAA AVHRR Pathfinder dataset. Boegh et al (Boegh et al 1998) related it to canopy and soil surface temperature based on the Ts - NDVI relation for certain vegetation when canopy is sparse. Association of the space with soil moisture content has been done by Smith & Choudhury (Smith & Choudhury 1991), Friedl & Davis (Friedl & Davis 1994), Goetz (Goetz 1997) and Goward et al (Goward et al 2002).

Sandholt et al (Sandholt et al 2002) determined a no moisture index called Temperature Vegetation Dryness Index (TVDI) by a simplified interpretation of Ts - NDVI space. They realised that the location of the image pixels in the scatterplot are indicative of their soil moisture or evapotranspiration status and defined TVDI. In the Ts - NDVI space the wet & dry edge are linearly regressed, giving different surface temperature for bare soil & full vegetation in no water stress condition. The upper limit or the warm edge where TVDI = 1 is the no moisture value & lower limit or the wet edge is when TVDI = 0.The conceptual diagram of the TVDI method is given in Figure 2.2. The equation that determines the index as derived by Sandholt et al (2002) is given below.

$$TVDI = (Ts - Tsmin) / (Tsmax - Tsmin) \qquad \textbf{Equation 2-4}$$

Where,

Ts = observed surface temperature

$\mathbf{Ts_{min}}$, $\mathbf{Ts_{max}}$ = minimum & maximum surface temperatures respectively at the same NDVI values.

From **Fig 2.1**,

$\mathbf{Ts_{min}} = b_2NDVI + a_2$

$\mathbf{Ts_{max}} = b_1NDVI + a_1$

$\mathbf{a_1}$, $\mathbf{a_2}$ = intercepts for wet and dry edges respectively

$\mathbf{b_1}$, $\mathbf{b_2}$ = slopes for wet and dry edges respectively

TVDI is found to represent soil moisture spatial variability well, though it is weak in reproducing temporal dynamics (Dadhwal & Patel 2007). Claps & Laguardia (Claps & Laguardia 2004), combined the TVDI and ATI concepts to formulate a modified TVDI in which they fixed the warm edge of the triangle based on the detection of the extreme dryness conditions on a monthly basis. They also tried using the day and night difference of the surface temperatures (DT) instead of Land surface temperature in the triangle and called it DTVDI. But DTVDI also is found to have good spatial stability and bad temporal stability.

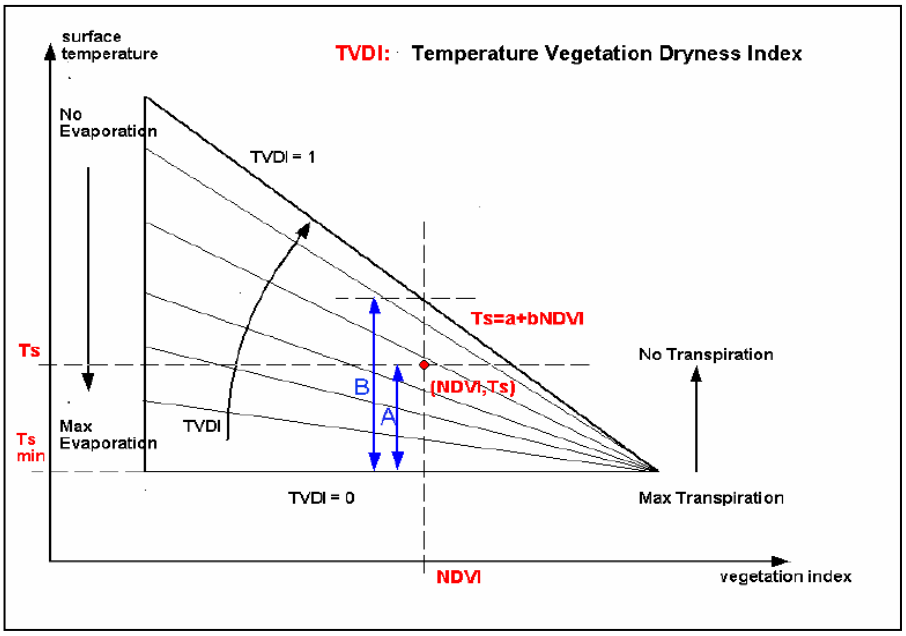

Figure 2-2: Schematic representation of Ts-NDVI Triangle (Sandholt et al 2002)

Liang (Liang 2003) described the concept of Ts – NDVI with the diagram in Figure 2-3. Points A & B belong to bare soils, A being dry so that there is no evaporation & so high LST and B being wet gives maximum evaporation & so low LST. As the vegetation fractional cover, increases, evaporation turns into transpiration & towards full cover, land surface temperature decreases. Points C & D represent full vegetation cover, C having water stress or less soil moisture available at the root zone, giving no transpiration & D having healthy vegetation giving maximum transpiration and so less leaf temperature.

Wang (Wang et al 2001) proposed VTCI, Vegetation Temperature Condition Index, for agricultural drought monitoring which also works with the Ts – NDVI space. It is determined by the equation.

$$VTCI = (\mathbf{LST}_{\mathbf{NDVIimax}} - \mathbf{LST}_{\mathbf{NDVIi}}) / (\mathbf{LST}_{\mathbf{NDVIimax}} - \mathbf{LST}_{\mathbf{NDVIimin}})$$ (Wang et al 2001)

Equation 2-5

Where,

$\mathbf{LST}_{\mathbf{NDVIimax}}$, $\mathbf{LST}_{\mathbf{NDVIimin}}$ = maximum & minimum land surface temperature of pixels which have the same NDVI in the region respectively.

As in TVDI, $LST_{NDVIimax}$ & $LST_{NDVIimin}$ is also determined by the regression equations of dry edge and wet edge of the Ts/ NDVI slopes respectively. The value of VTCI ranges from 0 to 1, the lower value indicating heavier drought and so lesser root zone soil moisture.

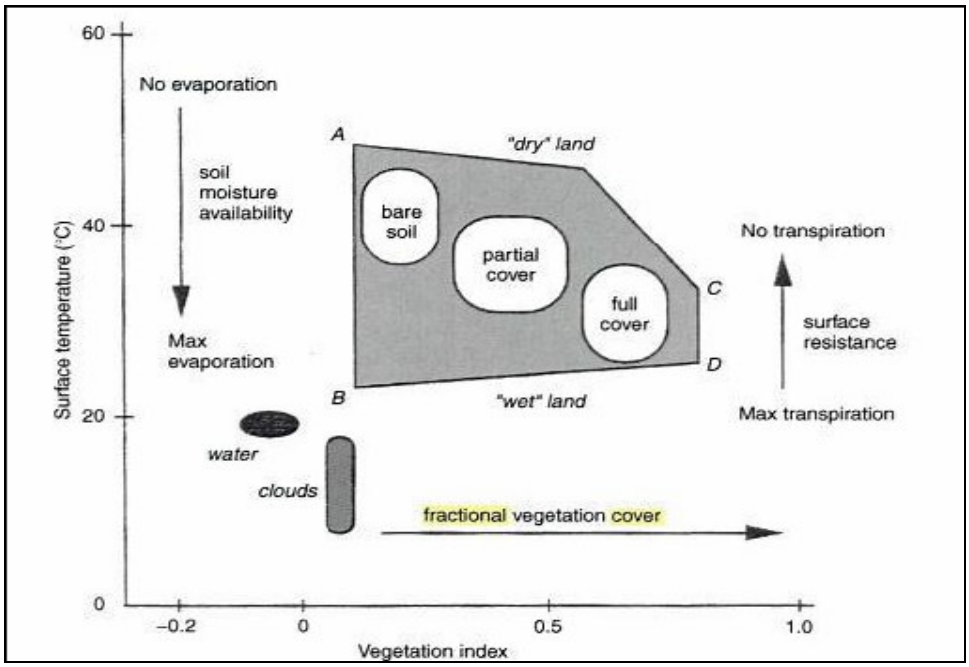

Figure 2-3: Schematic plot of vegetation index -Ts space, and the conceptual relationships with evaporation, transpiration and fractional vegetation coverage (Liang 2003)

The triangular Ts –NDVI space concept called the Universal Triangle Method by Carlson et al (Carlson et al 1994), Gillies et al (Gillies et al 1997) and Chauhan (Chauhan 2003) was again used for soil moisture estimation by Wang et al (Wang et al 2007a). They developed a regression relationship between ground measured soil moisture and NDVI and LST scales using the Universal Triangle and estimated soil moisture in the spatial resolution of optical data.

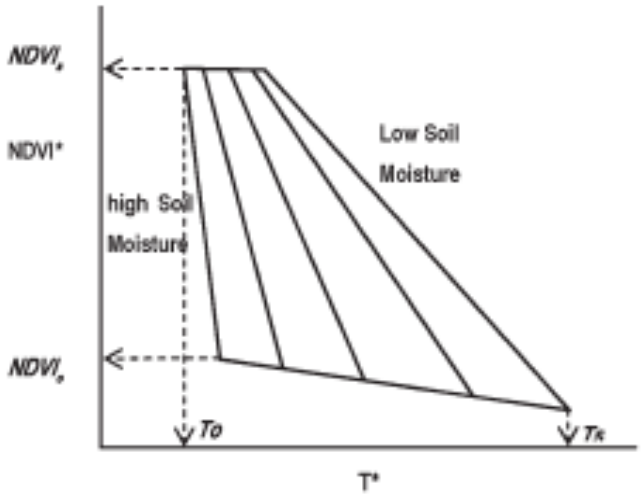

Figure 2-4: Universal Triangle Relationship between soil moisture, temperature and NDVI (Chauhan 2003)

These methods were all mainly built upon data from Advanced Very High Resolution Radiometer on the National Oceanic and Atmospheric Administration. After the launch of Moderate Resolution Imaging Spectroradiometer (MODIS), on the Terra satellite, in 1999, data is obtained at an improved spatial and radiometric resolution, so as to better the results on the application of these concepts. For the realisation of Ts / NDVI space, MODIS provides visible and infrared remotely sensed data at 250 meters and LST at 1kms spatial resolution. The data comes as a composite of 8 days i.e. a single image gives the average values of the following 8 days.

2.2.2. Soil Moisture through Microwave Remote Sensing

Microwave Remote Sensing operates in the frequency range of 0.3 GHz to 300 GHz .i.e. a wavelength of 1mm to 1m (Van Oevelen 2000). The principle behind the use of microwave remote sensing for soil moisture content assessment is the contrast in dielectric properties of liquid water (~ 80) and dry soil (< 4). Research on the dielectric properties of wet soil have been done by several investigators (Dobson et al 1985, Wang & Schmugge 1980) and it has been established that as the soil moisture content increases, the dielectric constant of the soil-water mix increases and this change is detected by microwave sensors (Njoku & Kong 1977).

The two types of microwave remote sensing differ in the source of electromagnetic energy. Passive microwave sensors measure the naturally emitted signals from earth surfaces and active microwave remote sensors or radars send out a pulse of electromagnetic radiation and measure the amount that is scattered back in the direction of the sensor (Jackson et al 1996). The two types are different because of their advantages also. One main difference is in the spatial resolution of data given. The amount of radiation emitted by the earth surface in the microwave region is relatively small. So it is difficult to obtain data with high spatial resolution using passive microwave remote sensing which currently gives data at tens of kilometers. On the other hand, active sensors can provide data on the order of tens of metres, though their sensitivity to surface roughness, topographic features and vegetation make their processing relatively complex (Van Oevelen 2000).

In the field of soil moisture measurement, a lot of efforts have gone into utilising microwave remote sensing because its unique advantages over visible and infrared remote sensing. Microwave measurements are independent of solar illumination and can be made at any time of the day (Jackson et al 1996). The attenuation of the signal received by the sensor by atmospheric gases and cloud is significant for radiation in the high frequency (short wavelength) region of the electromagnetic spectrum, but negligible for frequencies below 10 GHz. The effects of non-raining clouds on microwave radiation are negligible for frequencies below about 15 GHz, and below 3 GHz even the effects of raining clouds are negligible (Schmugge 1985).

Use of Passive Microwave Remote Sensing

Retrievals of root-zone soil moisture content from passive microwave remote sensing are limited as the retrieved signal mainly results from the upper soil layer. But as the surface soil moisture content is typically coupled with the underlying root-zone soil moisture content, the latter can be estimated by using physical land surface process models (Soil Vegetation Atmospheric Transfer Models (SVAT)) and a physical relationship can be obtained between the upper soil layer and the underlying ones (Loew 2007). Several studies have shown the potential of using time series of surface soil moisture to estimate the root-zone soil moisture content (Entekhabi et al 1994, Reichle et al 2002, Walker & Houser 2001).

A microwave radiometer measures the emitted or reflected radiation from the earth's surface in the microwave region of the electromagnetic spectrum. The intensity of the amount of radiation received is characterised by the brightness temperature T_B, which is the temperature of a blackbody that would emit the same amount of radiation. In the context of soil, the amount of energy generated at any point within the soil volume depends on the soil dielectric properties and the soil temperature at that point.

Depending on the orientation of the electromagnetic waves with respect to the surface, from microwave sensors are categorised into horizontally polarised and vertically polarised. Using the dielectric constant (k), viewing angle (θ) and the polarisation of the sensor (H = horizontal & V = vertical), the surface reflectivity can be calculated from Fresnal's Equations and Emissivity is equal to 1 minus reflectivity (Jackson 2005). The value of T_B is the product of soil temperature and emissivity (Schmugge 1985). A microwave radiometer measures T_B above a surface using the equation given below (Jackson et al 1981, Schmugge 1985).

$$T_{b(P)} \approx e_{s(P)} T$$

Where,
T_B observed brightness temperature
T physical temperature of the emitting layer
P refers to vertical or horizontal polarization and
e_s smooth-surface emissivity.

The emissivity is further computed as

$$e_{s(P)} = 1 - R_{s(P)}$$

where R_S is the smooth surface reflectivity which is obtained from Fresnal's equation.

$$R_{sV} = \left| \frac{k\cos u - \sqrt{k - \sin^2 u}}{k\cos u + \sqrt{k - \sin^2 u}} \right|^2 \qquad \textbf{Equation 2-6}$$

$$R_{sH} = \left| \frac{\cos u - \sqrt{k - \sin^2 u}}{\cos u + \sqrt{k - \sin^2 u}} \right|^2 \qquad \textbf{Equation 2-7}$$

Where,
u is the incidence angle (with respect to the normal) and
k is the absolute value of the soil bulk dielectric constant.

$$T_B = \tau(\Gamma_p \, T_{sky} + e_p \, T_{soil}) + T_{atm} \qquad \textbf{Equation 2-8}$$

Where,
T_B is the brightness temperature in Kelvin
Γ_p is the surface reflectivity for polarisation p,

e_p is the surface emissivity for polarisation p and
τ is the atmospheric transmission

This equation accounts for contributions from reflected sky radiation, land surface and atmosphere with the terms in the equation representing the effects from right to left respectively.

Methods to estimation of soil moisture from passive remotely sensed data is mainly categorised into statistical and model based inversion techniques (Prigent et al 2005). Jackson et al (Jackson et al 1981), Schmugge (Schmugge 1985), Engman and Chauhan (Engman & Chauhan 1995), Jackson et al (Jackson et al 1987), Galantowicz et al (Galantowicz et al 1999), Njoku and Kong (Njoku & Kong 1977), Njoku and Entekhabi (Njoku & Entekhabi 1996), Raju et al. (Raju et al 1995), Wilheit (Wilheit 1978) and Wang et al (Wang et al 1983) have used inversion models. The disadvantage of these methods is the influence of surface roughness and vegetation on the microwave response of soil. Roughness of the soil surface increases soil emissivity. The sensitivity to soil moisture content decreases because of this and reduces the range of T_B from wet to dry soils (Van de Griend & Engman 1985). In passive remote sensing, vegetation contributes to total surface emission along with attenuation and rescattering of emission from bare soil surfaces. The parameters influencing the effect are plant biomass and temperature and the sensor frequency (Van Oevelen 2000). The most common model that is used to describe this vegetation effect is the radiative transfer model by Mo et al. (Mo et al 1982) which is very simple so that it disregards many important factors, limiting its applicability to the global scale. (Holmes 2003, Jackson & Schmugge 1991, Wigneron et al 1993) have investigated and successfully developed other models that use information on vegetation type and vegetation water content estimated from visible and infrared remote sensing for this purpose.

Statistical techniques based on regression analysis have also been used to estimate soil moisture. It is found that the horizontally polarised T_{BH} is more sensitive to soil moisture than vertical polarisation (Choudhury & Golus 1988, Choudhury et al 1987, Jackson 2005). Choudhury et al (Choudhury et al 1987), Choudhury & Golus (Choudhury & Golus 1988), Teng, Wang, & Doraiswamy (Teng et al 1993) worked in relating T_{BH} to Antecedent Precipitation Index (API), a soil moisture indicator obtained from meteorological data. Polarisation Difference (PD) & Microwave Polarisation Difference (MPDI) are vegetation indices developed from microwave remotely sensed data (Felde 1998, Jackson 2005). The slope and intercept of the regression of T_{BH} and API were used to estimate soil moisture by developing a regression relation with Polarisation Difference so as to minimise the effect of vegetation on T_{BH}.

The best soil moisture information is provided by microwave sensors at very low frequencies (< 6 GHz) as the attenuation and scattering problems associated with the atmosphere and vegetation are less significant. Also they have higher sensitivity to soil moisture content and the instruments explore further deep into the soil profile. Generally the relevant bands for earth system studies are K (18-27 GHz), X (8-12 GHz), C (4-8 GHz) and L (1-2 GHz) (Jackson 2005).

Satellites containing passive remote sensors are not large in number. The first one that was in operation from 1978 to 1987 was the Scanning Multifrequency Microwave Radiometer (SMMR) onboard the NIMBUS – 7 satellite. It was a polar orbiting satellite providing dual polarised T_B in 5 frequencies, but at a very coarse spatial resolution of 150 km and with a very long repeat cycle. The special Satellite Microwave/ Imager (SSM/I) onboard the Defense Meteorological Satellite has been operational since 1987. It provides free data at high frequencies .i.e. above 19 GHz, dual polarised at all frequencies except 22 GHZ and at very coarse resolution. Another, passive satellite system, The Tropical Rainfall Measurement Mission (TRMM) Microwave Imager (TMI) has five channels providing free dual polarised data at frequencies above 10 GHz for the tropics at a higher spatial resolution than SSM/I. It could collect daily data making possible multi-temporal and diurnal analyses. Two sensors sharing the same name, Advanced Microwave Scanning Radiometer (AMSR) was

launched in 2002 onboard the satellites, the National Aeronautics and Space Administration (NASA) Aqua and the Japanese Advances Earth Observation Satellite (ADEOS – 2). AMSR includes soil moisture as a product which is comes as a daily swath product and also a global product composited to a standard grid to generate surface soil moisture with a nominal spatial resolution of 25 km. Other satellite missions include the Naval Research Lab Windsat, the European Space Agency Soil Moisture Ocean Salinity Mission (SMOS) and the NASA Hydrosphere States Mission (Jackson 2005).

2.3. Soil Moisture from Hydrological Models

A model is a conceptual representation of a real world system and theoretically it is possible to apply models to any hydrological problem. It is in hydrological modelling that modern hydrology has found its base. Different types of models are appropriate depending on the purpose, data availability, spatial scale, time scale, cost and computer resources. It can be empirical describing how the world behaves with little attempt to explain the underlying principles or conceptual, based on limited representations of the processes occurring in the hydrological system, on a perceived system behaviour or it can be physically based models which represent all the relevant processes in the hydrological system under consideration in a physically meaningful way (Watts 1997).

Recent developments in hydrologic models for estimating soil moisture profiles provide an alternative to directly or indirectly measuring soil moisture content in the field. A variety of hydrological models have been published. They differ in the level of detail they use in representing the physical system and temporal variation of the driving forces. Computation of evapotranspiration, partitioning between infiltration and runoff, temporal definition of evapotranspiration demand and precipitation, computation of vertical and lateral redistribution and number of soil layers used are some of the main differences in these models (Schmugge et al 1980). The advantage of hydrologic models is that they can provide timely information on the spatial soil moisture distribution without the necessity of field visits. The error associated with their estimates is a general disadvantage of hydrological models. They are mainly related to the fact that soil moisture exhibits large spatial and temporal variations (Engman & Chauhan 1995, Wigneron et al 1998), as a result of heterogeneity of soil properties, vegetation, precipitation and evaporation (Ottle & Vidal-Madjar 1994).

Water balance models are hydrological models that give information on the components of the water balance, may it be global, continental, regional, of a basin, of a watershed or an experimental field. They are usually semi distributed or distributed and incorporate remotely sensed data which are direct measurements of the water balance components or inputs to calculate the components. Three ways in which remote sensing observations can be input into water balance models are as parametric input data, including soil properties and land cover data such as land use classes or as data on initial conditions, such as initial soil wetness; and as data on hydrological state variables such as evaporation or soil moisture content (de Troch et al 1996). In simulating soil moisture over the entire soil profile using a soil moisture model, large errors are unavoidable due to the highly dynamic nature of the near-surface zone. Thus when measured soil moisture data are available, their use in place of the simulated data should improve the overall estimation of the soil moisture profile with the assumption that measurement errors are less than simulated errors (Arya et al 1983).

Water balance models or soil water budget models have been widely used to simulate regional water balances and to study hydrologic effect of climatic change. The Thornthwaite and Mather Method

(Thornthwaite & Mather 1955) for catchment water balance developed for long term monthly climatic condition in 1955 and modified in 1957 has since been one of the most popularly used water balance model for catchment, regional or continental scale. All simple water balance models adopt the law of conservation of mass equation Based on it, a general water budget equation to determine the root zone soil moisture content can be written as (Yang & Tian 1991).

$$\frac{\partial W}{\partial t} = (P + I) - E - R + D - G$$ **Equation 2-9**

Where
W is the water content of the root zone (cm),
P is Precipitation (cm),
I is the irrigation provided (cm),
E is the Evapotranspiration (cm),
R is Runoff (cm)
D is Discharge from the groundwater (cm), and
G is Recharge to the groundwater (cm)

This equation can be simpler if the model considers the soil as a single bucket. The recharge and discharge can be incorporated into the bucket and irrigation can be added with the precipitation. Then, the equation, in an integrated form for days or weeks, can be simplified for the increment in soil water storage as

Wt – Wt-1 = Pt – Et -Rt (Jupp et al 1998) **Equation 2-10**

Where,
W_t = Total soil moisture at time-step t
W_{t-1}= Soil moisture at the previous time-step

The water balance can be applied to any region taking into consideration the law of mass conservation, which states that the changes of water storage within the reservoirs must be equal to the difference between inflows and outflows (Pimenta 2000). The rainfall, irrigation and runoff from another area account for the inflows and surface runoff away from the area, evapotranspiration and infiltration are taken as the outflows. What remains is the moisture retained by the soil which in a future timestep, which is considered to be part of the inflow, but can be utilised as a part of the outflow. In a GIS environment, the water balances can be calculated on a grid basis or by pixel. Most regional models handle the temporal and spatial variations of the water balance components by first solving the temporal variation of each hydrological component for a single grid cell spatially over the region (Alemaw & Chaoka 2003).

The differences between these models are the methods used to calculate the water balance components, especially potential evapotranspiration and runoff, which are governed mainly by the scale of the application and the data availability. There are several empirical methods to calculate the potential evapotranspiration of a region. The PET is defined as the evapotranspiration which would

result when there is adequate water supply available to a fully vegetated surface. It is difficult to estimate evapotranspiration due to the complexity of plant size, bare soil and soil texture. These empirical equations have been developed from simultaneous observations of evaporation and a number of climatological factors (Mutreja 1986). The most sophisticated method is found to be the Penmann-Montieth method as it uses principles of both energy-budget and mass-transfer theories. The guidelines to calculate evapotranspiration, prescribed by the Food and Agriculture Organisation of the United Nations, FAO (Allen et al 1998) uses the same method. It uses relative humidity, windspeed, maximum temperature, minimum temperature, solar radiation and rainfall. The IMD, Indian Meteorological department, uses the Penmann method alone. The Thornthwaite Method which uses mean daily temperature, the latitude of the place and the month of the year is the most popularly used because of its data simplicity. The method assumes that a high correlation exists between the mean temperature and other variables. Blaney and Criddle developed a method which is similar to Thorthwaite & Mather model but simplified by the assumption that heat budget is shared in fixed proportion between heat, the air and evaporation, making it obvious that potential evapotranspiration is somehow related to the hours of sunshine and temperature, a measure of solar radiation. It uses crop type as a parameter unlike the Thornthwaite Method. Another method using the Hargreaves Equation is recommended when specific data are not available. It uses rainfall and maximum and minimum temperature, considering average values for the other parameters. Christensen method is a very practical though not analytical one for estimation of evapotranspiration. For data not available, it gives a default option developed by correlating the pan evaporation measurements with climatic data at different locations (Mutreja 1986). Jensen and Haise developed another that uses rainfall, maximum and minimum temperature along with solar radiation.

For calculation of runoff, most water balance models adopt the SCS curve number method developed by the United States Soil Conservation Service in 1972. The SCS method is simple to apply to a variety of basins and yields consistent results for particular land use categories; consequently it is popular among regulatory agencies (Masek 2002). The hypothesis of the method is that the ratios of two actual quantities to two potential quantities are equal and calculates daily runoff with the use of a graph plotted between rainfall and rainfall excess from many watersheds. These graphs have been standardised using a dimensionless curve number (CN) which depends on the rainfall received in the previous five days, land use and the hydrological soil group of the study area (Chow et al 1988).

Alemav (Alemaw & Chaoka 2003) developed a continental scale model for southern Africa in which they considered the soil profile as the surface and subsurface zones. The Thornthwaite & Mather method (Thornthwaite & Mather 1955) was used for estimation of subsurface processes .i.e. actual soil moisture, actual evapotranspiration and total runoff on a monthly basis where as the surface processes were accounted for daily using a distributed GIS based hydrological model.

Mandal et al (Mandal et al 2002), developed a soil water balance model to estimate the profile water dynamics. They assumed the soil to be a reservoir of two layers. One termed as the active layer in which the crop roots are always present and moisture extraction and drainage takes place. The lower one is a passive layer, from which only drainage will occur. Its depth is the difference of the maximum rooting depth and the root depth attained any day after sowing. They calculated evapotranspiration using Modified Penmann method. For run off, the SCS (Soil Conservation Service) curve method was adopted with some soil moisture accounting procedure. The characteristics of crops especially the rooting depth, need to be known to simulate soil moisture at the required depth. So they used an

empirical model from Borg & Grims (Borg & Grimes 1986, Mandal et al 2002) root growth model to simulate the rooting depth of the crop on each day after sowing. Mandal et al (Mandal et al 2007), applied the same for a crop specific yield estimation on sorghum.

Brogaard,S et al (Brogaard et al 2005) came up with a bucket model to compute water limitations to plant growth. The model treated bare soil evaporation and actual transpiration separately, a refinement which they say is more biophysically realistic, and leads to enhanced precision in the water stress term especially across vegetation gradients. In the model to calculated actual transpiration, runoff and drainage were not treated as they were considered relatively unimportant.

3. Study Area

This section explains the area chosen for the study. It includes general information about the state of Rajasthan, part of which has been selected for the study, reason for selecting the area, climate and agro-climatic zones in the study area, its physiography and soils and finally agriculture and the prominent crops grown.

3.1. Rajasthan: General Information

Rajasthan is located between 23°3'to 30°12'N latitudes and 69°3'to78°17'E longitudes. The state is the largest in India, with a land area of 342,239 sq. km and a population of 56.47 million. It is bound by Pakistan in the west, Punjab and Haryana in the north, Uttar Pradesh and Madhya Pradesh in the east and Gujarat in the south. Rajsthan is divided into 32 districts, 237 Panchayat Samities and 41,353 villages. The state proudly constitutes 11% of the country's total geographical area but is humbled by its share of only 1% of the country's water bodies. It is predominantly an agrarian state and 70% of the population's livelihood is dependent on agriculture-based activities.

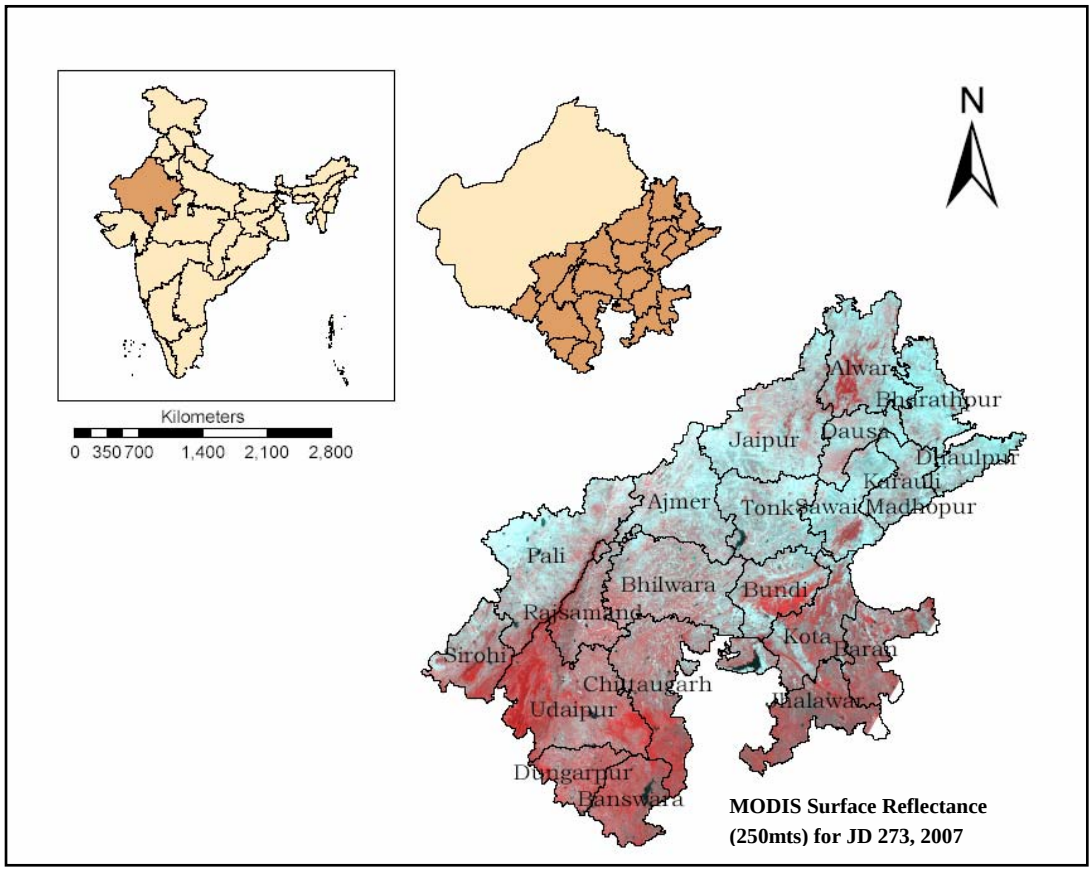

Figure 3-1: Location of Study Area

Rajasthan is landlocked from all four sides split into 2 by the Aravalli Hills which stretch all the way from South-West to North-East. This geographic feature causes the distinct climatic regimes in the state, obstructing the South West Monsoon from going to the western side of the state.

3.2. Choice of Study area

The need for studies on soil moisture in Rajasthan arises due to its high degree of drought propensity. Lack of suitable measure of soil moisture as an indicator of frequently occurring drought in Rajasthan is the main motivation to undertake this study. It can be visualized from the frequency of drought occurrence status given by The Disaster Management and Relief Department, Govt of Rajasthan.

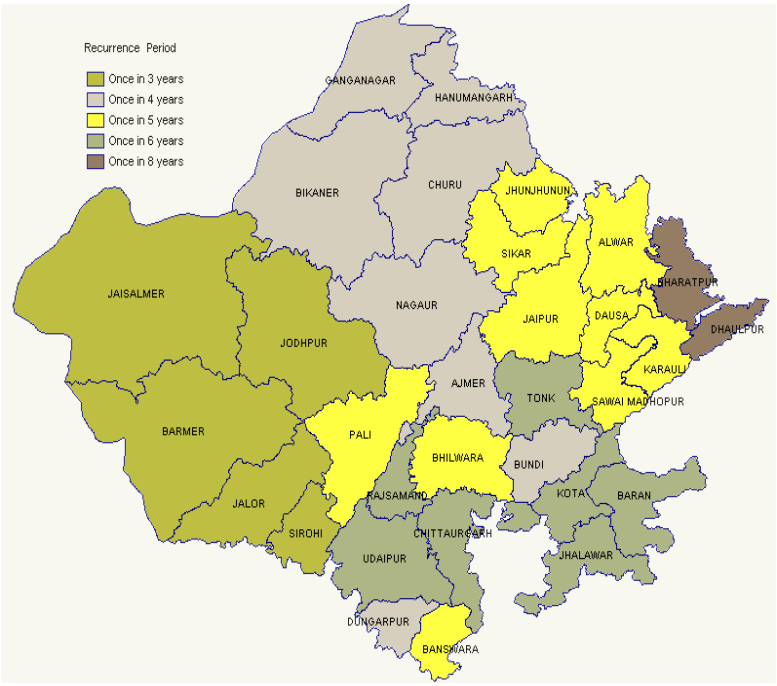

Figure 3-2: Drought frequency for districts of Rajasthan
Source: The Disaster Management and Relief Department, Govt of Rajasthan.

As the map shows, the Western Arid desert is most frequently drought affected. The area receives very low rainfall which varies from 100 to 400mm and is not suitable for rain fed agriculture due to the infertile and parched land. Natural drainage in this part is nil, except for the Luni river basin which drains till the eastern end of Barmer. Hence the moisture variability is highly determined by the irrigation provided by the Indira Gandhi Canal system which runs all the way from Punjab to Barmer in the south western end acting as the life line of the desert region. Any soil moisture study there would have to consider the effect of the canal, integrating natural and man made processes.

Unlike the western side, the eastern part of Rajasthan receives rainfall between 600 to 1000mm. There are 13 river basins and their network has formed well drained fertile land for agriculture. Even then, the eastern side remains drought prone at a frequency of once in 4 to 8 years. Agriculture in this part depends hugely on the amount of rainfall received in the monsoon period. Depending on their economic capability, farmers do use tube wells and other minor irrigation facilities, but most of them, with agriculture as their sole livelihood means, wait for the rains to wet their crops and fill their stomachs. To assess regional soil moisture in the area, one needs to be concerned only with natural phenomena.

The reason cited above, and the time limitation for field work inspired splitting up the state for the study. 21 districts in the eastern part of the state were chosen, avoiding the very arid ones. The difference in agro-climatic zones in the area, which consists of both semiarid plains and sub humid hills were taken into account, so that the spatial variation of soil moisture can be analysed with difference in climate also. The study area lies between 23^{o} and 28^{o}15'N latitudes and 72^{o}15' and 78^{o}16' E longitudes and the total area comes to about 146800 km^{2}.

3.3. Climate

The agro-climatic zones in the study area are classified as given below in the figure below

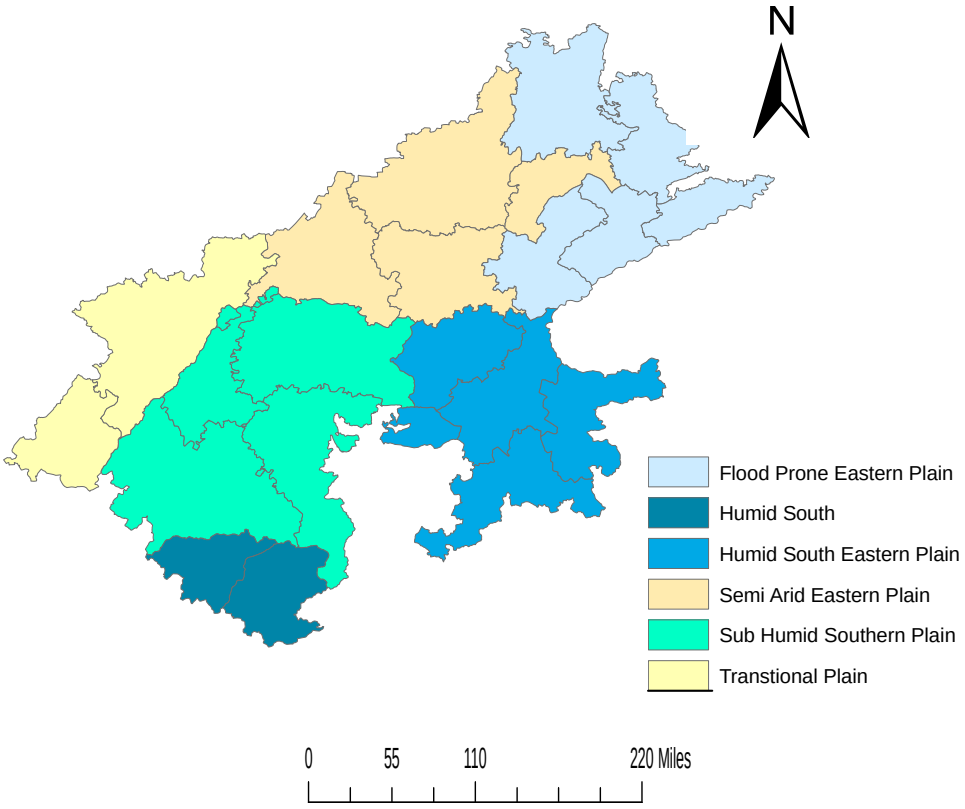

Figure 3-3: Agro climatic zones of Eastern Rajasthan

Source: Reproduced using data from Department of Agriculture, Govt of Rajasthan.

As shown in the map, the climate in the study area ranges from semi arid to humid. In general, the climate is divided into four seasons, namely summers, monsoon, post-monsoon and winters. The summer months are from April to June, after which the monsoon starts and lingers till September. October is the post monsoon month, followed by the winters from November to March. The monsoon season is of interest to this study as this period gifts 90% of the annual rainfall amount and this is when the farmers sow their rain-fed crops. The temperature in this season varies from 30 to 45^{o}C. The difference of rainfall and temperature in the semi arid and sub humid regions of the study area are depicted in the graphs given below. The difference in rainfall and temperature in the two agro-climatic zones are evident in the graphs. Higher rainfall and lower temperature in the monsoons characterize the sub humid region where as the semi arid has relatively lesser rainfall and higher temperature which starts going down as the winters approaches

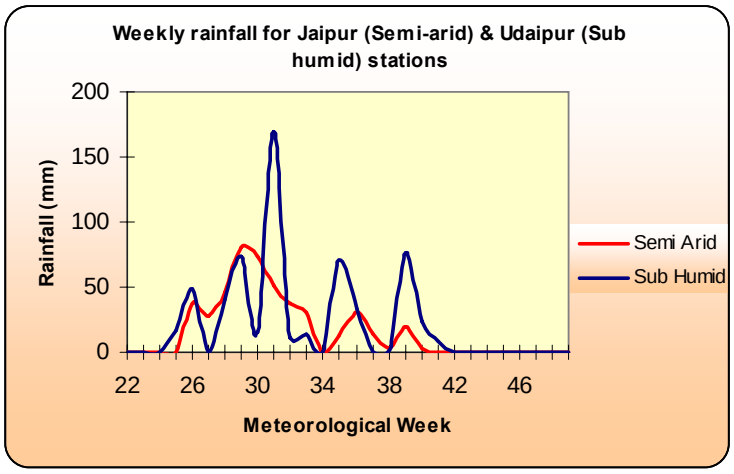

Figure 3-4: Weekly Rainfall pattern for the Khariff season in year 2003 for Jaipur and Udaipur
Source: Reproduced using data from Department of Revenue, Govt of Rajasthan

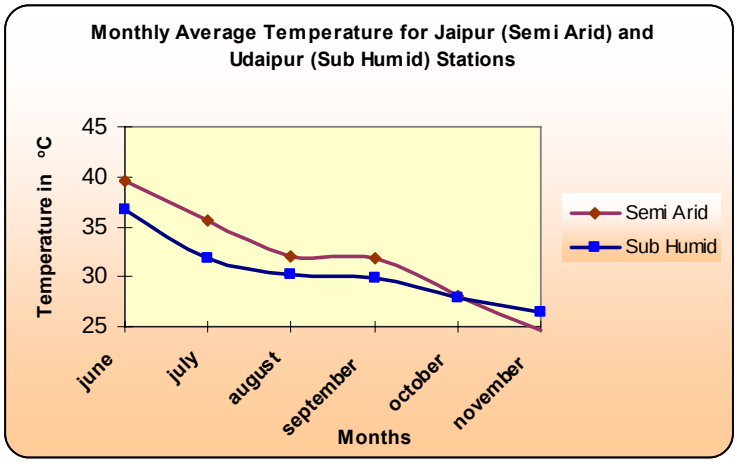

Figure 3-5: Monthly Mean Temperature during the Khariff season in the year 2003 for Jaipur and Udaipur
Source: Reproduced using data from Department of Revenue, Govt of Rajasthan

3.4. Physiography and Soils

The physiography of Rajasthan is product of long years of erosional and depositional process. The present landform and drainage systems have been greatly influenced and determined by the geological formation and structures. The study area can be classified into 5 physiographic units. The two districts, Pali & Sirohi, belong to the Semi-arid Transitional Plain which stretches from the western foot of the Aravalli hills to the western Thar Desert. To the east of the plain, the discontinuous hilly tracts of the Aravalli Landscape extend diagonally across the state. Further east and north east, the area is called Eastern Uplands. Towards Madhya Pradesh, in the eastern tip of the state lie the Pather and Bundelkhand upland which belong mainly to the Vindhyan system. In the south eastern extreme, small parts of Banswara and Jhalawar belong to the Malwa Plateau.

The soils in the area vary all the way from sandy to clayey. The Semi Arid Transitional Plain consists of coarse loamy to fine loamy, deep and well drained soils. They are formed by the alluvium deposits laid by Luni, Gagar, Saraswati, Chouthan and Sutlej river systems. The Aravalli landscape is

characterized by loamy and loamy skeletal in the hills with very low available water capacity, but the intermediate valleys and plains have fine and coarse loamy which are suitable for agriculture, as they have medium to high available water capacity. The Eastern Uplands consist of soils with mixed texture, parts near Ajmer having sandy soils and the others ranging from the loamy to fine. The soils are very deep except for the dissected hills and ridges in between. They are formed largely by the older and recent alluvium laid by the Banas and Mahi river systems originating in the Aravalli hills. The alluvial plains in the Pather and Bundelkhand Upland consist of fine to very fine soils having high available water capacity. They are formed by the alluvium laid by river Chambal and its tributaries. The Malwa Plateau consists of basaltic formations. The soils are clayey and clayey skeletal and they are generally prone to salinization and water stress. These soils are also formed by the alluvium laid by river Chambal and its tributaries (Shyampura & Sehgal 1995).

3.5. Agriculture

Agriculture, as similar to all over India, is done in two crop seasons. The Rabi, the winter crop, is sown in the months of October and November and harvested in the months of March and April. Barley, wheat, gram, pulses and oil seeds are the major crops in this season. The Khariff crops are sown with the starting of the monsoons, seeded in the months of June and July and harvested in the months of September and October. The main crops include bajra, jowar, maize, pulses and groundnuts. As the thesis involves the rainfed crops, the prominent crops in the Khariff season were identified as Bajra, Jowar and Maize.

Pearl Millet or Bajra or RajBajra, as called locally, is the major food crop of Rajasthan. The state holds the first position for Bajra production in India, producing 46% of the country's total bajra yield. This millet can be grown in sandy soils under rain-fed conditions and hence assumes importance in the semi arid region of the study area. The temperatures during the growing season remain between 25^{o}C and 35^{o}C. The optimum rainfall requirement ranges between 35 to 50cm. Bajra can be grown in areas, which receive less than 35 cm of annual rainfall, though prolonged spells of warm, rainless weather may be detrimental and may lead to crop failures. The major Bajra growing districts are the semi arid ones, Jaipur, Alwar, Karauli, Pali, Dausa, Bharathpur, Sawai Madhopur, Ajmer, and Tonk. Jaipur is the highest producer of Bajra, with a figure of 137310 tonnes in 2003.

Figure 3-6: Field photographs of Maize and Bajra in Maturity stage.

Maize or Makka or Makki is the staple food grain of southern districts of Bhilwara, Udaipur, Dungarpur, Banswara, Chittaurgarh and Jhalawar. These districts have good well-distributed rainfall throughout the crop season with 50 to 100cms mean annual rainfall. They also have sandy loam to loamy soils with good drainage and therefore are most suited for this crop. It is grown in areas where

the average maximum and minimum temperatures remain around 35 ^{o}C and 12 ^{o}C, respectively. Maize is mostly sown in July with the commencement of the first monsoon showers and harvesting is done in October-November. The crop yields higher when grown in fertile loamy soils. Stagnation of water in the field causes decay of plants and so the crops are mostly grown on well-drained soils.

Figure 3-7: Field photograph of Jowar in Maturity stage

Sorghum or Juar or Jowar is produced as fodder in almost all the districts in the study area, the major contribution being from Pali, Ajmer and Tonk. The crop has many qualities that make it drought resistant and it does well on most soils but better so in light to medium textured soils.
The statistics of area sown for these three crops for the year 2003 are given below

Crops	Area Sown in Hectares	Percentage of total agricultural area
Bajra	1465853	29.19%
Maize	1109740	22.2 %
Jowar	617799	12.5 %
Other Crops	1827193	36.4 %

Table 3-1: Area & percentage of the prominent crops in the study area for the year 2003
Source: Data from Dept of Agriculture, Govt of Rajasthan, www.rajasthankrishi.gov.in

4. Materials Used and Methodology

The study attempts 2 approaches to measure soil moisture at the upper root zone 1) using optical remote sensed data and 2) using passive microwave remote sensed data. In the optical approach, Vegetation Temperature Condition Index (VTCI) was derived from optical data. The index is derived using 3 different methods for 2007. The method which is best representative of in-situ soil moisture is used to develop a regression relationship to estimate soil moisture for 2003 Khariff season. The estimated measure is compared with simulated soil moisture from a simple water balance model (SWBM) which uses meteorological data and satellite data, combined with ancillary data. For the passive microwave approach, parameters from passive microwave remote sensed data are used to estimate Antecedent Precipitation Index (API), a widely used indicator of soil moisture. API is also derived using meteorological data and ancillary data together with satellite data. The passive microwave parameters are also tested for their ability to represent soil moisture at the root zone by correlating with simulated soil moisture from the SWBM. This chapter explains the data used to achieve the objectives of the study and the elaborates the methodology adopted

4.1. Materials Used and Pre-processing

4.1.1. Satellite Data

Data from the Terra – MODIS satellite was used for the optical approach to estimate soil moisture in the upper layers. For the passive microwave approach, data from Aqua – AMSRE were utilised for the study. Root zone soil moisture measures derived from ERS Scatterometer, AMSRE and Solar Radiation data derived using different bands of Meteosat were used for the simple water balance model. The details are discussed below.

MODIS Data Products

The **MOD**erate Resolution **I**maging **S**pectroradiometer (MODIS) is a key instrument for NASA's Earth Observing System (EOS). It was launched on board the Terra spacecraft in Dec. 1999 (first light on Feb. 24, 2000) and on board the Aqua spacecraft in May 2002 (first light on June 24, 2002). It has a viewing swath width of 2,330 km and views the entire surface of the Earth every one to two days. Its detectors measure 36 spectral bands between 0.405 and 14.385 µm wavelength, 20 reflective solar bands (0.405 - 2.2 µm) and 16 thermal emissive bands (3.5 - 14.385 µm). It acquires data at three spatial resolutions i.e. 250m, 500m, and 1,000m (http://edudaac.usgs.gov/modis/dataproduct.asp).

MODIS gives products categorised into 3 sections, land, atmosphere and ocean. Its products have come a long way in 7 years. The Level 3 MODIS products available at present, are corrected for atmospheric gases and aerosols and comes georeferenced. The latest Version 5 products are Validated Stage 1, i.e. accuracy has been estimated using a small number of independent measurements obtained from selected locations and time periods and ground-truth/field program efforts and ready for use in scientific publications. It provides daily and composite data. The 8 day composite data sets give the

best possible observation during a day period as selected on the basis of high observation coverage, low view angle, the absence of clouds or cloud shadow, and aerosol loading. A brief description about the MODIS Land products used in this study are given below

MODIS/Terra Surface Reflectance 8-Day L3 Global 250m SIN Grid V005:

The MODIS surface reflectance products are an estimate of the surface spectral reflectance for each band as it would have been measured at ground level if there were no atmospheric scattering or absorption. MOD09Q1 provides Bands 1 and 2 at 250-meter resolution in an 8-day gridded level-3 product in the Sinusoidal projection. Science Data Sets provided for this product include reflectance values for Bands 1 and 2, and a quality rating. Data for the dates corresponding to field campaigning .i.e. the Sept 30th, were downloaded. Also 20 images for the whole of the Khariff season, June to Oct 2003 were obtained. Figure 4-1(a) illustrates an example of the product

MODIS/Terra Land Surface Temperature/Emissivity 8-Day L3 Global 1km SIN Grid V005:

Land Surface Temperature, LST, is a key parameter in the physics of land surface processes because it combines the surface-atmosphere interactions and the energy fluxes between the atmosphere and the ground. The MODIS LST product is created using various methods. A view-angle dependent, split-window algorithm is used to calculate temperature to the nearest Kelvin if the land surface has high and stable emissivity. For land cover types with varying emissivity, the calculation is done with daytime and night time observations in seven MODIS thermal infrared (TIR) bands using a statistical regression approach, a least-squares fit approach, or both(Parida 2006). The level-3 MODIS global Land Surface Temperature (LST) and Emissivity 8-day data are composed from the daily 1-kilometer LST product and stored on a 1-km Sinusoidal grid as the average values of clear-sky LSTs during an 8-day period. MOD11A2 is comprised of daytime and nighttime LSTs, quality assessment, observation times, view angles, bits of clear sky days and nights, and emissivities estimated in Bands 31 and 32 from land cover types. It has twelve layers and out of these only layer1-MODIS _LST_Day_1km has been used in this thesis. The dataset for September 30th 2007 and for the Khariff season, June to October of 2003 were acquired. An example image of the product is given in Figure 4-1(b).

Preprocessing:

The MODIS data are put through the following pre-processing steps before it was used for analysis.

1. Conversion of file format
2. Layer Stacking
3. Reprojection
4. Scaling with a multiplication factor
5. Subsetting

MODIS products are available to the users in HDF (Hierarchial Data Format) which is a multi object file format for sharing scientific data in a multi platform distributed environment. It is imported to img format. The surface reflectance layers from band 1 & 2 are separately stacked. The stacked layers are then reprojected from Sinusoidal projection to Alberts Conical Equal Area projection, retaining the datum, WGS 84. The parameters for India for Alberts Conical Equal Area projection are given below. After reprojection, the MODIS data products were scaled with their respective multiplication factors, which is 0.002 for LST images and 0.0001 for the surface reflectance images. All the pre-processing

steps were done in ERDAS imagine 8.7. The Normalised Difference Vegetation Index (NDVI) is then calculated using the surface reflectance bands. Figure 4-1 (c) illustrates an example image of NDVI.

Albers conical equal area
Parameters:
a=6378137.00
b=6356752.31
1/f=298.25
b/a= (1-1/f)
Central Meridian: 78°
Central Parallel or Central Latitude of origin: 20°
Standard Parallel 1:12°
Standard Parallel 2:28°
False Easting: 2000000.00
False Northing: 2000000.00

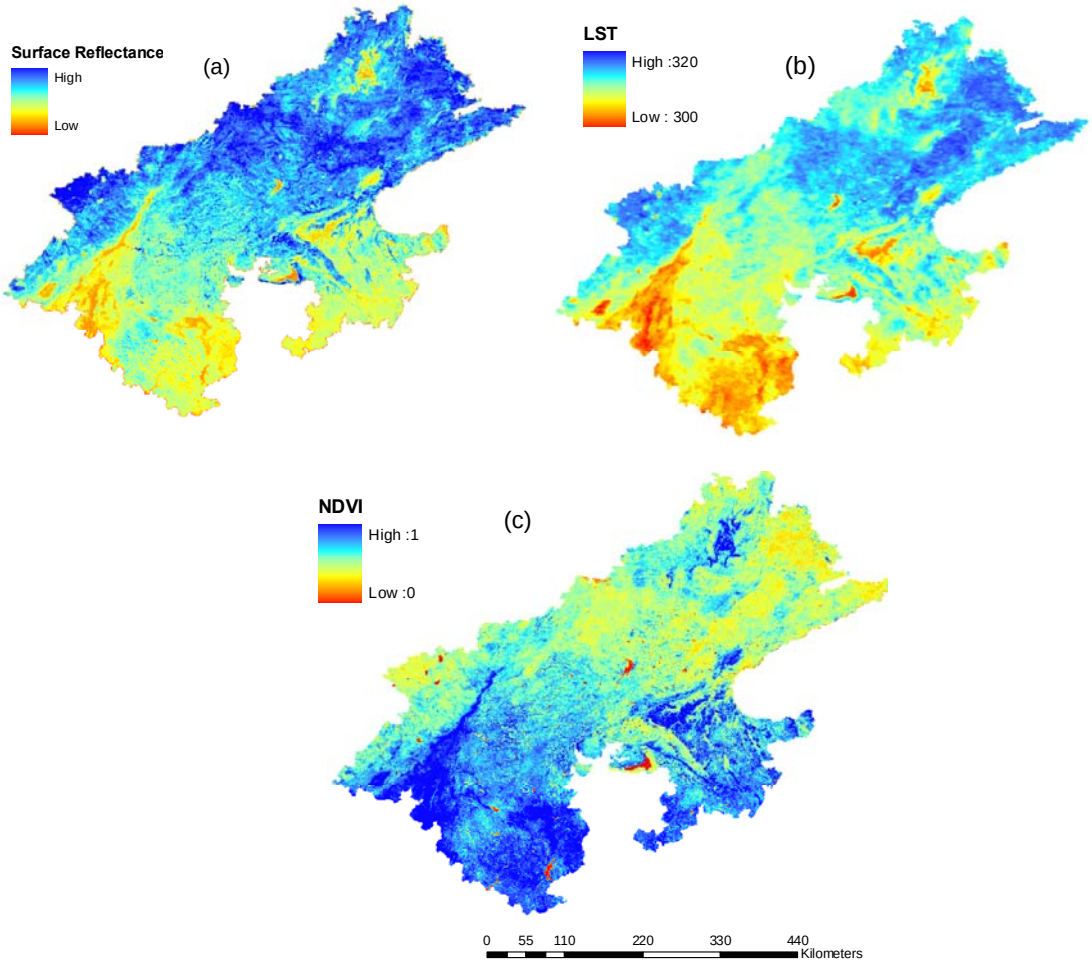

Figure 4-1: (a) Surface Reflectance (b) Land Surface Temperature and (c) NDVI Images for JD 273, 2007

AMSRE Data Products

The Advanced Microwave Scanning Radiometer - Earth Observing System (AMSR-E) instrument on the NASA EOS Aqua satellite provides global passive microwave measurements of terrestrial, oceanic, and atmospheric variables for the investigation of water and energy cycles. It gives daily

measurements of surface soil moisture and vegetation/roughness water content interpretive information, as well as brightness temperatures (T_B) and quality control variables. Ancillary data include time, geolocation, and quality assessment.

Temperature Brightness (Vertically and horizontally polarised (T_{BH} & T_{BV})):

Input brightness temperature data, corresponding to a 56 km mean spatial resolution, are resampled to a global cylindrical 25 km Equal-Area Scalable Earth Grid (EASE-Grid) cell spacing (http://nsidc.org/data /docs/daac/ae_land3_l3_soil_moisture.gd.html). So the effective spatial resolution of the products is 25 km^2. The T_B data come from different frequencies namely, 6.9 GHz, 10.7 GHz, 18.7 GHz, 36.5 GHz and 89 GHz. The vertical and horizontal polarised T_Bs are daily global data available from June 2002. The Level -3 data include images of both, descending and ascending paths.

The AMSRE products were downloaded through the EOS data Gateway. 170 images for the whole of the 2003 Khariff season were obtained and pre-processed.

Pre-processing:

The level-3 AMSRE Brightness Temperature data are subjected to the pre-processing steps given below which were done in ENVI.

1. Composition of data to alternate days.
2. Layer stack
3. Georeferencing
4. Resizing
5. Scaling

Every other day, there is a shift in the swath of the satellite. So the T_Bs of descending modes of every other day were combined to make alternate day composite data. The products are not georeferenced, but their parameters are provided in a separate file. The georeferencing can be done in ENVI and the output file is in Geographic latlong projection with WGS 84 datum. After georeferencing the data can be subsetted or resized for the study area. The resized data was subjected to scaling by multiplying with a factor of 0.1. Figure 4-2 illustrates a pre-processed image of T_{BH}

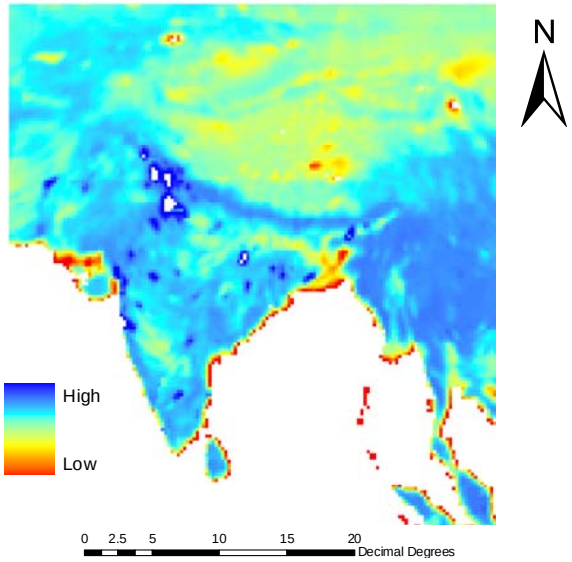

Figure 4-2: Horizontal polarised Brightness Temperature as given by Aqua AMSRE for JD 273

Soil Moisture at the root-zone upto 1m depth estimated using the AMSRE surface soil moisture product by Bonn university is available for 2003 and 2004. The temporally constant soil moisture is calculated using long-time precipitation, vegetation density, soil texture and terrain slope. A linear regression is used to retrieve the local climatological mean constant soil moisture within the uppermost meter. The temporal variability is incorporated in the second step. The 18 Ghz brightness temperature from Aqua/AMSR is used to estimate the remaining temporal variance of soil moisture at each grid point. Finally, the complete soil moisture field is retrieved by combining the results of the two steps. The product is available at a temporal interval of 10 days and spatial resolution of 0.5^{o} in geographic latlong projection.
(http://postel.mediasfrance.org/en/BIOGEOPHYSICAL-PRODUCTS/Soil-Moisture).
The pre – processing involves resizing the product for the study area and reprojecting it to Alberts Conical Equal Area projection with WGS 84 as the datum. The product is used in this study to compare the trend of the simulated soil moisture from SWBM.

Soil Water Index from ERS Scatterometer

Scatterometers onboard the ERS -1/2 are active microwave remote sensing sensors with three antennas simultaneously observing the Earth surface at different look directions. The high quality C- band frequency backscatter data supplied by the scatterometers are used to retrieve soil moisture. The Vienna Institute of Technonogy (VUT) Model developed by The Institute of Photogrammetry and Remote Sensing (IPF), Vienna University of Technology, Austria when applied to the data resulted in the first multi-year global remote sensed soil moisture dataset. The model is based on a change detection algorithm proposed by Wagner et al which accounts for environmental conditions, heterogeneous landcover and surface roughness effects. It uses the multiple incidence angle viewing capabilities of the sensor in order to separate soil moisture and vegetation effects. To retrieve soil moisture in the root zone up to one meter below the surface, a two-layer water balance model, which only considers the exchange of soil water between the topmost remotely sensed layer and the "reservoir" below, was used to establish a relationship between the ms series and the profile soil moisture content (Ceballos et al 2005). The parameter thus obtained is named Soil Water Index (SWI). Its physical definition can be the soil moisture content in the 1^{st} meter of the soil in relative units ranging between wilting level and field capacity. Its physical values range from 0 to 100 %. The Global SWI data is validated by comparing with model data and in-situ soil moisture of 360 stations in Russia, Ukraine, India, Illinois, China and Spain.
(http://postel.mediasfrance.org/en/BIOGEOPHYSICAL-PRODUCTS/Soil-Moisture).
The product has been found to give an accuracy of 10%. The product is available from 1992 to 2006 with a temporal resolution of 10 days and spatial resolution of 33km. The image of mid-June 2003 was used in this study as initial soil moisture input for the SWBM. The product is multiplied with a factor of 0.5 to get its original values from the encoded data.

Solar Radiation from MIVSSR EUMETSAT

Data from visible, water vapour and thermal IR channels of The Meteosat Visible and Infrared Spin Scan Radiometer on- board METEOSAT -5 were used to produce a measure of insolation. The spatial resolution of the product is 0.04^{o} with a temporal resolution of 10 days. The product for acquired from June to November 2003 for its use to compute potential evapotranspiration for the SWBM. It was reprojected to Alberts Conical Equal Area before further processing.

4.1.2. Meteorological Data

Meteorological data were required for the SWBM and for computing API. Daily rainfall and minimum and maximum temperature were acquired from the Department of Revenue, Govt of Rajasthan. The data are from mandal or sub-district level offices.

Daily Rainfall

Daily Precipitation data of 284 mandal level rain gauge stations as illustrated in Figure 4-3(a) for the year 2003 were obtained. 284 stations inside the study area and 24 stations in the surrounding area were taken. The daily data was added up to get the weekly sum. Modified Inverse Distance Weighted Average was used for interpolating the point data to acquire the daily and weekly spatial rainfall patterns. Inverse Distance Weighted Average is an averaging procedure. It gives each neighbouring station a weight which is proportional to a power of the inverse of the station distance. The modified method gives a smoothened version of the same. Thus, closer stations have more weight in the averaging procedure than stations that are further away. 1km * 1km grids of weekly rainfall was obtained for 24 weeks from June 18th (25th meteorological week) to Nov 30th (48th meteorological week).

Daily maximum & minimum temperature

The daily minimum and maximum temperature for 16 stations as illustrated in Figure 4-3(b) were interpolated using the thin plate spline technique to obtain spatial patterns. This interpolation method is a basic minimum curvature technique which ensures that the surface must have minimum curvature i.e. the cumulative sum of the squares of the second derivative terms of the surface, taken over each point on the surface must be a minimum. This concept ensures a continuous, smooth interpolated surface. The interpolation was done in FAO Loc Clim 1.03 because it considers altitude also, which is an important factor for the spatial variation of temperature.

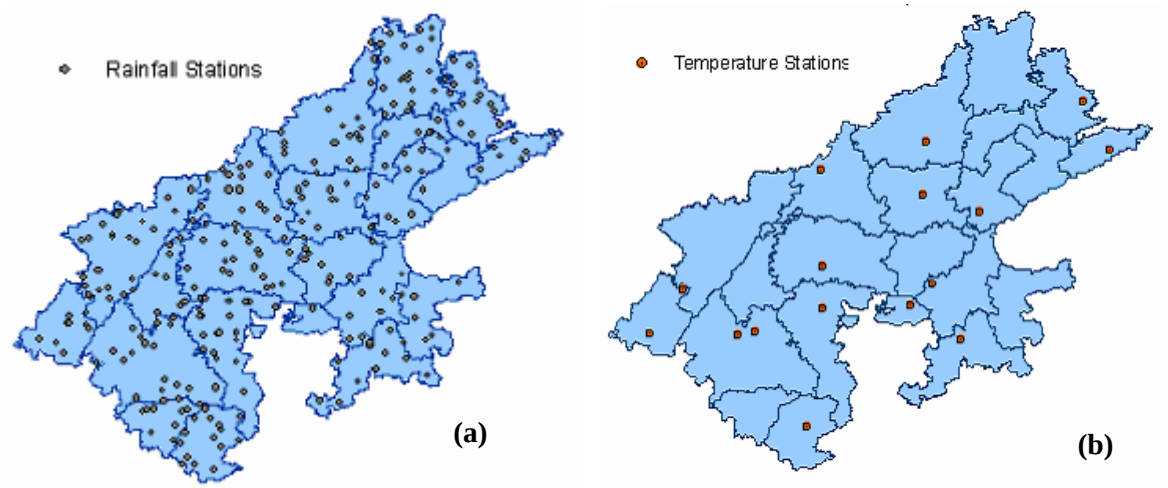

Figure 4-3: Stations with daily (a) Rainfall (b) Temperature data used for interpolation.

4.1.3. Ancillary Data

The ancillary data used for in various approaches of the study are listed below. The soil properties maps are used for the SWBM and API computation. The rest were used to make the crop distribution map of prominent crops in Eastern Rajasthan.

1. Properties of soils in Rajasthan mapped at a scale of 1:250,000 and published at 1:500,000 scale by

the National Bureau of Soil Survey and Land Use Planning (Shyampura & Sehgal 1995).

2. Land-use Map 1km Grid (www.gvm.jrc.it/glc2000/Products).
3. District wise Agricultural Statistics (www.rajasthankrishi.gov.in).
4. Crop calendars for Pearl Millet, Sorghum & Maize in the study area during the Khariff season (literature).

4.2. Methodology

This section details the methodology adopted in the study. It begins with the methods used to produce the crop cover map for the prominent crops in the area. The second section describes the field investigation conducted followed by elaborate discussion on the various approaches used.

4.2.1. Crop Cover map

For a study related to the prominent crops in the area, it is necessary to generate a map which provides the spatial distribution information of the crops. The crop cover map was produced based on the NDVI profiles from the MODIS 8 day surface reflectance of 250 mts spatial resolution. NDVI is an effective measure of photo synthetically active biomass and it has been used to study vegetation phenology especially those of crops. Each NDVI profile is said to represent changes in green biomass over time and is assumed to relate to a specific mix of land cover. This capability of NDVI is put to use in the stepwise methodology discussed below, to generate the crop cover map.

Step 1: Extraction of Agricultural area

NDVI profiles of different scrubs and plants in the forest area may come similar to the crops. So it was necessary to first mask out the agricultural area from the NDVI images. The level 1 land use map was used to extract the agricultural land present in the study area.

Step 2: Cloud Correction

The Khariff season in India is from June to November. It starts with the southwest monsoons which bring showers in July, August and September. So, using optical remotely sensed data for the Khariff season has the limitation due to cloud cover. For this reason, the NDVI images of July and August need to be cloud corrected for crop classification. The quality file accompanying the surface reflectance data was put to use here to identify the cloudy pixels. The QA file comes as a 16 bit data file, each value representing the cloud situation of that pixel. The 2 and 3 bits give information on the cloud status (http://edudaac.usgs.gov/modis/dataproduct/mod09q1v5_.asp). To interpret the cloud information the values have to be converted into binary. The combination of 2 & 3 bit spaces highlighted in the Table 4-1 give the cloud info.

Binary places →

Pixel Values ↓

	12	11	10	9	8	7	6	5	4	3	2	1	0	Cloud Status
4096	1	0	0	0	0	0	0	0	0	0	0	0	0	clear
4100	1	0	0	0	0	0	0	0	0	0	1	0	0	cloudy
4104	1	0	0	0	0	0	0	0	0	1	0	0	0	mixed
8204	1	0	0	0	0	0	0	0	0	1	1	0	0	assumed clear

Table 4-1: Binary codes of QA file provided with MOD09Q1

For eg. 4096, 4100, 4104 & 8204 are some of the pixel values from the QA file. They give the values given in Table 4-1 when converted into binary. The combinations in the 2, 3 bits, i.e. 00, 01,10 & 11 indicate different cloud situations.

The cloudy pixels were identified in each image of July and August. NDVI becomes relatively very low in the presence of clouds. So the identified pixels were replaced by the maximum value in the three adjacent weeks i.e. for a cloudy pixel in July 2nd week's image, the maximum of the NDVI values for the respective pixel, in the images of July 1st week, 2nd week and 3rd week is substituted. Considering more than 3 weeks would give considerable change in the NDVI profile, so the maximum value was selected between 3 weeks, though there are pixels which are cloudy throughout the 3 weeks. An example has been illustrated in Figure 4-5.

Julian days (June 1st – Nov 30th)	*NDVI value before cloud correction*	*NDVI value after cloud correction*
145	0.158	0.158
153	0.143	0.143
161	0.137	0.185
169	0.185	0.185
177	0.149	0.185
185	0.155	0.254
193	0.254	0.426
201	0.426	0.426
209	0.228	0.716
217	0.716	0.716
225	0.458	0.716
233	0.488	0.488
241	0.173	0.488
249	0.450	0.450
257	0.371	0.371
265	0.413	0.413
273	0.327	0.327
281	0.278	0.278
289	0.275	0.275
297	0.228	0.228

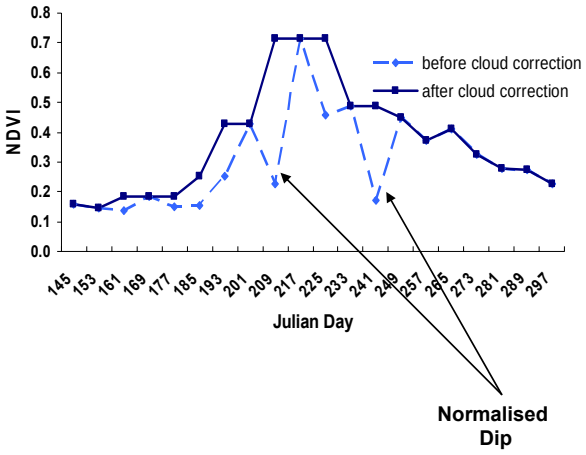

Figure 4-4: Sample Cloud Correction table & NDVI profiles

Step 3: Unsupervised classification

After cloud correction, the NDVI images consisting of agriculture pixels alone were classified using the ISODATA clustering algorithm in ERDAS Imagine™. The method is iterative i.e. it repetitively performs an entire classification and recalculates statistics. It uses the minimum spectral distance formula to locate the clusters that are inherent in the data. At first the image was classified into 35 clusters. The average NDVI profiles of the 35 clusters were then visually explored. Clusters with visually similar profiles were merged.

Step 4: Naming of the clusters

To identify the crop that each cluster represents, the crop calendar for the area was used. But as the three prominent crops taken for the study share almost the same period (as shown in Table 4-2) for sowing and harvesting, the land use points collected during the first field investigation were used to differentiate between them. Examples of NDVI profiles for the crops are illustrated in Figure 4-6.

Crop	Months of sowing	Months of harvesting
Pearl Millet	June – July	Sept – Nov
Sorghum	June - August	Oct – Dec
Maize	June – July	Sept – Nov

Table 4-2: Months of sowing and harvesting for the major crops in the study area

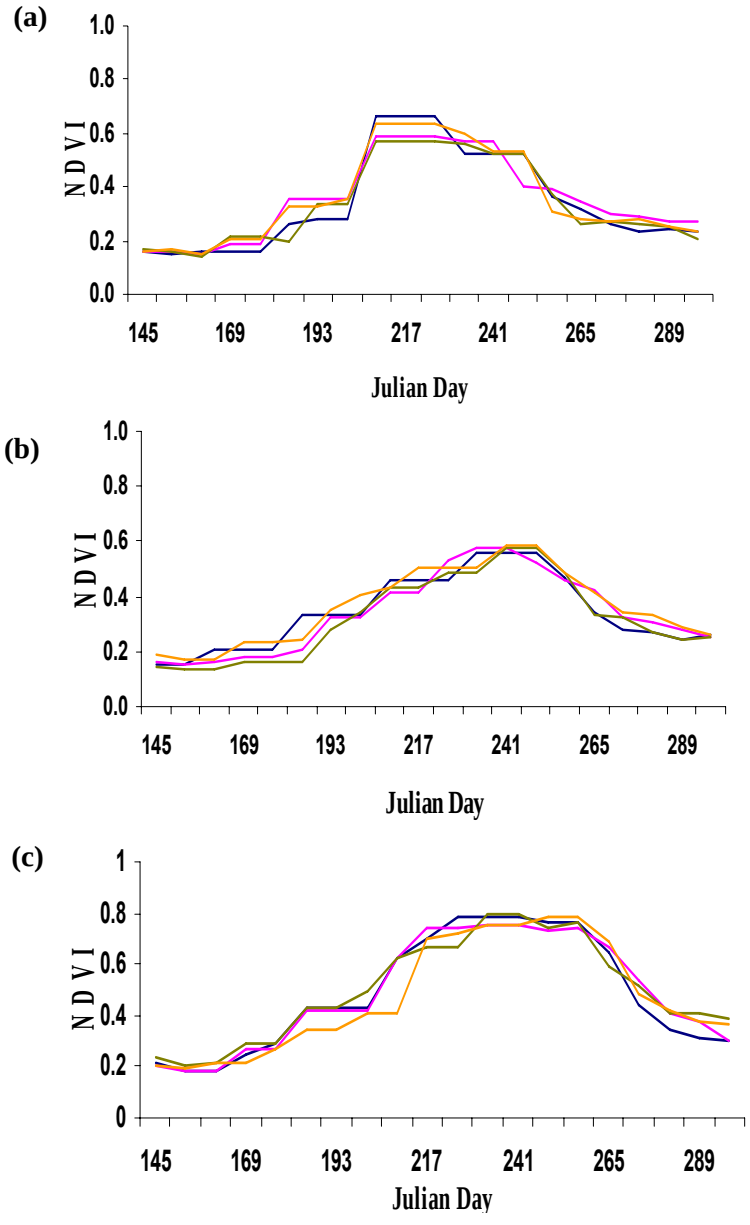

Figure 4-5: NDVI profiles of different prominent crops (a) Bajra, (b) Jowar and (c) Maize

Step 5: Comparison with Crop Statistics

The results were then compared with the district wise crop production statistics for the year 2003 available online at the official website of the Department of Agriculture, Rajasthan

(www.rajasthankrishi.gov.in). The area of production of Bajra, Jowar, Maize and other crops were compared. The relative deviation of the estimated from observed for each crop has been illustrated in Figure 4-7. The resultant crop cover map is presented in Figure 4-8.

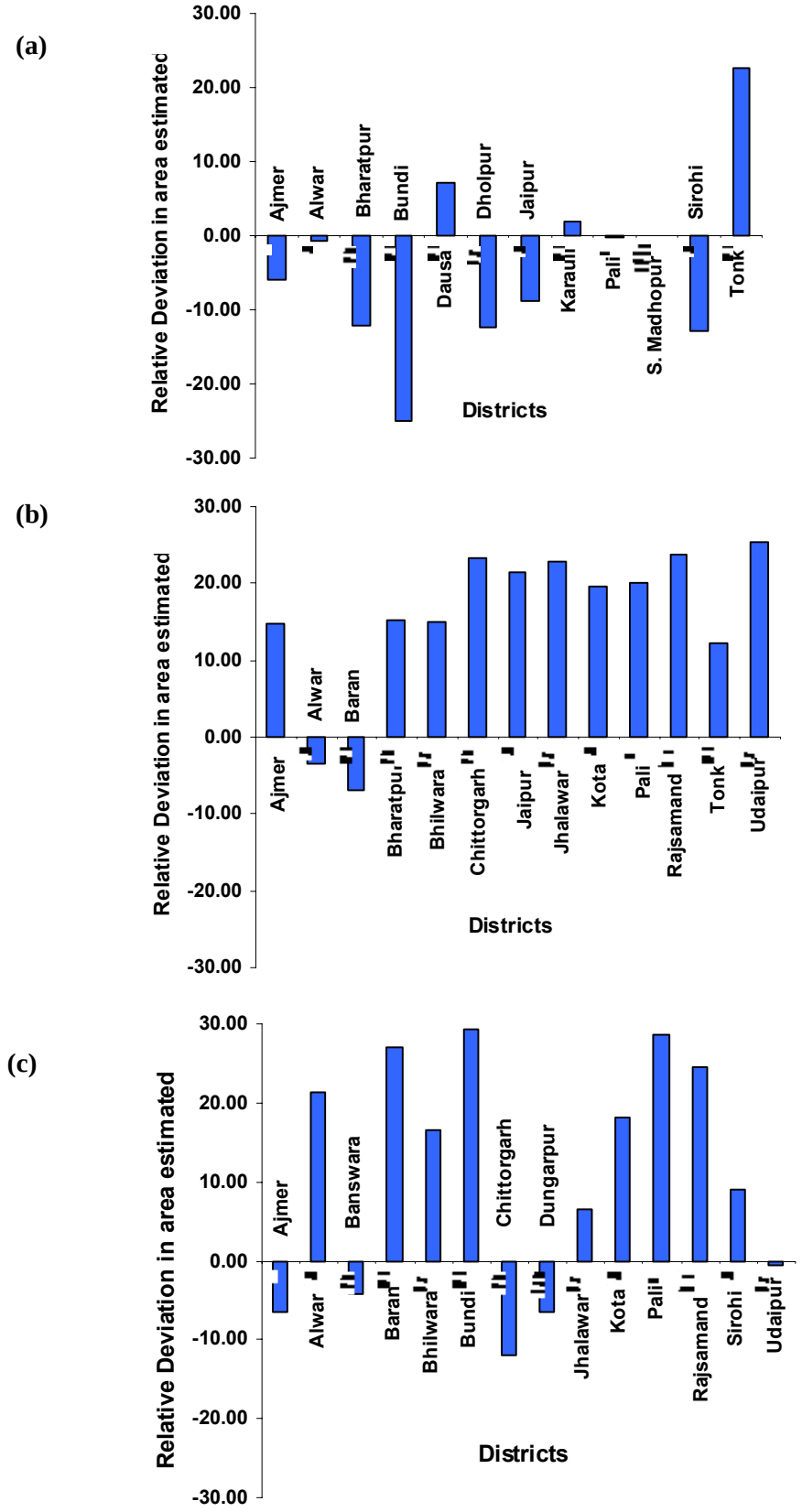

Figure 4-6: Relative Deviation of area estimated for a) Bajra b) Jowar and c) Maize

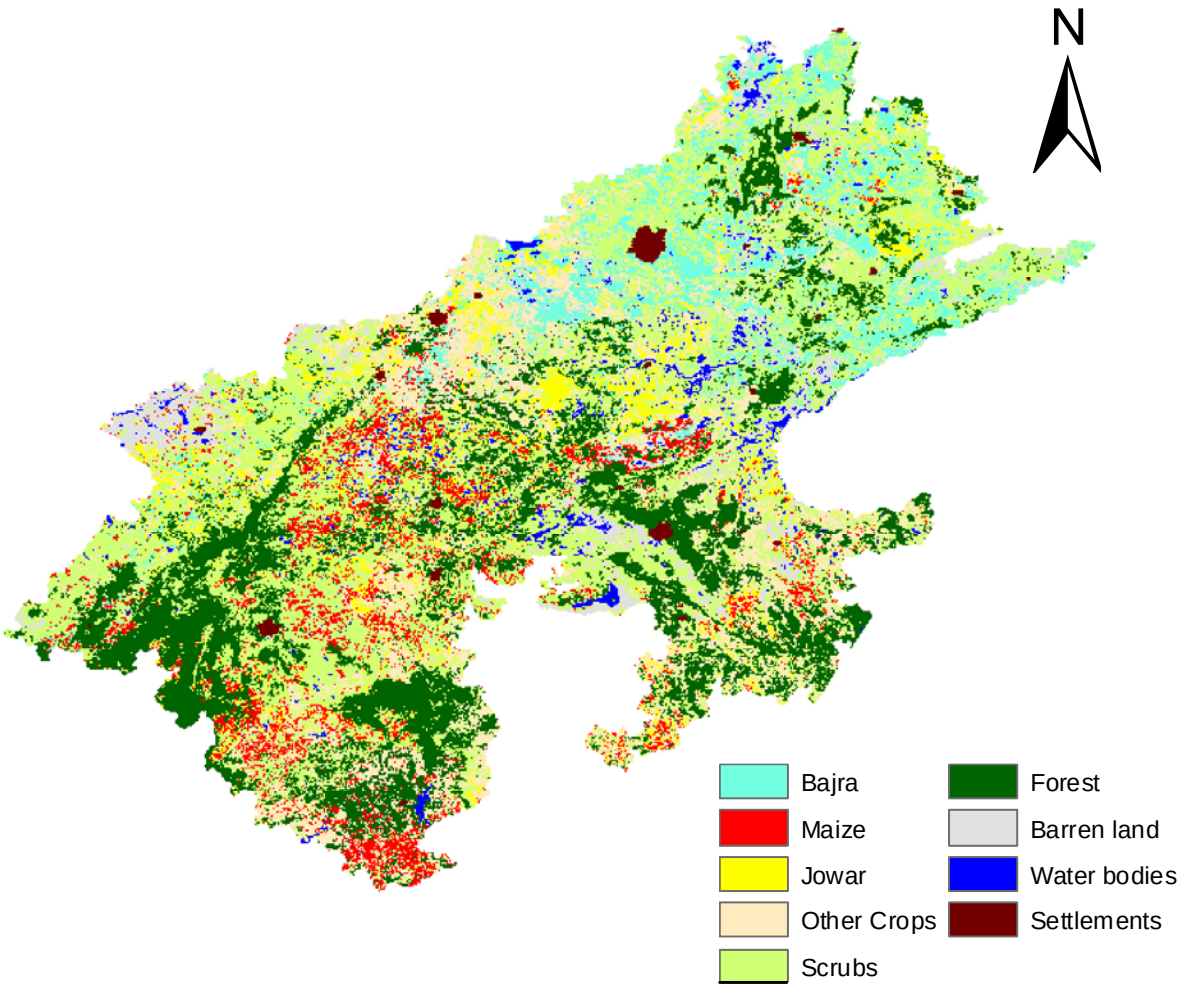

Figure 4-7: Crop Cover Map produced from NDVI profiles

4.2.2. Field Investigation for In-situ Soil Moisture Measurement

Fieldwork in the study is necessary to obtain in-situ soil moisture measurements and points for land-use classification. As the study concerns the prominent crops in the area in different phenological stages, the fieldwork was planned accordingly in two phases. The primary purpose was to collect in-situ soil moisture measurements during different growth stages of the crops. The first field visit was planned from August 5th to 15th 2007, when the crops are in their development stage and the second while they were in the last stage, form September 28th to October 8th.

Pre-field preparation

The study area consists of both semi arid and sub humid regions. So, two field sites, of 50 * 50 kms each, were demarcated nearby the main cities, Jaipur in semi-arid and Udaipur in sub-humid area. Twenty sampling grids, each of 1 km * 1km area, were planned in both the field sites. The sampling grids were decided based on the soil texture and crop type i.e. soil- crop variation.

Procedure

In each 1km * 1km soil sample grids, three to five sample points were taken and at each point, soil moisture was measured at four different depths to obtain profile values. At each point, the first reading

was taken on the surface and the succeeding readings at 15cm, 30cm and 45cm respectively by digging a trench as illustrated in Figure 4-9. In-situ soil moisture measurements were taken using the Theta probe. It gives the average reading at a depth of 5cm from the surface of measurement. For the first field, as there was no crop cover information available, sampling was done referring to the 1: 50,000 Survey of India topo-sheets of the two sites. Accessible sampling points were taken depending on the proximity to motorable roads. A total of 16 points were collected in this field. For the second field, the crop-use map generated using the first field land-use information was used with the NBSS soil texture map to obtain soil- crop units required for sampling. The sampling sites were taken within soil crop units of 1km^2 area. Three to five points from each sampling site were obtained to average out the heterogeneity of soil properties in the area. The sampling done is shown in Figure 4-10. A Total of 31 points were collected during the second field session. The details of the collected points and their measurements are given in Appendix 7.

Figure 4-8: Trench dug for in-situ soil moisture measurement at 45 cms

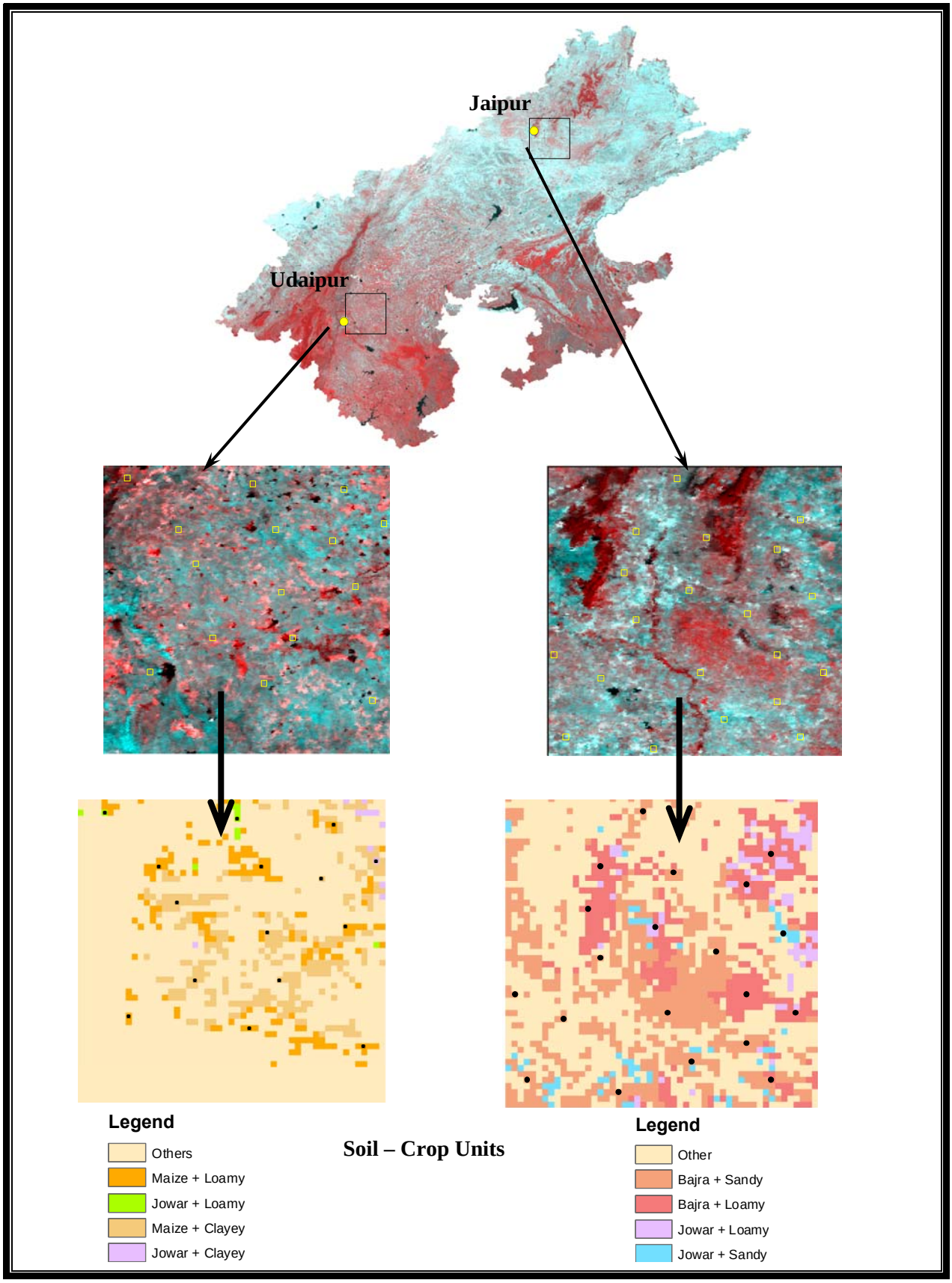

Figure 4-9: Sampling done for field investigation as per different soil – crop units

4.2.3. The Optical Remote Sensing Approach

The approach to estimate upper root zone soil moisture using optical remote sensing data was done by developing a relationship between an optical drought index and in situ soil moisture. The regression was done for 2007 and soil moisture was estimated for 2003 using the linear relationship developed. The estimated soil moisture was then compared with the simulated soil moisture from the Simple Water balance model. The detailed approach is presented in a flowchart in Figure 4-10.

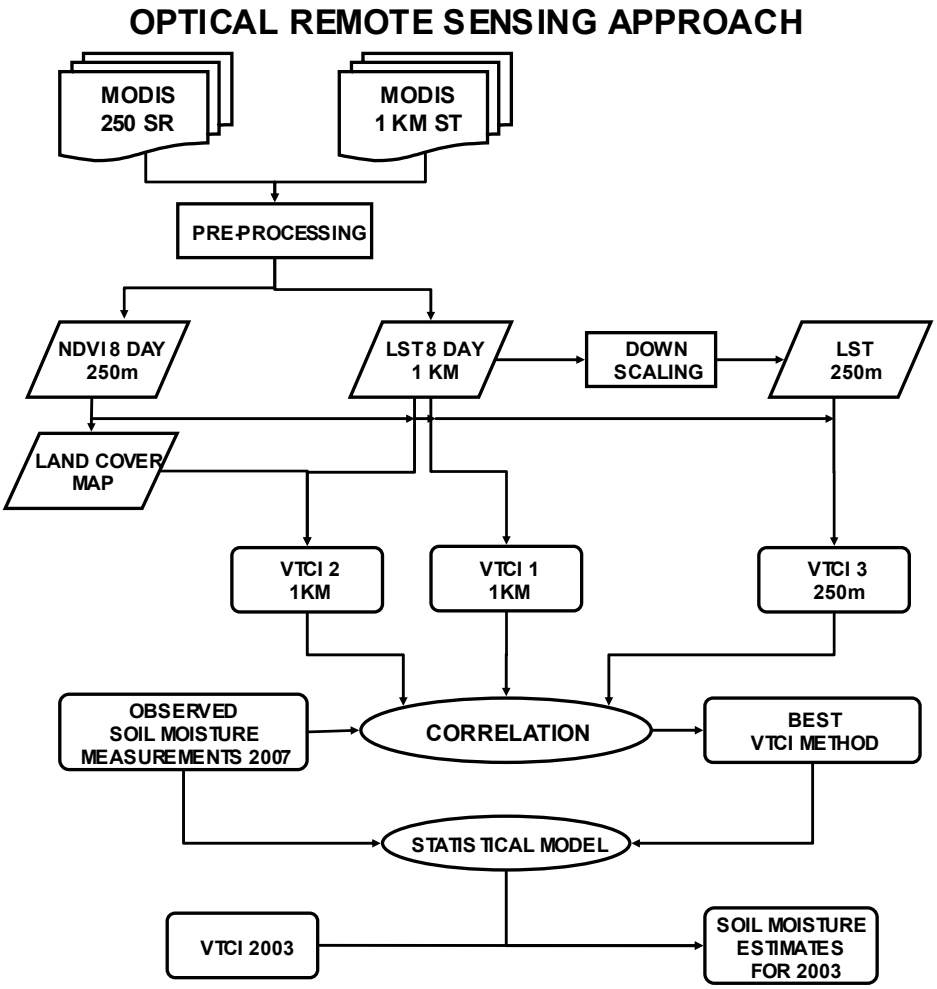

Figure 4-10: Flow chart for Optical remote sensing approach

Vegetation Temperature Condition Index (VTCI)

The Optical Remote Sensing Approach uses Vegetation Temperature Condition Index (VTCI). The approach integrates land surface reflectance and thermal properties. The index is derived by interpreting the NDVI- Ts space using NDVI from the 250mts surface reflectance and 1 km LST provided by MODIS. It is sensitive to NDVI and the LST variations for each NDVI value in the image. VTCI was originally developed for regional drought monitoring. Theoretically, it is an index to be considered only for areas large enough to provide a wide range of NDVI and surface soil moisture conditions. Our study area has both semi arid and sub humid regions, making it suitable for this index. The index was calculated on the images during the field work from Sept 28 to Oct 8. The MODIS image of Sept 30th (Julian Day 273) was used.

VTCI is, as per its definition, the ratio of LST differences among pixels with a specific NDVI value in the study area. The numerator is the difference between maximum LST of the total pixels and LST of each pixel and the denominator is the difference between maximum and minimum LSTs of the total pixels in the study area. The value of VTCI ranges from 0 to 1; 0 indicating dry pixels i.e. less moisture at root zone and 1 is that of very wet pixels, i.e. enough and more water available for plant growth.

The equation for the index is

$$VTCI = \frac{LST_{NDVIi\,\max} - LST_{NDVIi}}{LST_{NDVIi\,\max} - LST_{NDVIi\,\min}}$$

Where

$$LST_{NDVIi\,\max} = a + bNDVI_i$$

$$LST_{NDVIi\,\min} = a' + b'NDVI_i$$

Where

$LST_{NDVIimax}$ is the maximum LST among pixels having same $NDVI_i$ value in the area

$LST_{NDVIi\,\min}$ is the minimum LST among pixels having same $NDVI_i$ value in the area

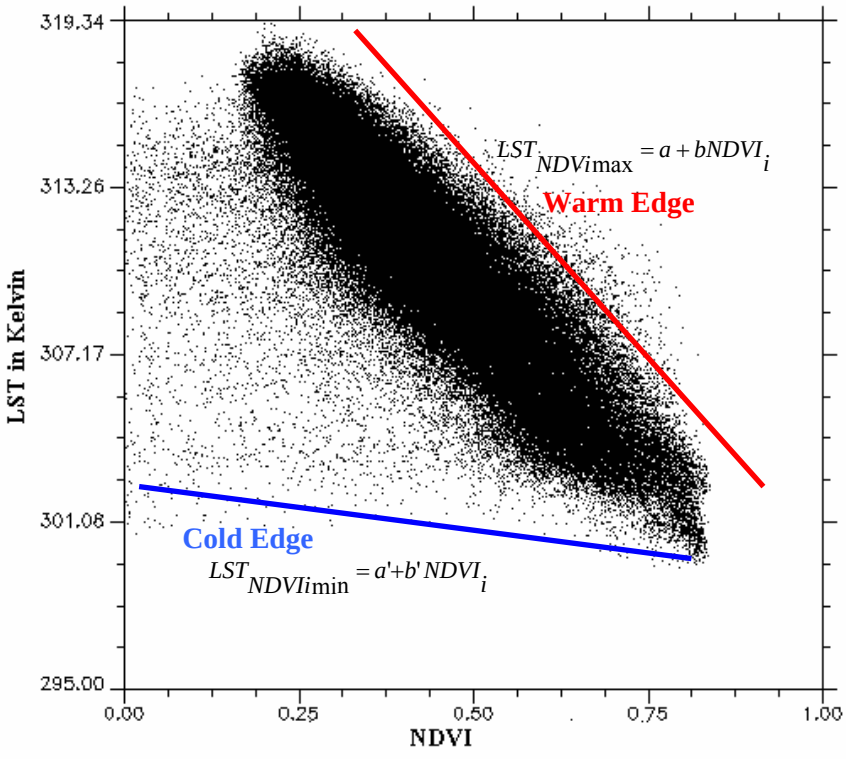

Figure 4-11: NDVI-Ts Space for Julian Day 273

In general, the coefficients a, b, a' and b' are estimated from the scatter plot of LST and NDVI (as illustrated in (Figure 4-11) in the area, i.e. the Ts/NDVI space. LST_{max} can be regarded as ' the warm edge where there is less soil moisture availability and plants are under dry conditions and LST_{min} can

be regarded as the 'cold edge' where there is no water restriction for the plants. Coefficient a, b, a' and b' can be estimated from an area large enough where soil moisture at surface layer should span from wilting point to field capacity at pixel level. The shape of the scatter plot is normally triangular at a regional scale (Gillies & Carlson 1995) and (Wang et al 2001), if the study area is large enough to provide a wide range of NDVI and surface moisture conditions. To determine the warm edge and cold edge, the NDVI and LST were plotted using the 2D scatter plot option in ENVI. The points were then converted into ASCII format and imported into Microsoft Access. The maximum and minimum LST of pixels with NDVI values at every 0.01 interval were queried out. The NDVI values and the corresponding LST_{max} and LST_{min} are again plotted. The line joining the LST_{max} values of all the NDVI values are regarded as the warm edge and the equation of this line provides the intercept, a and slope b to determine $LST_{NDVI\max}$. Similarly, the line joining the LST_{min} values of all the NDVI values are regarded as the cold edge and the equation of the line gives the 'a' and 'b' to determine $LST_{NDVI\min}$.

Literature reviewed about VTCI (Parida 2006, Wang et al 2001)have aggregated NDVI of 250 m to 1 km, the spatial resolution of LST thereby causing loss of information. The advantage of NDVI's higher resolution can be exploited only if the LST is downscaled to 250mts. This possibility was investigated using the Disaggregation Procedure for radiometric surface temperature (DISTRAD) devised by Kustas et al (Kustas et al 2003). And also, the objective of the thesis is to use VTCI to estimate soil moisture in agriculture fields. So there is an unexploited possibility that the warm edge and cold edge can be obtained, taking into consideration only the agricultural fields than plotting the whole image. Thus, three methods to obtain the warm edge and cold edge to calculate VTCI were tried out.

1st Method:

In this method NDVI is aggregated from its 250 mts spatial resolution to the resolution of the LST product, 1km. The whole of the1km NDVI image is then plotted with the LST image to obtain the scatter plot. All the pixels in the study area are considered and the resultant VTCI image is of 1km spatial resolution.

2nd Method:

In the second method, the agricultural pixels are extracted from the aggregated NDVI and corresponding LST images and they alone are taken for plotting. The resultant VTCI is of 1 km but reflects the condition of the agriculture land alone.

3rd method:

The third method applies a downscaling method on the 1km LST image to bring it to the spatial resolution of the NDVI image, 250mts. The DisTrad Technique is done by obtaining a relationship between aggregated NDVI and LST of 1km, and applying the relation on NDVI of 250 metres to obtain LST of 250 meters. The procedure was implemented as given below.

Step 1: Removal of cloudy pixels.

Pixels with cloud effect were also removed because they can act as outliers in the relation. The image of Julian Day 265 has pixels with cloud effect giving LST as 0 K which were masked out.

Step 2: NDVI is aggregated to 1km from its existing 250 meters to obtain the mean NDVI for 1 km.

Step 3: The next step is to understand the heterogeneity of each aggregated NDVI pixel so that uniform pixels can be extracted to build a true relation. In each aggregated NDVI pixel, there are 16 NDVI pixels of 250mts. The coefficient of variance of the 16 pixels in each 1 km aggregated NDVI pixel is calculated using block statistics. The lower the coefficient, the higher will be the uniformity or homogeneity.
Coefficient of Variance = (Standard Deviation / Mean)* 100

Step 4: After recognising the most uniform pixels in the image, 25% of those belonging to each range of NDVI were extracted. For this purpose, the aggregated NDVI was classified as given below.

- Sparse Canopy (0 < NDVI < 0.2)
- Moderate Canopy (0.2< NDVI < 0.5)
- Fully vegetated (0.5 < NDVI)

From the total pixels in each of these classes, 25% of the most uniform, i.e. with the 25% of pixels in each class which have the least coefficient of variance were selected.

Step 5: The aggregated NDVI and LST values of the uniform pixels were then extracted so that they can be plotted against each other to obtain the relationship.

Step 6: The extracted NDVI and LST of 1km of the uniform pixels were plotted against each other. They were found to share a clear inverse linear relationship except for the water pixels which have low NDVI and low LST. So downscaling of LST using NDVI is not possible for the water pixels.

Step 7: Using the regressed relationship, with NDVI of 250 mts as the independent variable, and LST as the dependent, LST was downscaled to 250 mts. The regression equation developed to downscale 1Km LST to 250m and its coefficient of determination is given in Figure 4-12.Figure 4-13 illustrates the downscaled image and the graph in Figure 4-14 presents the one to one plot obtained between the LST at 1 km and LST downscaled to 250mts.

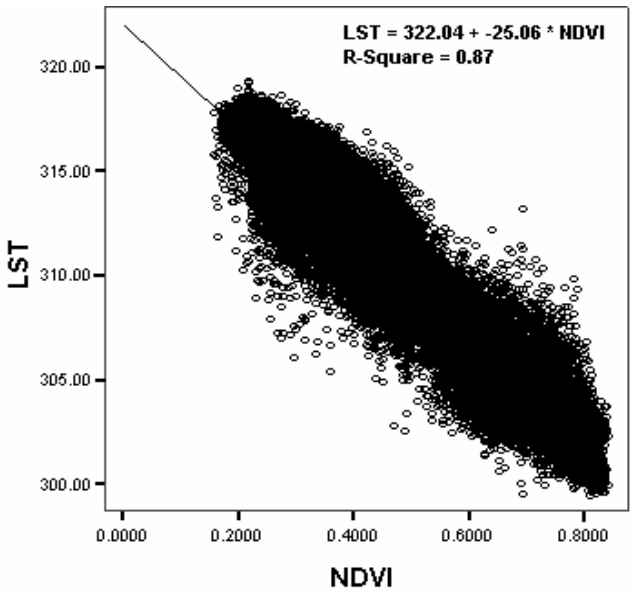

Figure 4-12: NDVI-LST plot of uniform pixels

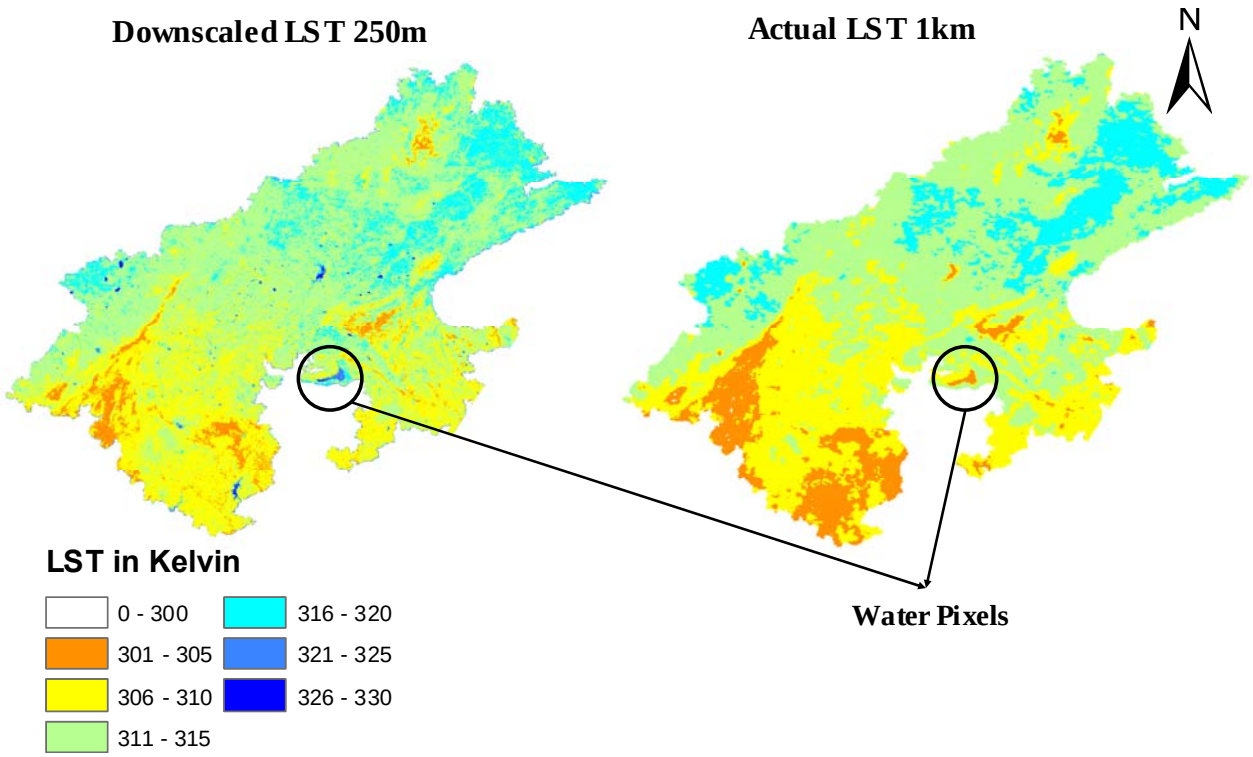

Figure 4-13: LST images, Actual LST and Downscaled LST for JD 273

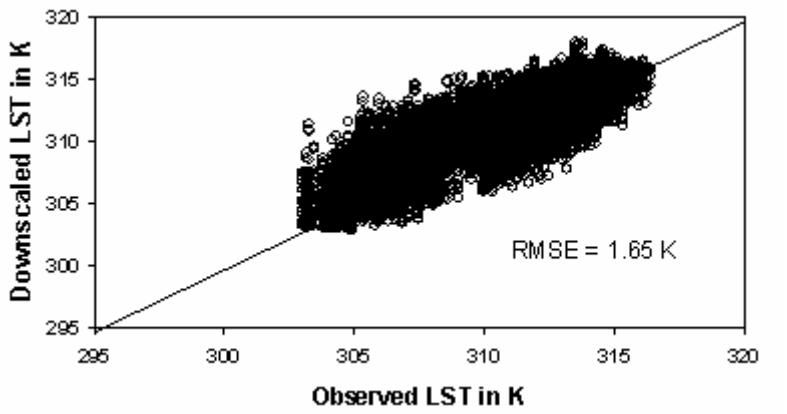

Figure 4-14: Plot of Observed LST at 1km and Downscaled LST at 250mts

The warm edge and cold edge for VTCI were found from the NDVI and LST plot of the uniform pixels. The equations for LST min and LSTmax, thus obtained were applied on the NDVI and the downscaled LST to obtain VTCI at 250mts.

Linear Regression Analysis between VTCI & In situ Soil Moisture

The best VTCI method was identified based on their ability to infer soil moisture status. VTCI obtained from different methods were correlated against in-situ soil moisture and best VTCI was identified based on statistical inferences. The regression equation thus obtained using the best VTCI and in-situ soil moisture was used to inverse estimate average soil moisture in the top 50cms. Estimation was done for the year 2003. The validation was not possible because of lack of in-situ soil

moisture measurements. So the assessment was done with weekly soil moisture simulated from a GIS based simple water balance model.

4.2.4. The Passive Microwave Remote Sensing Approach

For assessment of soil moisture using passive microwave remote sense data, two parameters were used namely horizontally polarised brightness temperature (T_{BH}) and the polarisation Difference (PD). Data of the frequencies, 6.9 GHz and 36.5 GHz were used for analysis. The parameters were used as illustrated in the flowchart in Figure 4-15.

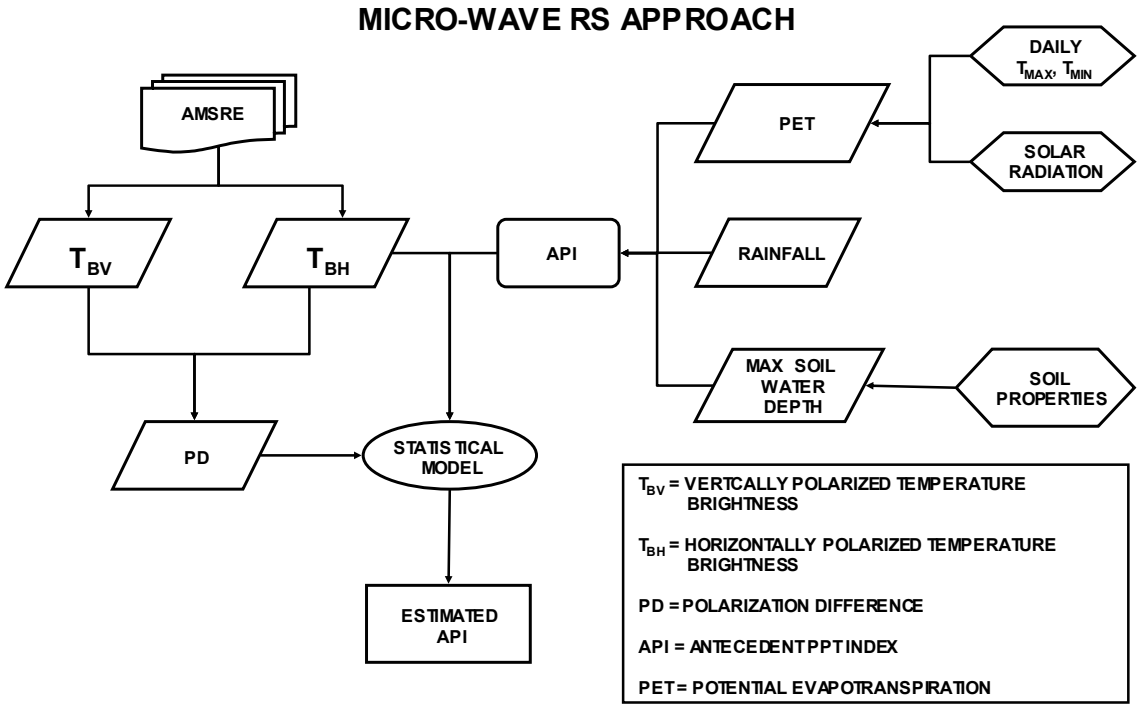

Figure 4-15: Flowchart for Microwave Remote Sensing Approach

Antecedent Precipitation Index

API is a daily measure of soil wetness computed using precipitation, potential Evapotranspiration and soil properties. It is commonly used as a substitute for in-situ soil moisture measurements when there is limited data (Teng et al 1993). API is computed using the model developed by Choudhury and Blanchard (Choudhury & Blanchard 1983). The same has been used by others in their respective study areas (Choudhury & Golus 1988, Teng et al 1993). So the validity of the model in the present study area is assumed.

$$API_j = K_j (API_{j-1} + P_j) \qquad \textbf{Equation 4-1}$$

Where,

API_j = API value for the j^{th} day

API_{j-1} = API value at the end of the previous day

P_j = Precipitation on the j^{th} day in mm

and

$$K_j = e^{\left(-E_j / W_m\right)} \qquad \textbf{Equation 4-2}$$

Where,

K_j = recession coefficient for the j^{th} day (dimensionless)

E_j = potential evapotranspiration in mm occurring on the j^{th} day

W_m = Maximum depth of soil water in mm available for Evapotranspiration.

The potential evapo-transpiration was computed by Jensen Haise Method(Jensen & Haise 1963). W_m was computed as the product of Available Water Capacity and soil depth. All the inputs were taken same as for the simple water balance model. API was computed from June 1st to Nov 30th. As the starting date was before the beginning of the monsoon, which is by mid - June, the initial value of API was taken as zero. It has been noted that any error in the selected initial value of API decreases with time and becomes insignificant after a few days (Teng et al 1993).

Polarisation Difference

Polarisation Difference is the difference between the vertically polarised brightness temperature (T_{BV}) and horizontally polarised brightness temperature (T_{BH}).

$$PD = T_{BV} - T_{BH} \qquad \textbf{Equation 4-3}$$

Prigent et al (Prigent et al 2005) has reviewed previous works on relationship of passive microwave data with soil moisture. It has been found that T_{BH} shares a negative linear correlation with soil moisture and PD, a positive linear relationship.

API estimation from PD and T_{BH}

Estimation of API solely from microwave data was attempted by regression analysis. This is desirable because of the high temporal resolution of microwave data. As the microwave T_{BH} is of 25 km resolution and of alternate day temporal resolution, the calculated API was aggregated to 25kms and averaged for 2 days. The alternate day API and T_{BH} was subjected to regression analysis, followed by the regression of the resultant slope and intercept with Polarisation Difference.

The regression between T_{BH} and API gives equation of the form

$$T_{BH} = a + b\ API \qquad (1)$$

The regression between the slope/intercept of the T_{BH}-API regression and Polarisation Difference gives

$$b = a_1 + b_1\ PD \qquad (2)$$

Substituting (2) in (1)

$$API = (T_{BH} - a) / a_1 + b_1\ PD \qquad \textbf{Equation 4-4}$$

This resultant equation of the regression analysis performed can be used to inverse estimate API, thereby obtaining a daily soil moisture measure from microwave data alone.

4.2.5. The GIS based Simple Water Balance Model Approach

The GIS based simple water balance model applied here is a soil water crop model which quantifies soil moisture for rain fed cropping areas and assesses their spatial variation (Patel et al 2006).The soil water crop model applied here is a single layer model that can be used for large scale applications in a simplified form. It can be used for both rain fed and irrigated crops as per the criteria given by Thornthwaite and Mather (Thornthwaite & Mather 1955). The model furnishes low accuracy results which are valid only for large scale applications. So it should be used only when particular accuracy is not required and when calibration is impossible because of lack of data.

As the requirement of this model in the thesis is as a modest substitute of in situ soil moisture to analyse the soil moisture estimated from optical remote sensed data, available in an interval of 8 days, weekly time series has been considered for model simulation. The model is a grid based model and the grid size was adopted as 5 km because of the difference in the spatial resolutions of the inputs. The flowchart in Figure 4-16 illustrates how the model works. The methods adopted to compute each of the inputs are tabulated in the Table 4-3.

The input variables required by the model are

1. Effective rainfall (ERF_t in mm)
2. Maximum crop Evapotranspiration (ETm_t in mm)
3. Maximum Water capacity (U in mm)
4. Initial Soil Moisture (SM_{t1} in mm)

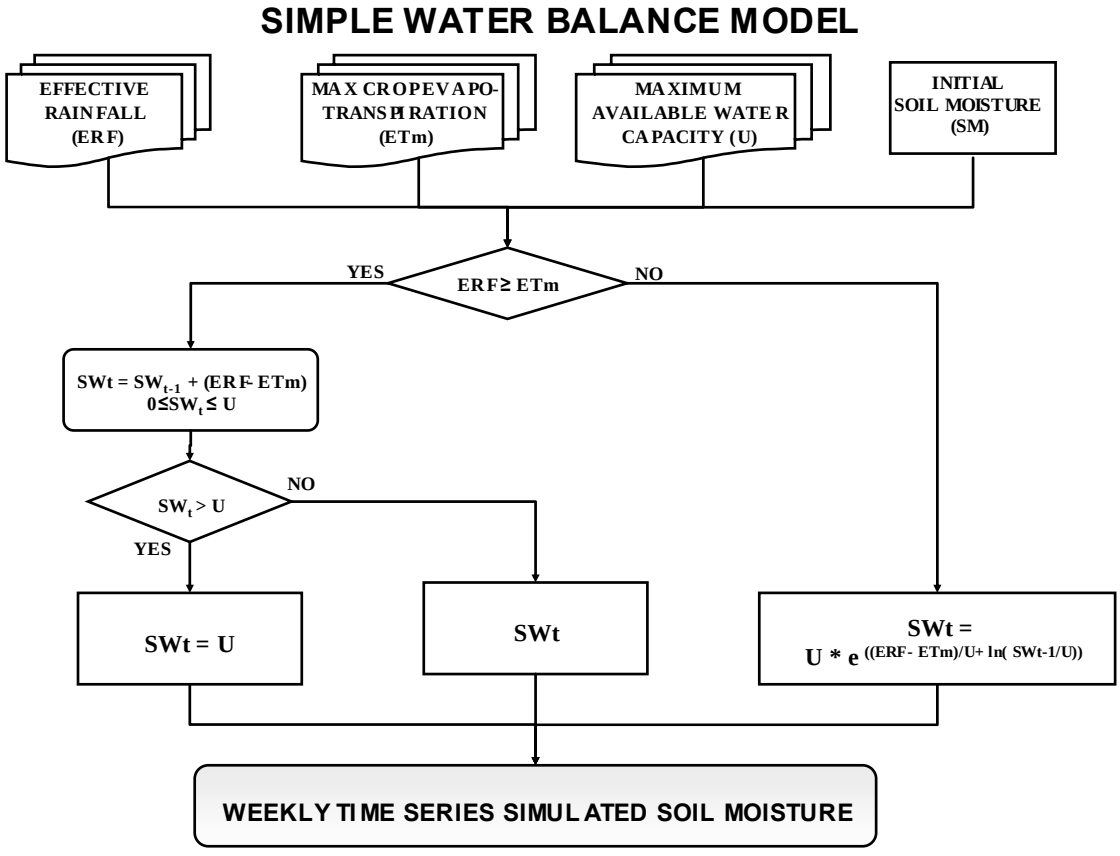

Figure 4-16: Flowchart for Simple Water Balance Model

The model considers the time in progress in 2 probable categories, dry period and wet period with reference to the first two input time series, ERF_t and ETM_t When effective rainfall is more than or equal to crop maximum evapo-transpiration, the soil stores water and recharges itself partially or totally and the period is termed as wet period. But when the effective rainfall is lesser, the soil transfers water to the crops and becomes dry, making it the dry period.

Model Variable	***Calculation parameters***	***Calculation Methods***	***Inputs required***
Effective Rainfall, ERF (mm)	Rainfall	Point measurement interpolated by Modified Inverse Distance Weighted Method	Rainfall
	Runoff	SCS Curve Method(USDA 1972)	Daily rainfall, Land use map, Soil texture map, Soil depth map, Soil particle size map, Soil drainage map.
Maximum Evapo transpiration, ETM (mm)	Potential Evapo transpiration, PET (mm)	Jensen Haise Method (Jensen & Haise 1963)	Maximum & Minimum Temperature, Solar Radiation
	Crop Coefficient, Kc (dimensionless)	Literature	
Maximum Water Capacity, U (mm)	Field Capacity FC (% Vol)	Soil Plant Air Water Version 6.02.75 (Saxton & Rawls 2006)	Soil Texture
	Rooting Depth RD(mm)	Borg & Grims Model (1986)(Borg & Grimes 1986)	Maximum RD (mm), No. of days after sowing when the crops attain maximum RD.

Table 4-3 : Inputs to the SWBM model and their computational methods

For the dry period, the simple water balance equation to simulate weekly soil water content is given by Thornthwaite & Mather (Thornthwaite & Mather 1955).

$$\frac{SM_t}{U} = e^{\left[\frac{(ERF_t - ET_m)}{U} + \frac{\ln SM_{t-1}}{U}\right]}$$

Equation 4-5

Where,

SM_t is the soil moisture content at a time step i.e. a week in this simulation.

SM_{t-1} is the soil moisture at the time step t-1, i.e. the previous week.

U is the maximum water capacity available to the plants during the week.

ERF_t is the effective rainfall during the week.

ET_m is the maximum evapo-transpiration in the week.

For the wet periods, the model is based on a hypothesis that the soil water zone is considered to be like a reservoir from which the crops can take a part of the stored water through their root systems. The hypothesis is justified because of the presence of the so called irreducible water in the soil contained by capillary and absorption forces. This soil water zone is characterised by the third input, U.

$$SM_t = SM_{t-1} + (ERF_t - ET_m) \qquad 0 \le SM_{t-1} \ge U$$ **Equation 4-6**

If SM_t is greater than U, then, the difference $SM_t - U$ is taken as surplus in an agricultural point of view. It is assumed to pass to deeper soil depths as deep percolation.

ERF_t, Effective Rainfall

Effective Rainfall represents the supply part of the water balance system. It is the net precipitation that enters the soil which is an aggregate effect of surface losses namely direct runoff and evaporation losses as interception (Alemaw & Chaoka 2003). The interception losses were not incorporated, assuming it is negligible. The spatio-temporal patterns of effective rainfall are given in Appendix 4.

$$ERF_t = RF_t - Q_t$$ **Equation 4-7**

Where,
ERF_t = Effective Rainfall for the week in mm
RF_t = Total Rainfall received in the week in mm
Q_t = Total Runoff occurred through the week in mm

Weekly Rainfall, RF_t:

The spatially interpolated weekly sum of daily rainfall was used to calculate the effective rainfall for the week. The spatio-temporal patterns of effective rainfall are given in Appendix 2.

Weekly Runoff, Q_t:

Daily Runoff is estimated using the Soil Conservation Service (USDA 1972), SCS Curve Number method (Ministry of Agriculture 1972, Sahu 1990, USDA 1972). The model is based on the water balance equation and two fundamental hypotheses; the first one equates the ratio of the actual amount of direct surface runoff (Q) to the total rainfall (P) to the ratio of the amount of actual infiltration (F) to the amount of potential maximum retention (S) and the second one relates the initial abstraction (Ia) to the potential maximum retention (Mishra & Singh 2003). The model gives daily runoff as output. So it was crucial to obtain daily values and sum them for a week. The final model derived from these hypotheses requires daily precipitation, P and the retention parameter S as the variables.

$$Q_t = \frac{(P_t - 0.2S_t)^2}{P - 0.8S_t} \qquad \text{if} \quad R > 0.2S$$

$$Q_t = 0 \qquad \text{if} \quad R > 0.2S$$ **Equation 4-8**

Where,

Q_t = Daily Runoff in mm

P_t = Daily Precipitation in mm

S_t = Potential Maximum Retention.

$$S_t = \frac{25400}{CN} - 254 \qquad \textbf{Equation 4-9}$$

The potential maximum retention is computed using the Curve Number (CN) which is a dimensionless quantity that depends on major surface characteristics such as soil type, vegetation cover, land use/ treatment, hydrologic condition, antecedent moisture condition and climate. The procedure adopted to calculate CN is explained in Appendix 3.

ETM_t, Maximum Evapotranspiration (in mm)

This variable is determined by the crop coefficient approach whereby the effect of the various weather conditions are incorporated into ET_o and the crop characteristics into the K_c coefficient (Doorenboos & Pruitt 1977). It indicates together, the amount of water evaporated from the soil and the amount transpired for the crop's survival. Its temporal variation depends on the climate and the phenological stage of the crop.

$$ETM_t = PET_t * Kc_t \qquad \textbf{Equation 4-10}$$

Where,

ETM_t = Maximum Evapotranspiration for the week in mm

PET_t =Total Potential Evapotranspiration for the week in mm

Kc = Average Crop Coefficient for the week

Weekly Potential Evapotranspiration, PET_t:

Daily potential evapotranspiration is estimated using Jensen Haise Method which accounts for the maximum and minimum temperature in a day and the average radiation received from the sun in a day (Jensen & Haise 1963).The Jensen & Haise Equation for the calculation of PET is as follows

$$ET_o = \left(\frac{Rs}{2.45} * \left(\left(0.025 * \left(\frac{T_{\max} + T_{\min}}{2} \right) \right) + 0.08 \right) \right) \qquad \textbf{Equation 4-11}$$

Where,

Rs = Daily solar radiation (MJ/m2/day)

$T_{\max}$ = Maximum daily air temperature (^oC)

$T_{\min}$ = Minimum daily air temperature (^oC)

The daily PET thus obtained were summed up according to the meteorological week calendar to obtain the weekly potential evapotranspiration. The spatio –temporal patterns of PET thus obtained are given in Appendix 6.

Average Crop Coefficient for the week, Kc:

Crop Coefficients incorporates the crop characteristics and the averaged effects of evaporation from soil. It depends mainly on the crop growth stages. FAO technical paper 24 (Doorenboos & Pruitt 1977) gives generic Kc values for specific crops. The localised values of those for North India were found in various literature. The crop growth stages were taken as initial, crop development, mid and

late season. The length of these seasons for the relevant crops, Pearl Millet, Sorghum & Maize and their corresponding Kcs are tabulated in the Appendix 1.

U, Maximum Water capacity (in mm)

U is a measure of the soil – crop characteristics in the grid. It is the amount of water that the soil can hold, i.e. within the depth of its roots with reference to a unit surface. The temporal variation of this parameter is also a function of the crop phenology.

F (soil properties):

This function indicates the maximum water capacity of the soil. It is the water content of the soil where all free water has been drained from the soil through gravity. It is the water content, (%v), of the soil matrix approximating the water content of a saturated soil that has been allowed to freely drain. The values adopted here have been estimated as a hydraulic tension of 33 kPa (0.33 Bar) and is dependant only on the soil texture and unaffected by salinity or gravel. The Field Capacity values adopted fro each soil texture are given Appendix 4.

Rooting Depth (mm):

The variation of rooting depth for the crops were predicted using an empirical model given by Borg & Grimes (Borg & Grimes 1986). The crop specific rooting depth was calculated for each day after sowing and averaged to obtain the weekly soil moisture.

$$RD_t = RDM\left[0.5 + 0.5\sin\left(3.03DAS / DTM - 1.47\right)\right] \qquad \textbf{Equation 4-12}$$

Where,

RD_t = Rooting Depth for the day.

RDM = Maximum rooting depth (mm).

DAS = No. of days after sowing.

DTM = Day on which maximum rooting depth is achieved.

4.2.6. Methodology for Comparison of Various Approaches with SWBM

Lack of in-situ soil moisture restricts the validation of the approaches adopted. So the performance of the optical and passive microwave approaches were analysed on the basis of comparison with the simulated output from the simple water balance model.

Optical Remote Sensing Approach with SWBM

The soil moisture estimated from VTCI and the weekly simulated soil moisture were statistically compared. For the comparison VTCI was aggregated 5 *5 km. Eighteen grids of 5 * 5 km^2 area, where the prominent crops of the study area, Pearl millet, Maize and Sorghum are dominant were selected for the comparison. Figure 4-17 illustrates the crop dominant grids with the crop cover presented in the background.

Passive Microwave Remote Sensing approach with SWBM

For the microwave approach, T_{BH} and PD of both 6.9 GHz and 36.5 GHz were statistically analysed with the simulated soil moisture from SWBM. The simulated soil moisture had to be spatially aggregated to 25 km. The microwave parameters were temporally averaged to match the weekly

resolution of the simulated soil moisture. Two sites, one in the semi – arid region and one in sub – humid region (as illustrated in Figure 4-18) were taken for the analysis. The average values of the variables for the selected sites were obtained using 3 * 3, 5 *5 km windows and also pixel by pixel. The analysis was aimed to find out the variation of soil moisture indicated by the T_{BH} and PD from different frequencies in the different climatic region at different window sizes

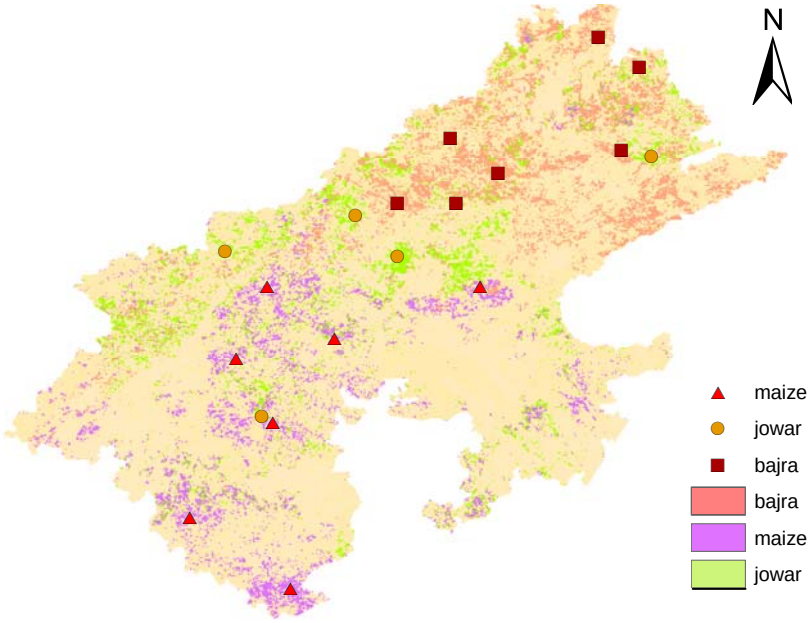

Figure 4-17: Crop dominant sites taken for analysis of optical approach with simulated soil moisture

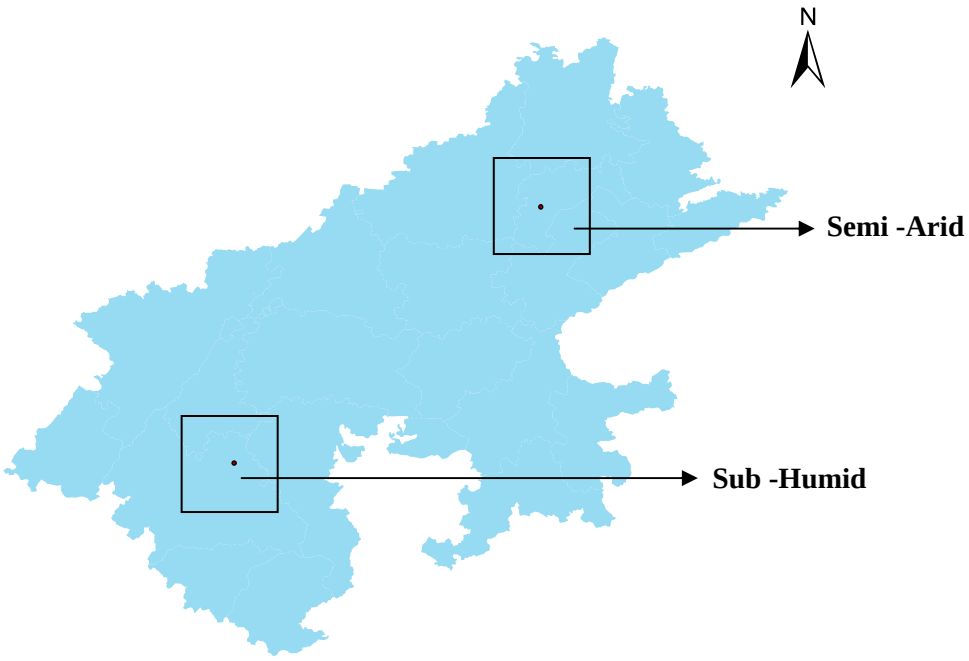

Figure 4-18: Sites chosen for analysis of microwave approach with simulated soil moisture

5. Results and Discussion

The present study attempts to assess the soil moisture status at the upper root zone layers in the prominent crops (Pearl Millet, Sorghum and Maize) in Eastern Rajasthan using optical and passive microwave remote sensing. Statistical inference has been made to exploit the use of optical and microwave measures to derive soil moisture status. Due to difficulty involved in obtaining in-situ soil moisture observations, effort is made to investigate sensitivity of optical and microwave parameters to simulated soil moisture from a GIS based Simple Water Balance Model (SWBM). The database creation and processing was done for the whole of Eastern Rajasthan and the analysis was done on specific sites where Bajra, Jowar & Maize are dominant. This chapter summarizes the results obtained in accordance with the objectives.

5.1. The Optical Remote Sensing Approach

In the optical approach, Vegetation Temperature Condition Index (VTCI) developed from the NDVI – Ts space from Terra MODIS optical satellite data was used to estimate soil moisture in the upper root zone after regression analysis with in-situ soil moisture for 2007. Soil moisture for 2003 Khariff season was estimated from the linear relationship obtained.

5.1.1. Vegetation Temperature Condition Index (VTCI) for 2007

The VTCI is computed based on interpretation of NDVI – Ts space derived from the MODIS observations, surface reflectance at 250 mts and Land Surface Temperature at 1 km. The MODIS images corresponding to the field campaign period (August 5th to 15th (JD 217) and September 28th to October 8th (JD 273)) were tried to be obtained. The Khariff cropping season in India goes in rhythm with the south –west monsoon which gives showers in the months of June, July and August. Persistent clouds are observed during this period. As optical data cannot penetrate clouds, their use during the Khariff season is limited. So, the 8 day composite LST images, which is highly sensitive to cloud cover, was not available for the JDs 217. The cloud cover recedes only by mid September. So images during the second field had minimum cloud interference. The MODIS products for JD 273 was successfully downloaded and processed. The resultant, VTCI from the three methods are discussed below.

Warm edge and Cold edge using different methods

The NDVI – Ts space of the 1st method was triangular in shape. This showed that the study area has a large range of soil moisture conditions which varies from wilting point to field capacity at pixel level. The LST at the lower NDVI side of the triangle range from 298K to 320 K which indicates vegetation of the same vigour with the same NDVI value has different conditions of soil moisture. The lesser LST denotes enough soil moisture and higher LST shows water stress. The scatter plots of Method 1 & 2 (illustrated in Figure 5-1(a) and Figure 5-1(b)) differ in the trend of the LST_{min} which implies that there is no agricultural land which has low NDVI and low LST. The agricultural land which had low soil moisture showing high LST are mainly concentrated on the left end of the scatter plot where as

those crops which had enough soil moisture, as indicated by low LST are fully vegetated with high NDVI and are observed to be accumulated in the right end corner of the scatter plot.

For method 3, the warm edge and cold edge to compute VTCI were taken from the scatter plot of uniform pixels. But as can be seen from Figure 5-1(c), by generating the uniform pixels, the triangular distribution has been lost. The pixels are concentrated on an inverse linear pattern, limiting the variation of range of LST_{min} for low NDVI pixels which is not recommended for VTCI inference. This may be because the water pixels, which usually contribute to the low NDVI and low LST that accumulate in the lower left corner of the NDVI- Ts space, have been removed prior to the extraction of uniform or homogeneous pixels, from the scatter plot of which, the warm edge and cold edge have been computed.

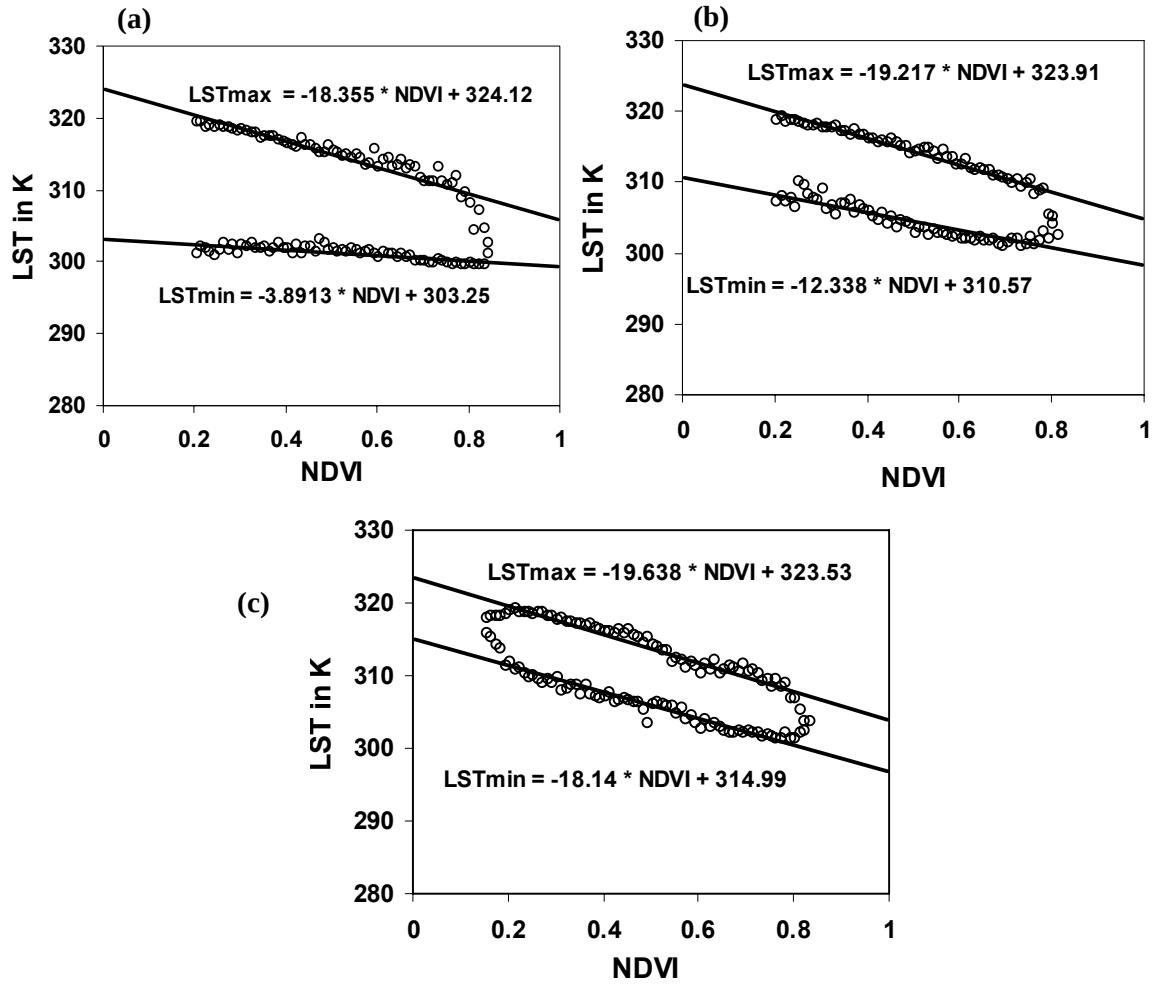

Figure 5-1: Warm Edge & Cold Edge for VTCI from (a) Method 1 (b) Method 2 and (c) Method 3 f or Julian Day 273

Spatial Variation in VTCI using different methods

The VTCI values, in theory, can range from 0 to 1, the higher the VTCI value, wetter the pixel. Figure 5-2 illustrates the relative difference in the spatial pattern of VTCI as obtained using the 3 different methods for JD 273 of the year 2007. The VTCI from Method 1 showed a normal variation as expected with values as low as 0.06 for barren land and a maximum of 1 for water pixels for JD 273. This variation was less in the output of method 2 where the VTCI values ranged from 0.23 to 0.81 for

JD 273. It can be deduced that the higher value of LST_{min} i.e. the cold edge, is responsible for the smaller variation.

Before computing VTCI by method 3, LST was downscaled to 250 mts. The NDVI and LST of the uniform pixels shared a linear relationship with a coefficient of determination of 0.8 for JD 273. Pixels of water bodies had very low, mostly negative values for NDVI. Their LST also being low, were not considered for the scatter plot as an inverse linear relationship like other land use cannot be expected from them. The LST downscaling was thus done successfully but VTCI, which solely depends on the NDVI –Ts spatial relationship did not give satisfactory results. VTCI was computed on the 250 mts NDVI and the downscaled 250 mts LST image. The linear relationship established between NDVI and LST during the downscaling procedure again lead to a compression of the VTCI value range. The computed VTCI belonged to a very narrow range of 0.31 to 0.67. VTCI, being the difference in the maximum and minimum LST isolines, the compressed values are theoretically justified.

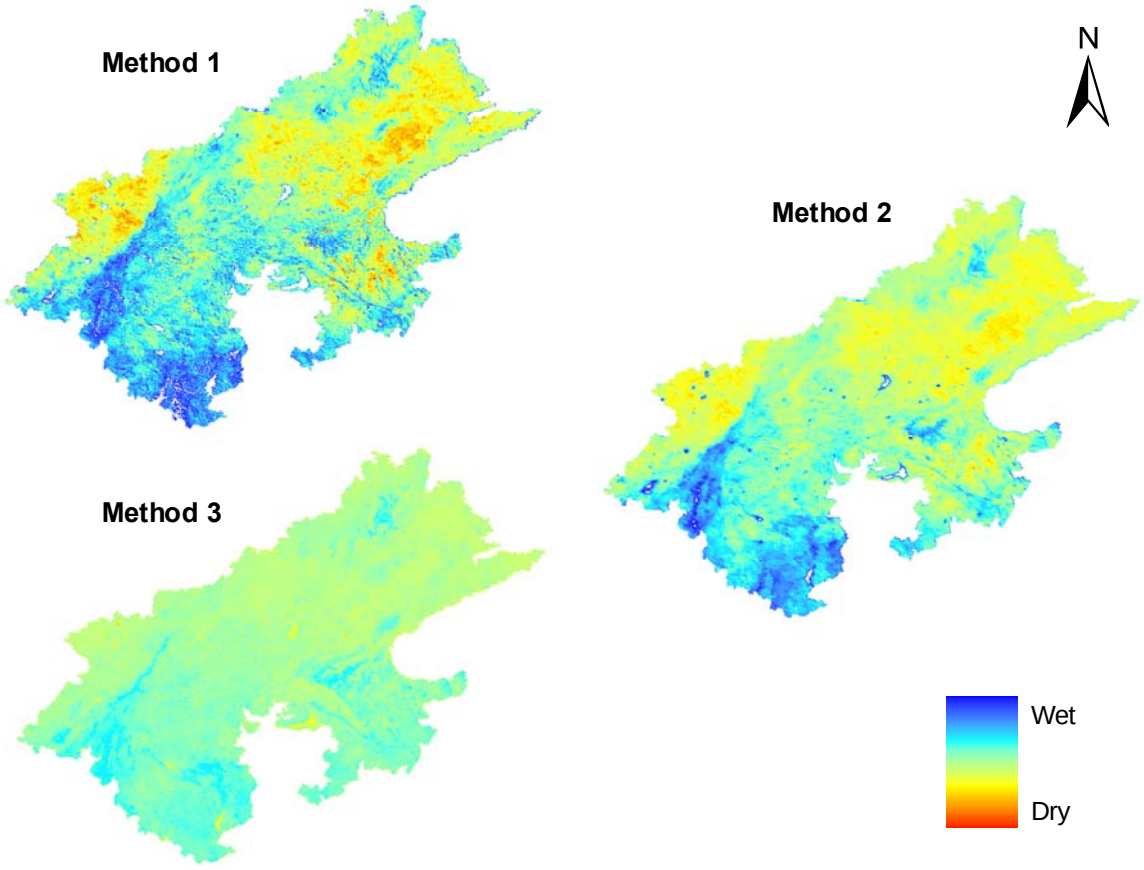

Figure 5-2: Spatial patterns of VTCI for JD 273, 2007 as derived from different methods.

5.1.2. Comparative Sensitivity of Vegetation Temperature Condition Index (VTCI) from different methods to Soil Moisture in the Upper Layers

The VTCI computed by the 3 methods were regressed against concurrent in-situ soil moisture to decide on which method yields VTCI that represents soil moisture in the upper 50cm relatively better. The regression was done with the average value for soil moisture content in the active root zone (i.e. 50cm). The graphs of VTCI versus the average in-situ soil moisture are given below in Figure 5-3. It can be clearly observed that method 1 is better correlated with the average soil moisture in the first 50

cm. Method 2 gave lower value of coefficient of determination than Method 1 but is seen to be better than Method 3. For Method 1 and Method 2, the correlation is significant at 0.01 level for 2 tailed analysis and Method 3 showed significance at 0.01 level for 1 tailed analysis. These results once again prove that VTCI is best calculated when the whole image is considered and when it is computed at the resolution of LST. So VTCI from Method 1 was used to estimate the average soil moisture in the top 50cms, representing the active root zone of the crops. The statistics of the samples used for regression is given in Table 5-1. The resultant regression equation had a slope and intercept of 0.5341 and 34.66 respectively.

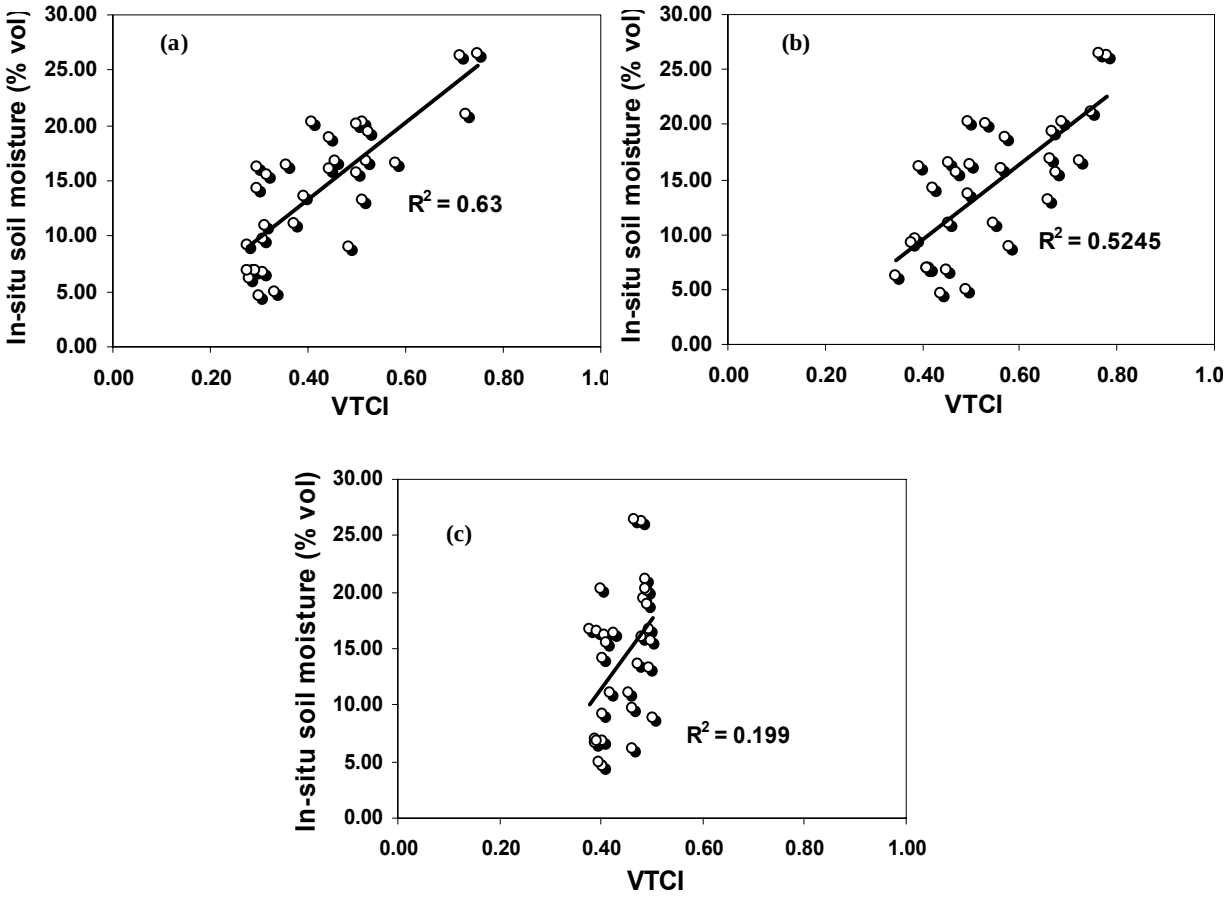

Figure 5-3: Correlation of VTCI with In-situ soil moisture (a) Method 1 (b) Method 2 (c) Method 3

Variable	Mean	Std. Deviation	No .of Samples
VTCI (Independent)	0.42	0.14	31
Average Soil Moisture in % Vol (Dependent)	14.09	6.02	31

Table 5-1: Statistics of the samples used for regression

5.1.3. Relationship of Vegetation Temperature Condition Index (VTCI) with Depth wise In-situ Soil Moisture

In- situ soil moisture collected in the field from the surface and at three different depths beneath the surface was analyzed with the single VTCI value. Thirty one in-situ moisture measurements were used for this analysis. The graphs in Figure 5-4 show the plots obtained between VTCI and in –situ volumetric soil moisture content at different depths. VTCI, being an indicator of the combined effect of vegetation vigour and land surface temperature, is observed to be strongly related to surface soil moisture condition with a coefficient of determination of 0.72 which is relatively better than those for other depths. A good relationship was also observed at 30cm with an R^2 of 0.65 while VTCI has explained relatively less variance in soil moisture content at 15 and 45 cm with a coefficient of determination of 0.54 and 0.55 respectively.

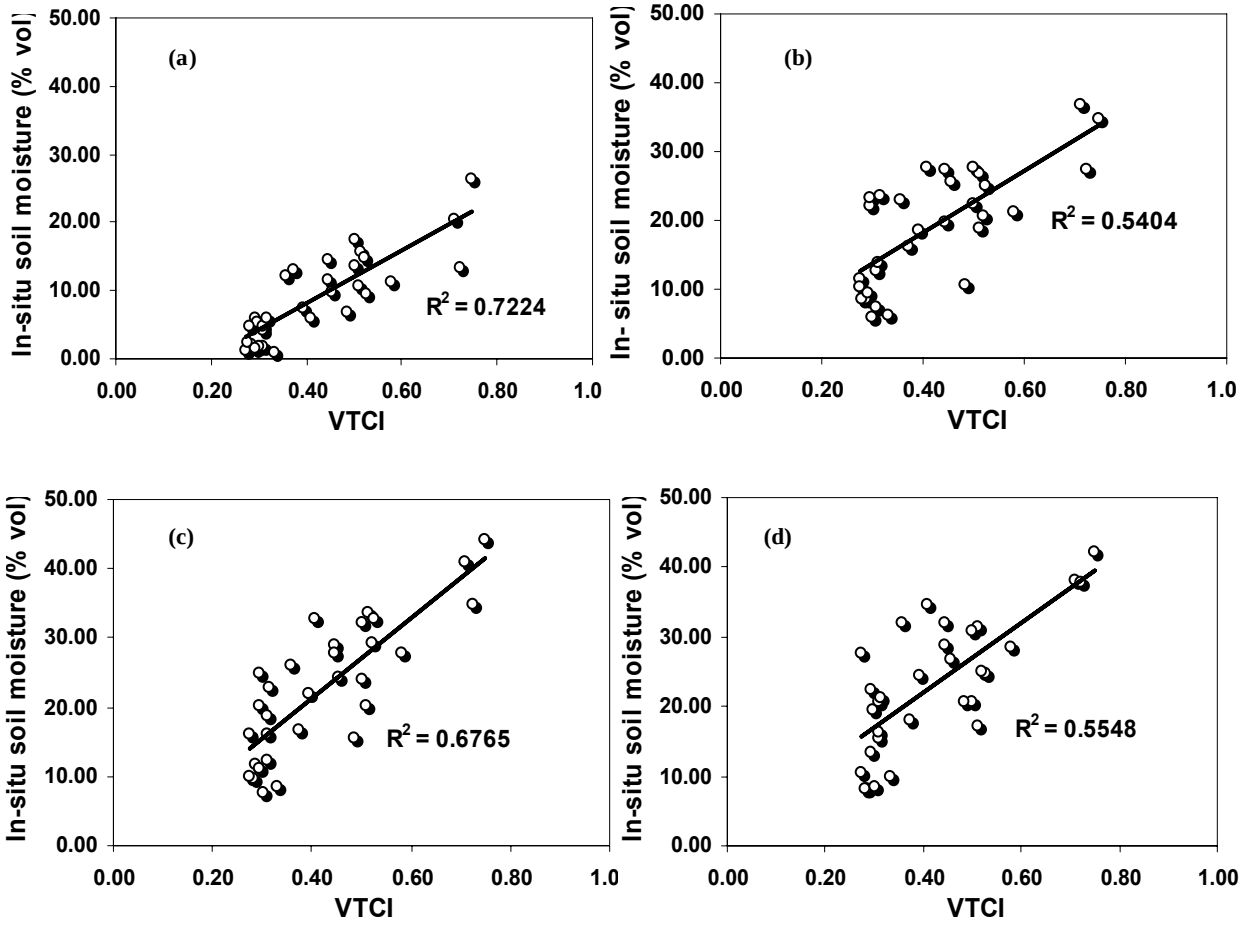

Figure 5-4: Regression of VTCI with observed soil moisture at different depths (a) Surface (b) 15cms c) 30cms and (d) 45cms

Wang et al (Wang et al 2007b) attempted a similar study with NDVI, which is a representation of vegetation vigour alone, instead of VTCI which incorporates the effect of LST. They examined the improvement in correlation with time lag as NDVI lags in its response to root zone soil moisture by 1 to 2 weeks. This was an exception at 10 cm depth, whose correlation coefficient decreased with time lag, signifying less contribution of surface soil moisture in transpiration. The LST factor in VTCI makes it a near real – time drought monitoring index unlike NDVI. The main determining factor of

LST is evapotranspiration in which evaporation is more than transpiration in sparsely vegetated fields and transpiration starts dominating with increase in NDVI. So when the crop cover is less in agriculture fields, evaporation plays a good role in determining the value of LST. As the field work was done at the stage of crop maturity, when the crop vigour is less, the values of LST has more contribution from evaporation than transpiration. It is the soil moisture at the surface which evaporates and that at the root zone which transpires through the plants. So the real time soil moisture correlated with VTCI shows more influence of surface soil moisture owing to more evaporation than transpiration, because the crops are in their later stages with less canopy cover and less NDVI.

The relationships reflect the effect of transpiration also, though with lesser correlation than evaporation. Transpiration occurs from the root zone of the crops which, in theory, spans till 1 – 2 metres, but in reality, differs and often, cereals find it difficult to vertically spread their roots more than 30cm, owing to lack of nutrients and limitations posed by soil depth and compactness(Peacock & Wilson 1984, Pearson 1984). The maximum rooting activities of Bajra and sorghum in the tropics is found to occur at 30cms. The higher correlation observed with soil moisture content at 30cm can be due to its higher contribution to transpiration. The lesser, though significant relationship shared by soil moisture at 15cm and 45 cm can be attributed to their lesser contribution to evapotranspiration.

5.1.4. Spatio – temporal Variation of Vegetation Temperature Condition Index (VTCI) for 2003

VTCI was computed from JD 257 to JD 297 for 2003. JD 257 and JD 265 which have about 30% cloud cover were considered for analysis. LST images for the rest of the Khariff season, June – August was found to be more than 70 % cloudy and could not be used for analysis. The VTCI from JD 273 to JD 297 are given in figure below.

The warm and cold edges or $LST_{NDVImax}$ and $LST_{NDVImin}$ isolines obtained to compute VTCI for six 8 day time periods in 2003 are given in Table 5-2. All the warm edges have negative slope, indicating the decrease in LST_{max} when the value of NDVI interval increases. They maintain a consistent good relationship with R^2 ranging from 0.86 to 0.98. The cold edges of the first two 8 day periods give a positive slope signifying the decrease in LST_{min} with the NDVI interval. From JD 273, as the effect of the rains decrease causing the value range of LST_{min} to become higher, the slope turns negative. This negative slope in the cold edge also indicates the rise in LST_{min} with decrease in the NDVI interval. The intercepts of cold edge show a steady increase from JD 257 to JD 297 which is due to the rise in the minimum temperature in the area as the days are further away from the monsoon period.

From JD 257 to JD 273, VTCI shows relatively higher values as the area is still under the effect of the monsoons. In the figure 5-5, for JD 273, VTCI shows higher values, throughout the image, and it goes decreasing for all land-cover except thick natural vegetation. For JD 281, the natural vegetation is seen to have higher values than JD 273, which depicts ground reality, the vegetation vigour being high just after the monsoons. But in the next two weeks, JD 289 & JD 291, when the monsoon has receded and soil moisture is going down, VTCI shows a decreasing temporal trend for the whole image.

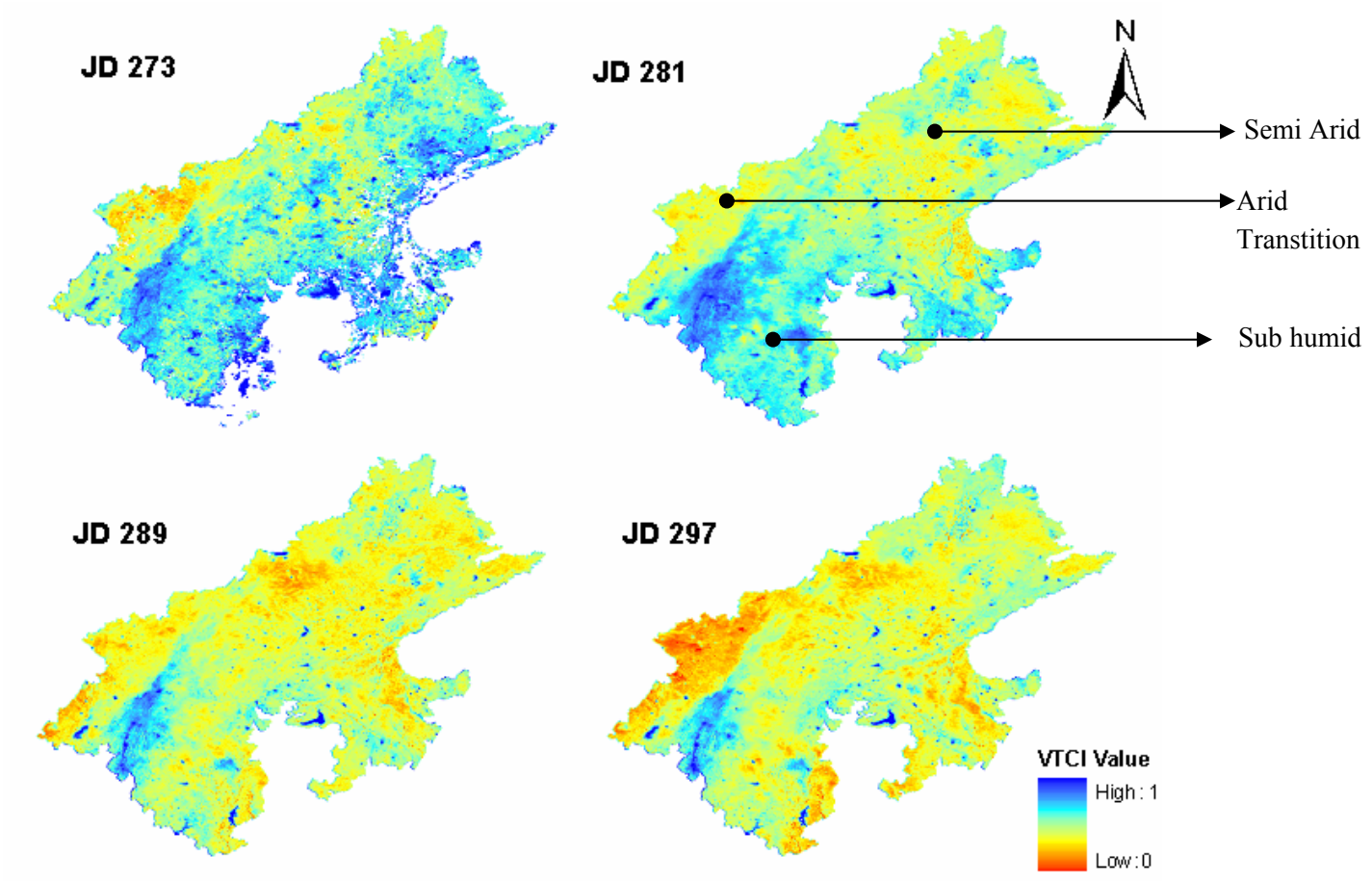

Figure 5-5: Spatial patterns of VTCI for October 2003

Spatially, VTCI shows large variation with the different climatic zones. It had relatively low values in all the weeks, for the districts of Pali and Sirohi which belong to the arid transitional zone in the south west corner of the study area. In the east of this zone lies the Aravalli Hills which consistently shows a high value of VTCI, owing to the thick natural vegetation which flourishes on the hills during the rainy season. Further east of the Aravalli hills; lay the sub humid region and northwards, the semi arid region. VTCI has distinguishable variation between these regions too with predominantly high values in the sub humid region compared to the semiarid area.

JD(8 day period)	Warm Edge ($LST_{NDVImax}$)		R^2	Cold Edge ($LST_{NDVImin}$)		R^2
	Slope	Intercept		Slope	Intercept	
257 (257-264)	-14.447	317.75	0.86	2.5681	293.26	0.38
265 (265-272)	-23.325	323.5	0.91	2.7884	293.78	0.60
273 (273-280)	-28.218	326.29	0.97	-1.3933	297.34	0.37
281 (281-288)	-20.321	323.58	0.96	-6.0995	304.12	0.74
289 (289-286)	-23.398	324.26	0.98	-7.1007	305.86	0.82
297 (297-304)	-21.86	323.24	0.98	-7.3885	305.72	0.79

Table 5-2: The warm and cold edges in NDVI – Ts space for 2003

5.1.5. Spatio - temporal Variation in Soil Moisture as Estimated from Vegetation Temperature Condition Index (VTCI) and In-situ soil Moisture

Average volumetric soil moisture content for the top 50 cm of the soil profile, at 1 km spatial resolution, as estimated using the developed VTCI – soil moisture relationship during 2003 follows the same trend as VTCI, both temporally and spatially. The spatio- temporal variation is shown in Figure 5-8. For further analysis, the pixels of agricultural area, consisting of Bajra, Jowar and Maize were extracted from the images of the whole study area as the objective of the study is to assess the variation of soil moisture for these prominent crops. Two Squares of $1^o * 1^o$ area were selected, one each from the semi-arid and the sub humid regions to get the representative statistics of both the regions. The squares consist of only the pixels attributed with the prominent crops in the chosen $1^o * 1^o$ area. There were 4864 pixels in the semi-arid region and 2717 pixels in the sub-humid region. The maximum, minimum and the mean values for the prominent crops in both the regions are given in the Table 5-3. The values have been tabulated for the month of October to show the temporal variation through the month. The graph in Figure 5-6 conveys the variation in the values for the whole study area and Figure 5-7, for the two climatic regions taken separately for JD 281. The soil moisture content is plotted against the % of pixels having the same values in the $1^o * 1^o$ squares, and analysed, assuming it is indicative of the whole area of the two climatic regions in the study area. It is evident from these figures that the measure of soil moisture as estimated from VTCI shows considerable spatial variation with different climatic regimes. The mean soil moisture content for the prominent crops in the whole study area is 16.45% for JD 281. For the semi-arid region, it goes down to 13.45% and for the sub-humid it goes up to 26.29%.

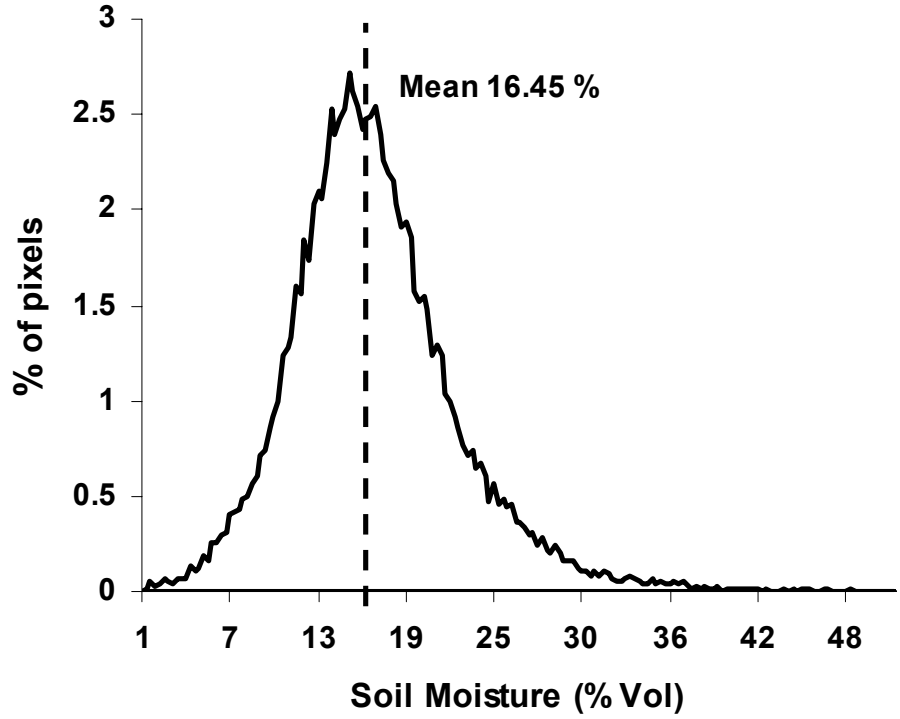

Figure 5-6: Spatial frequency of volumetric soil moisture content in the study area for JD 281

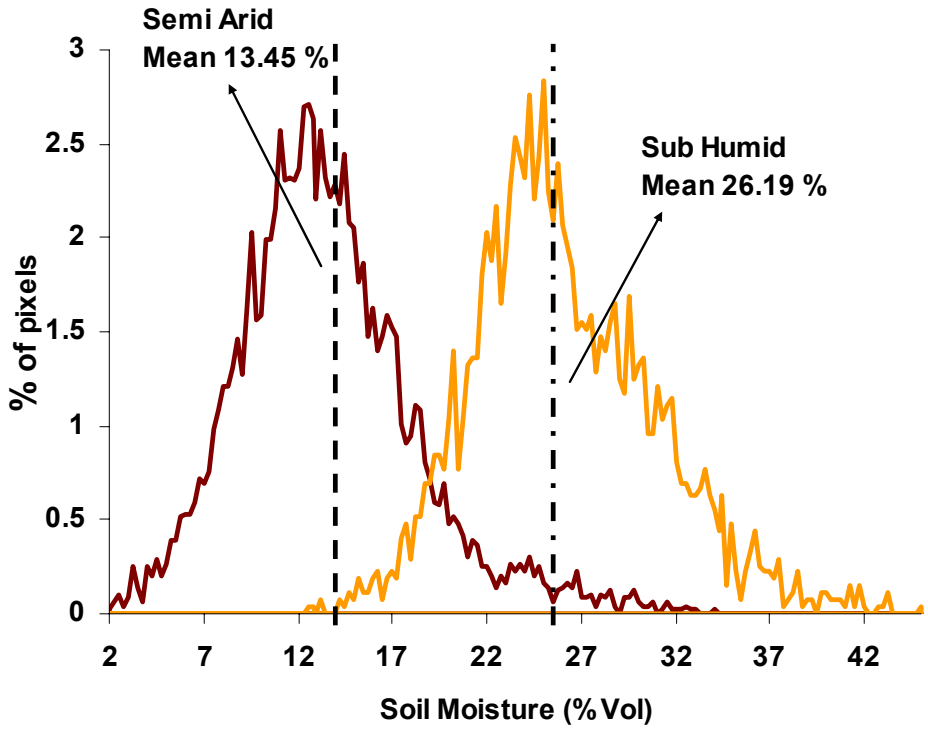

Figure 5-7: Variability in the spatial frequency of volumetric soil moisture content with different climatic regions for JD 281

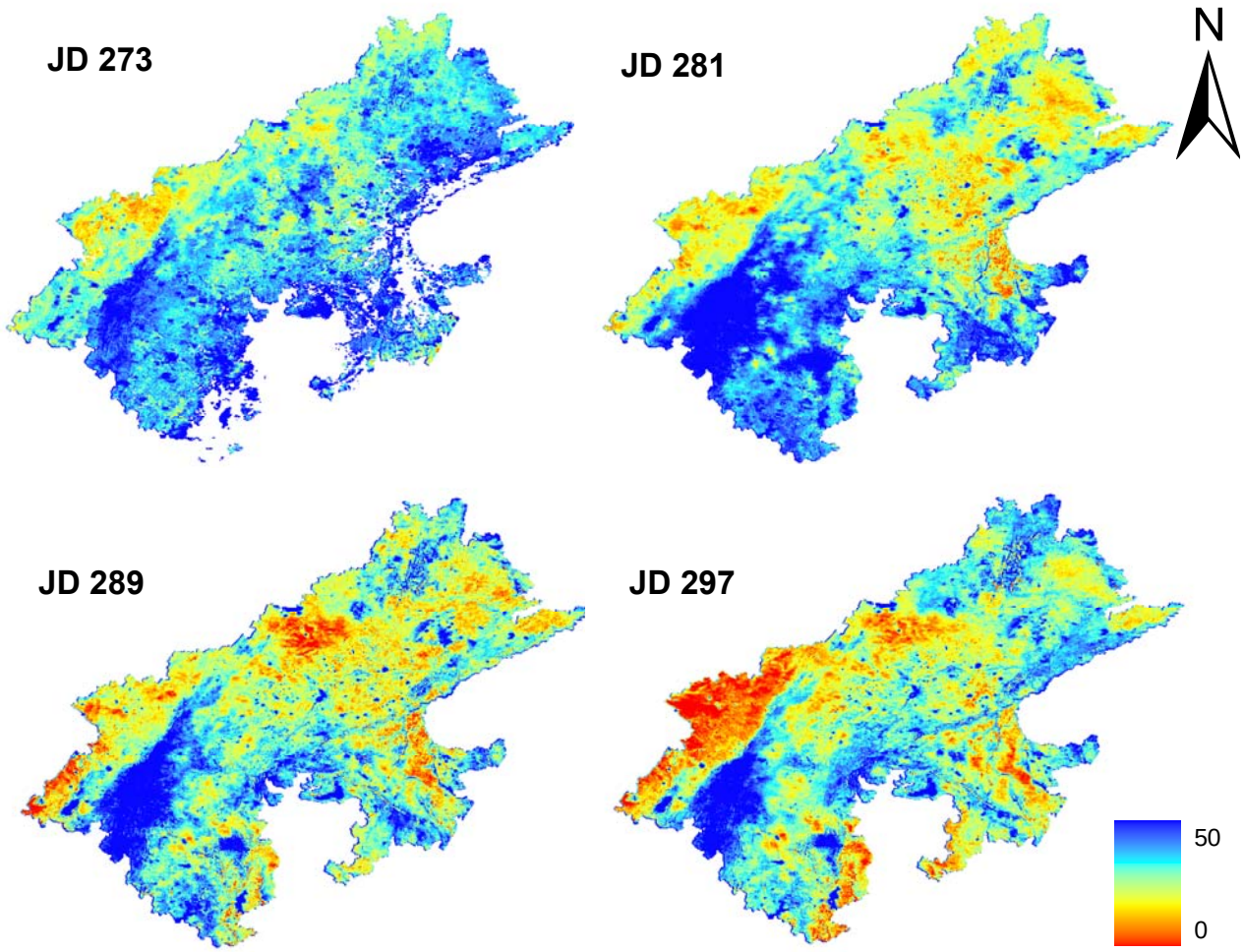

Figure 5-8: Spatial Patterns of Soil Moisture as estimated from VTCI

JD	Semi Arid			Sub Humid		
	Min	Mean	Max	Min	Mean	Max
273	1.99	16.77	44.88	8.82	26.97	49.12
281	1.78	13.45	34.26	12.43	26.19	45.42
289	1.42	12.62	31.65	6.70	20.51	41.91
297	1.09	10.49	31.49	5.86	18.52	41.13

Table 5-3: Variability in the statistics of volumetric soil moisture content with climate regions for different JDs

Further, from the images depicting the spatio – temporal variability in Figure 5-8, the arid transitional plain can be observed to be having the minimum values of soil moisture for all the JDs. It can also be noticed that VTCI attributes very high root zone soil moisture to the Aravalli ranges, partitioning the arid transitional and sub- humid regions, because of the dense vegetation cover just after the monsoons. Temporally, the soil wetness is seen to be steadily decreasing as the Julian day goes further away from the monsoon season.

5.2. The Passive Microwave Remote Sensing Approach

The passive microwave approach to assess soil moisture variability at coarse resolution was done with 3 parameters, API (Antecedent Precipitation Index), T_{BH} (Horizontally Polarized Brightness Temperature) & PD (Polarization Difference). The spatio –temporal variation of the parameters and their relationship to root zone soil moisture have been explored and discussed here.

5.2.1. Spatio – temporal variation of Horizontally Polarised Brightness Temperature (T_{BH}) & Polarisation Difference (PD)

The spatio-temporal variation of horizontal brightness temperature, T_{BH} and the polarisation difference, PD of the horizontally polarized from the vertically polarized brightness temperatures, PD, are analyzed in this section. The alternate day T_{BH} and PD datasets, with a spatial resolution of 25 km were analyzed for the whole of Khariff season, from first week of June to last week of November. The spatio – temporal trend is shown in Figure 5-9 for T_{BH} and in Figure 5-11 for PD. Previous work by Prigent et al (2005) has reported negative correlation of T_{BH} with soil moisture and positive correlation with vegetation density. For PD, they have observed positive correlation with soil moisture and negative correlation with vegetation density.

The temporal trend of T_{BH} is observed to start from a high value and goes down with the onset of monsoons, when the soil moisture starts rising. It reaches its maximum dip, a few days after the start of the monsoon and is seen to be rising up till the end of the Khariff season. This phenomenon can be interpreted with the crop phenology in the period that the T_{BH} values begins to increase once the crops are in their vegetative stage in July, August and September, i.e. when the vegetation density is higher. By mid-October when the crops have matured and the effect of soil moisture T_{BH} is dominant, the values again start going down. The trends of both 6.9 GHz and 36.5 GHz are shown in the graph in Figure 5-10 .Its inverse variation with the local rainfall can be observed, especially for the semi - arid

region. Spatially, no definite trend can be noticed in the variation of $T_{BH.}$ This observation is due to the simultaneous effect of both vegetation and soil moisture on the T_{BH} value. In Figure 5-9, in the image of JD 305, a particular pixel has been pointed out. In most of the JDs, this pixel can be seen to be having relatively higher $T_{BH.}$ This pixel is dominated by dense vegetation with an average NDVI value of 0.61 for the Khariff season. Majority of the 25 km in the pixel has been classified as forest or thick vegetation. It is highlighted at this juncture, as an example of the positive variation of T_{BH} with vegetation density.

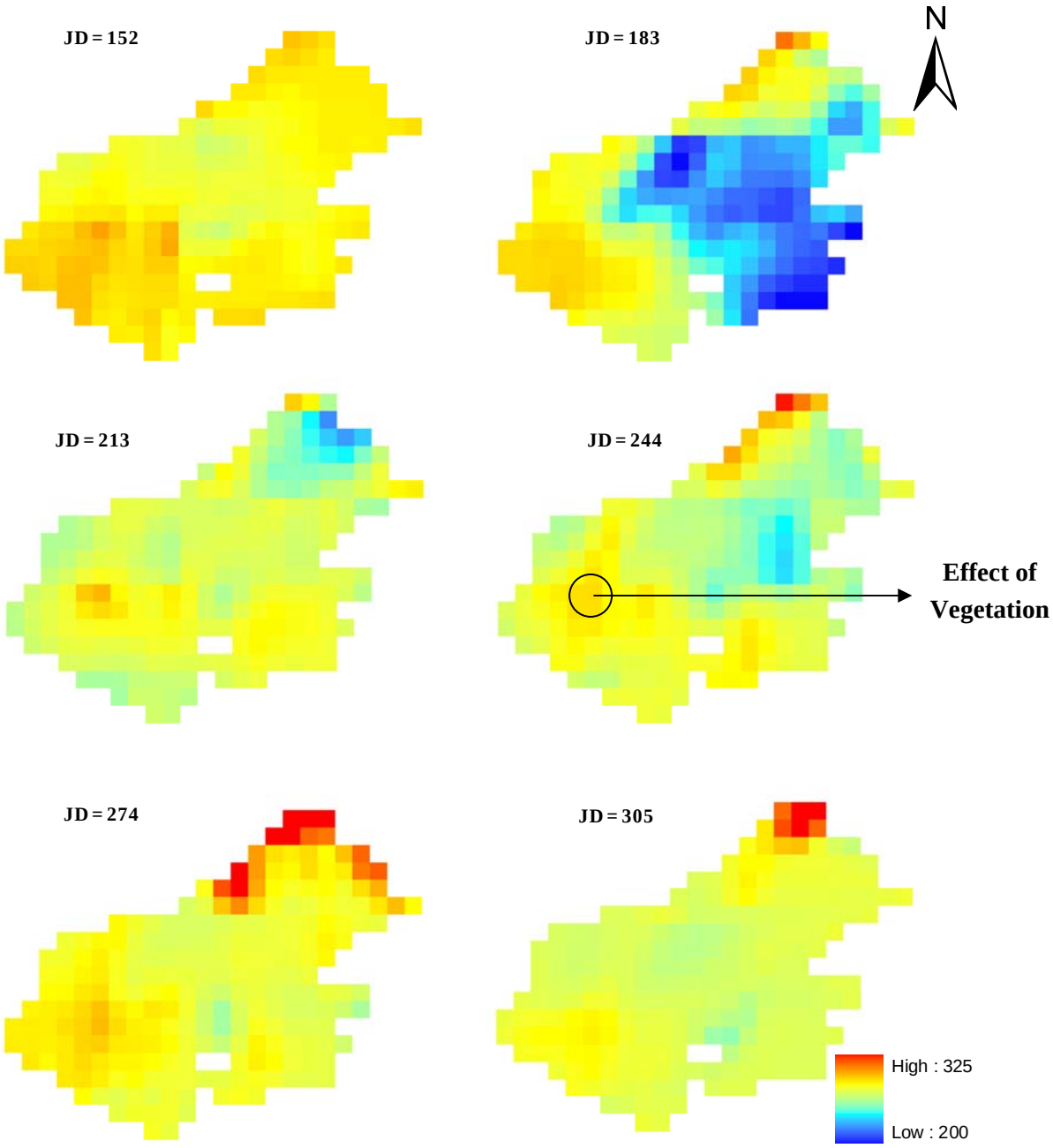

Figure 5-9: Spatio –temporal variation of T_{BH} from June to November (6.9GHz)

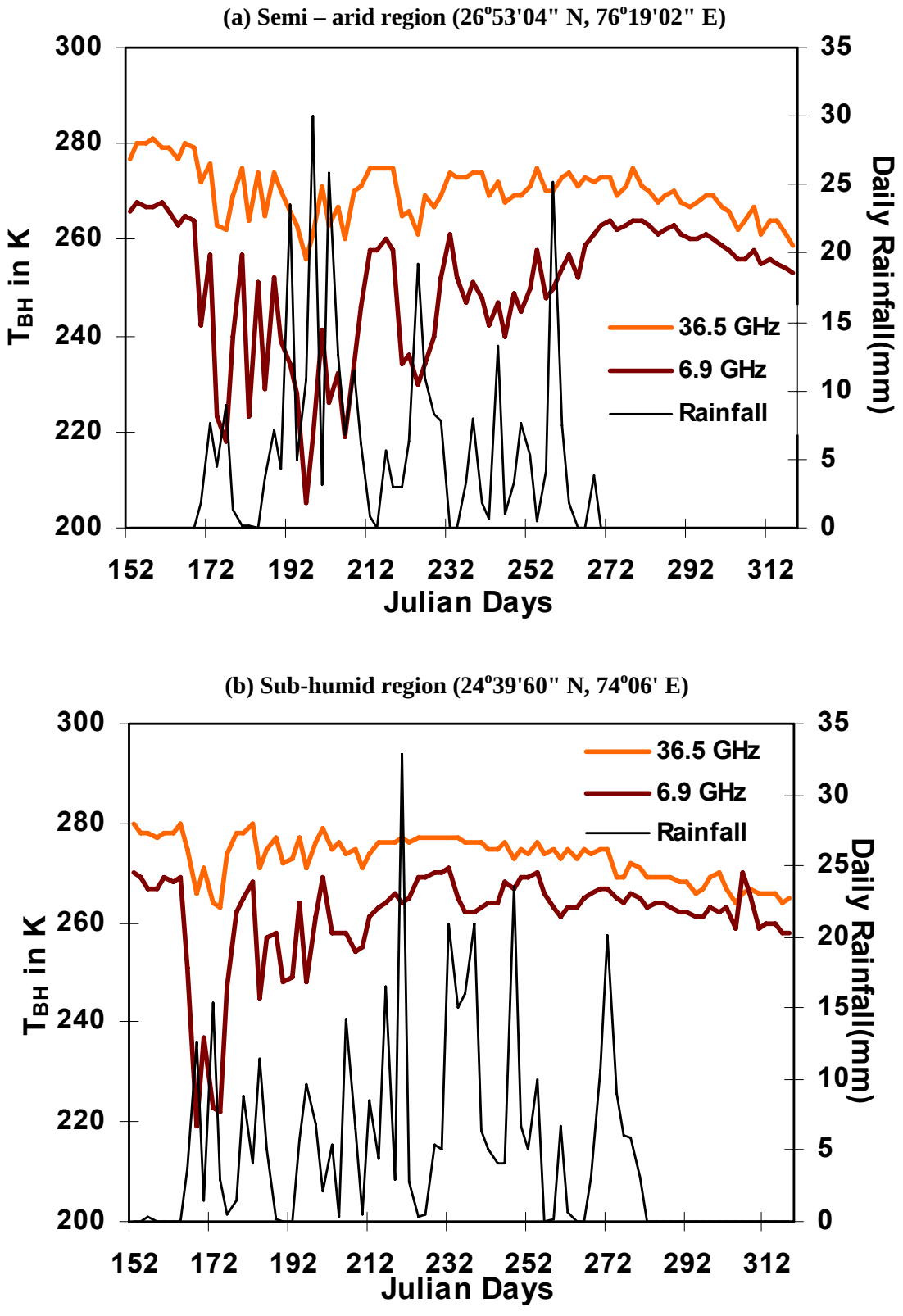

Figure 5-10: Temporal Variation of T_{BH} in the Khariff Season for different climatic region

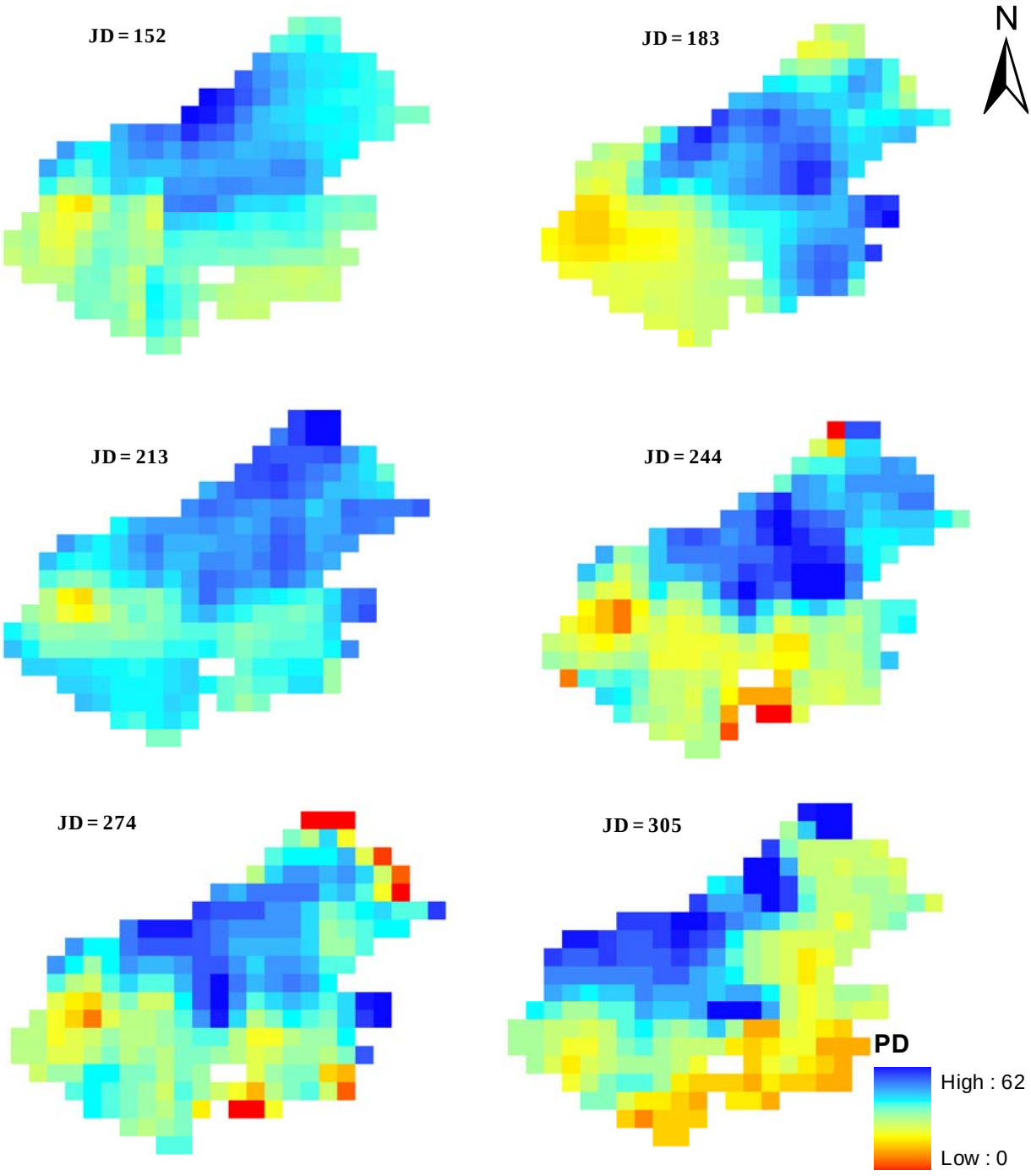

Figure 5-11: Spatio –temporal variation of PD from June to November (6.9GHz)

The temporal trend of Polarisation Difference is the inverse of that observed for $T_{BH.}$ The temporal profiles of PD for semi-arid and sub-humid regions for both the frequencies are presented in Figure 5-12. PD also shows a logical variation with rainfall particularly in the semi-arid region. It is seen to rise with the beginning of the monsoon season and starts decreasing when the crops reach their vegetative stage. The spatial variation in PD, unlike T_{BH}, is seen to be varying from one climatic region to another. It can be observed in the graphs in Figure 5-12 that till the end of the rainy season in the semi –arid region, by JD 272, PD in the semi – arid region shows higher values than the sub – humid region. After JD 272, the sub –humid region gives an increasing trend while the semi-arid region presents a decreasing trend.

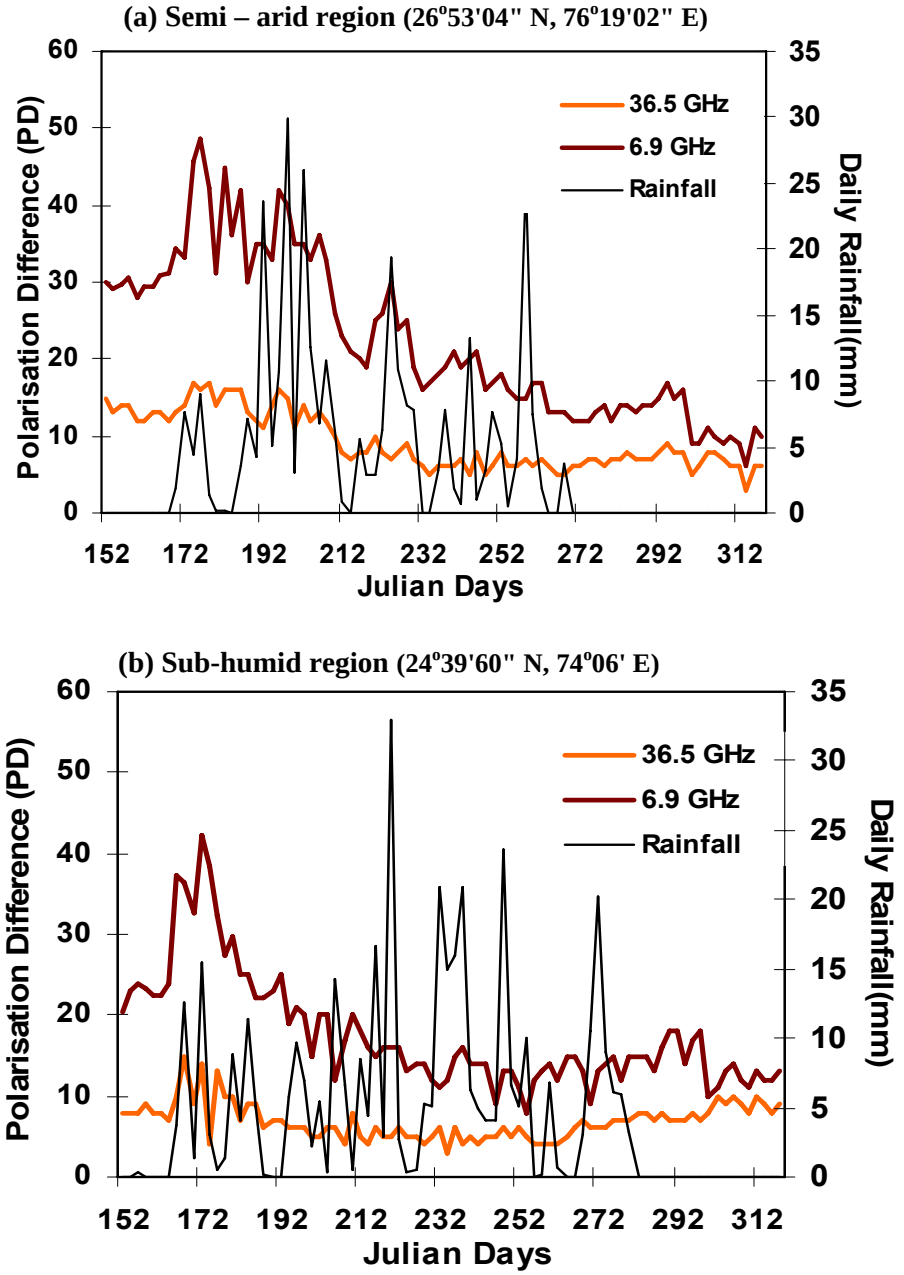

Figure 5-12: Temporal variation of PD in the Khariff Season for different climatic region

5.2.2. Antecedent Precipitation Index (API) from Horizontally Polarised Brightness Temperature (T_{BH}) & Polarisation Difference (PD)

API was computed from meteorological and ancillary data on a daily basis at 5 km and aggregated to 25 km to make it comparable with the spatial resolution of the passive microwave data. It was also averaged for every two days. API was attempted to be estimated from solely microwave data of a single year, for 2003. The estimation was tried to be done in two steps, first regressing API with T_{BH} and then regressing the slope and intercept thus obtained, with PD. The double regression is done to incorporate the vegetation effect as indicated by PD. The regression equation of API and T_{BH} was obtained from the pooled data of 4 months from July to October 2003. To regress API – T_{BH} slopes and intercepts with PD, two grids of 1^o * 1^o were adopted, one in semi arid and one in sub humid

consisting of pixels with best r value. The 16 pixels of 25 km * 25 km each in the $1^{o}*1^{o}$ grids were taken to obtain the daily slope and intercept.

Relationship of Temporal Antecedent Precipitation Index (API) with Horizontally Polarised Brightness Temperature (T_{BH})

The relation of soil moisture with brightness temperature is generally found to be negative without the interference of vegetation (Prigent et al 2005). The trend was found to be true as shown in the spatial plot given below. For 6.9 GHz, good inverse correlation was found almost everywhere in the study area except for a few pixels in the sub-humid region. For 36.5 GHz, the trend decreased and most of the sub-humid region gave positive correlation, as the density of vegetation became higher. The spatial variation is depicted in the Figure 5-13. The spatial profile of the Pearson's coefficient of correlation from semi – arid to sub – humid region is shown in Figure 5-15. The relationships of API and T_{BH} for individual pixels in semi-arid and sub-humid region are illustrated in graphs in Figure 5-14.

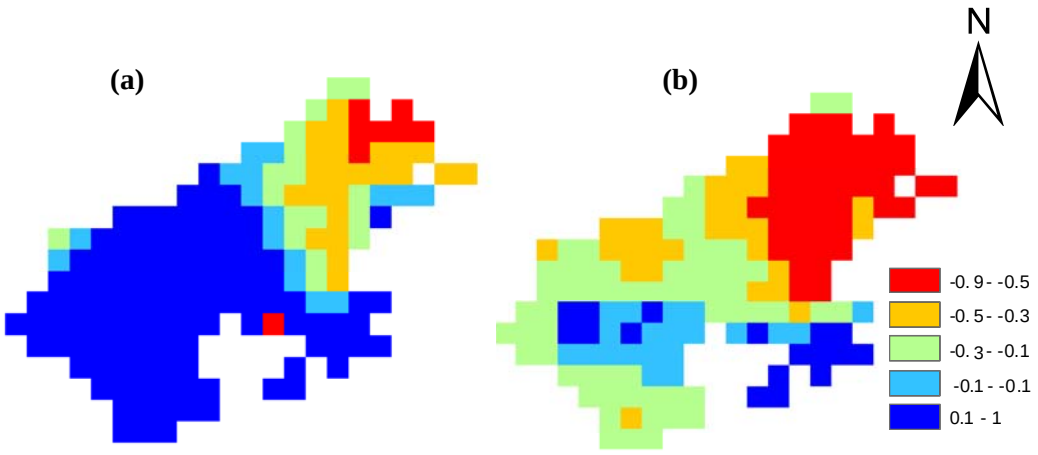

Figure 5-13: Spatial Variation of r for API – T_{BH} with climatic regions for a) 36.5 GHz and b) 6.9 GHz

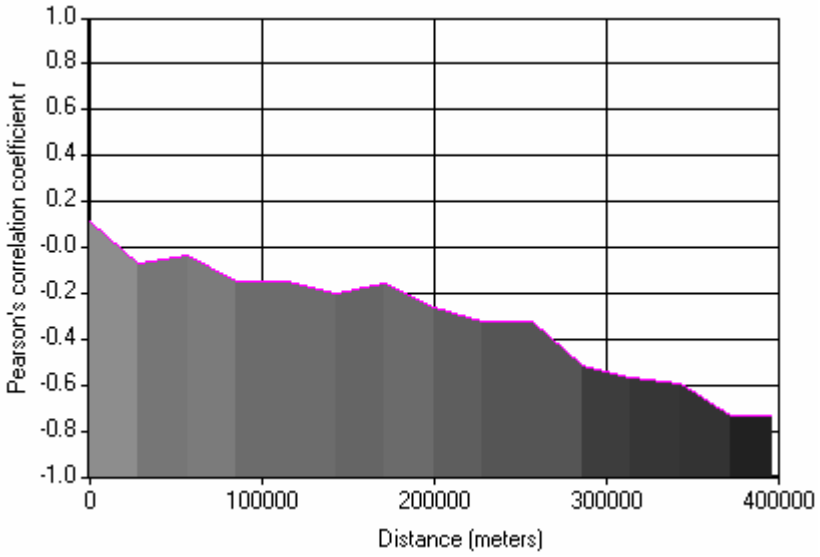

Figure 5-14: Spatial variation of correlation of API & T_{BH} from Sub-humid (24^{o} 33' 10" N, 73^{o} 38'04"E) to Semi –arid (26^{o} 57' 06" N, 76^{o} 57' 08"E) Climatic regions (6.9GHz)

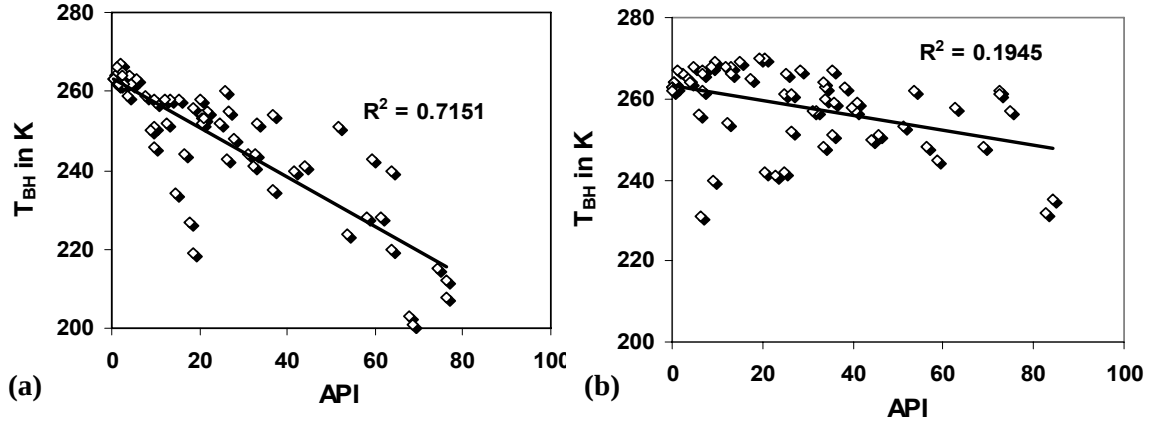

Figure 5-15: API- T_{BH} Relationship for individual pixels (a) Semi-arid (26° 53' 04" N, 76° 06' 02"E) (b) Sub-humid (24° 39' 60" N, 74° 06' E) for 6.9 GHz

Relationship between daily API, Horizontally Polarised Brightness Temperature (T_{BH}) and Polarisation Difference (PD)

API was regressed with T_{BH} with the average of 16 pixels from the starting of rains, by mid July to October so as to obtain the daily slope and intercept for further regression with PD. The correlation did not come out as good as the pixel to pixel inverse relation. Microwave brightness temperature emission has intense geographical dependence and the relations with soil moisture and vegetation density varies with different locations on the globe as observed by Prigent et al (Prigent et al 2005). The averaging of the 16 spatially variant pixels deteriorated the relationship which was obtained for temporal data of individual pixels. The regression was done separately for the 84 alternate days to obtain the slopes and intercepts for each day. The relationships varied from negative to positive without any particular trends. The graphs in Figure 5-16 illustrate the average relationship of the 16 pixels for 84 alternate days. Nevertheless, the slopes and intercepts were regressed with PD. The r values of the results obtained for the two frequencies in the two climatic region are tabulated in Table 5-5. As no definite trend could be observed from the results, the methodology could not be further analyzed to inverse estimate API from T_{BH} and PD. The 16 pixels taken together may give better results if yearly data are pooled and regressed as done by Teng et al (Teng et al 1993).

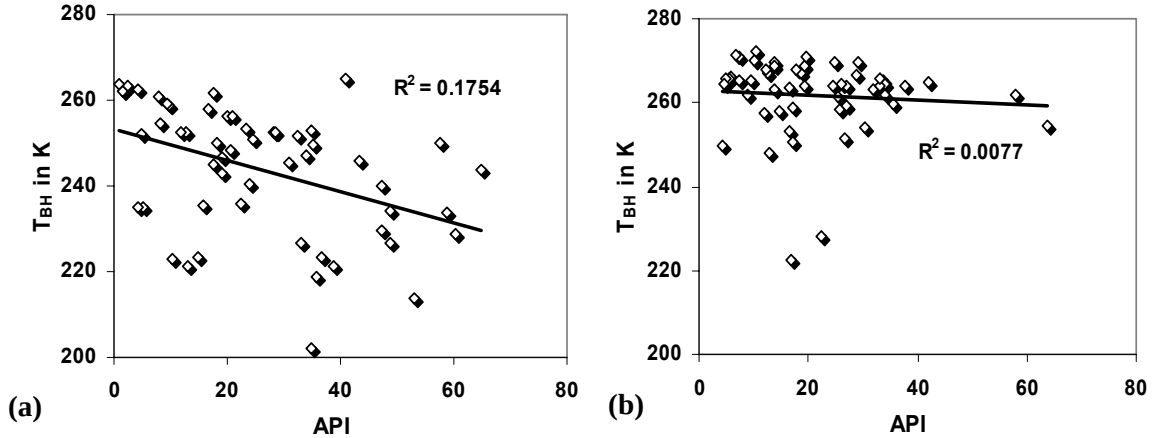

Figure 5-16: Average API- T_{BH} Relationship for 16pixels (a) Semi-arid (b) Sub-humid for 6.9 GHz

Climatic Region	Frequency in GHz	Pearson's Correlation Coefficient, r	
		Slope	Intercept
Semi- arid	6.9	-0.23	-0.69
	36.5	-0.22	-0.27
Sub-humid	6.9	-0.71	-0.08
	36.5	0.06	0.03

Table 5-4: Value of r for relationship between slope and intercept of API -T_{BH} relationship and PD

5.3. The GIS based Simple Water Balance Approach (SWBM)

The water balance model is based on the simple algorithm soil water balance according to the criteria given by Thornthwaite & Mather (Thornthwaite & Mather 1955). The algorithm can give time series soil moisture, actual evapo-transpiration and water surplus as outputs. As the present context demands the spatial and temporal patterns of soil moisture only, the program was limited till the computation of the same. The algorithm was programmed using IDL 6.3. The model is adopted on a grid base with a grid size of 5kms. The 5 km grid size was chosen to match with the corresponding resolution of the input data (Solar Radiation, Rainfall, Temperature etc). The database was prepared for Eastern Rajasthan for the Khariff season of 2003. The analysis of the results was done for selected grid cells where Bajra, Jowar and Maize are dominant and the field capacities of the soil are different. The model was run from the third week of June to last week of November. The period was chosen to cover the crop calendar of the three prominent crops.

The results were compared with the soil moisture from AMSRE which is validated for 1 m. This product is available at a temporal interval of 10 days and a spatial resolution of 0.5^{o}. It was made into monthly average to facilitate the comparison. The monthly values were normalized for the monthly average rooting depths in which the soil moisture from SWBM was simulated. The weekly simulated soil moisture from SWBM was also averaged for the 6 months in the Khariff season and aggregated to 0.5^{o}. The temporal trend for the season is shown below in Figure 5-17 for 2 locations, one in semi arid region and the other sub humid. From the graphs, it can be observed that there is underestimation of soil moisture as simulated with the SWBM after august in both the regions. Conventional methods used to compute the inputs in the SWBM must be the reason for the underestimation. The Penmann and Montieth method provides the most accurate measure of Potential evapotranspiration but it demands a lot of meteorological data which is unavailable for the study area. The adopted method of Jensen and Haise (Jensen & Haise 1963), has a tendency to overestimate PET and probably this might be the cause of more extraction of water resulting in the underestimation of soil moisture.

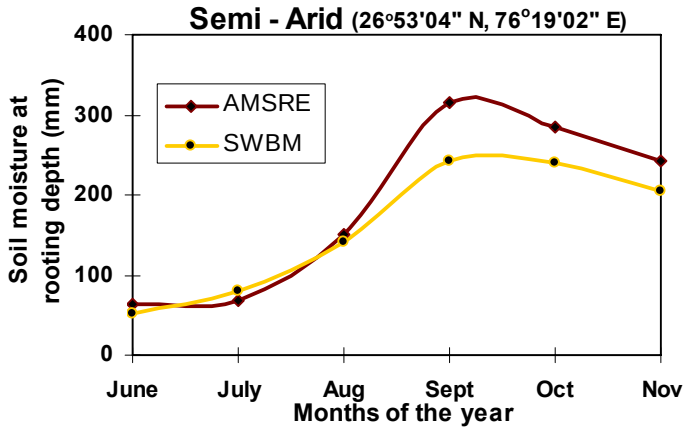

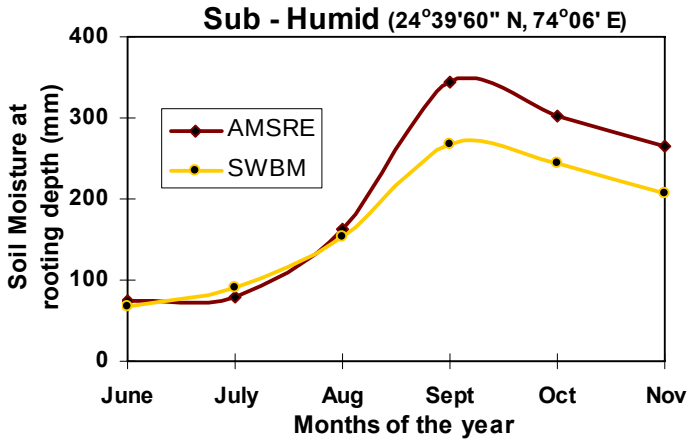

Figure 5-17: Temporal trend of simulated soil moisture and AMSRE soil moisture (University of Bonn, Ref .Section 4.1.1)

5.3.1. Spatio - temporal Variation of Soil Moisture Content from the SWBM

Soil moisture as simulated at 5 km spatial resolution, by the simple water balance model varies spatially and temporally in the study area as illustrated in Figure 5-19. Significant variation can be observed in soil moisture spatially, which is highly dependant on the water retention capacity of each soil regime indicated by the field capacity (FC). Same has been observed by Alemaw and Chaoka (Alemaw & Chaoka 2003). The range of the values in which soil moisture varies temporally is also based on this field capacity. Soil regimes of five different field capacities, 42%, 37.1%, 35 %, 26.7 % and 12.1 % are present in Eastern Rajasthan and they occupy 0.1%, 14.3 %, 40.3%, 18.8% and 26.3% of the study area respectively. It is observed that the minimum and maximum of the range in which soil moisture values occur for each week is linearly correlated to the values of field capacity. This causes 26.3 % of the area having a low FC of 12.1% to have relatively lower soil moisture range than the others in all the weeks. The maximum and mean soil moisture values for each regime in the months of the Khariff season are given in the Table 5-4.

Months	***FC =12.1%***	***FC =26.7%***	***FC =35%***	***FC =37.1%***
June	43.59	65.49	69.47	77.34
July	50.52	78.94	96.35	101.08
August	90.52	126.95	154.47	171.07
September	140.2	183.58	215.35	282.56
October	111.7	161.15	191.68	261.95
November	85.0	134.13	165.9	225.54

Table 5-5: Mean Soil moisture (mm) for different soil regimes for the Khariff season months

The spatial variation of soil moisture shows no relation with precipitation, though for individual grids, when the precipitation is very high, the temporal soil moisture profile shows a small peak and dips slightly when the precipitation goes extremely down. Sub-humid region receives 20% more of rainfall. This does not seem to have any effect on the resultant soil moisture because of high runoff obtained in the sub-humid region owing to the undulating terrain. So the distribution of effective rainfall does not vary as significantly with climatic region as actual rainfall is seen to be varying.

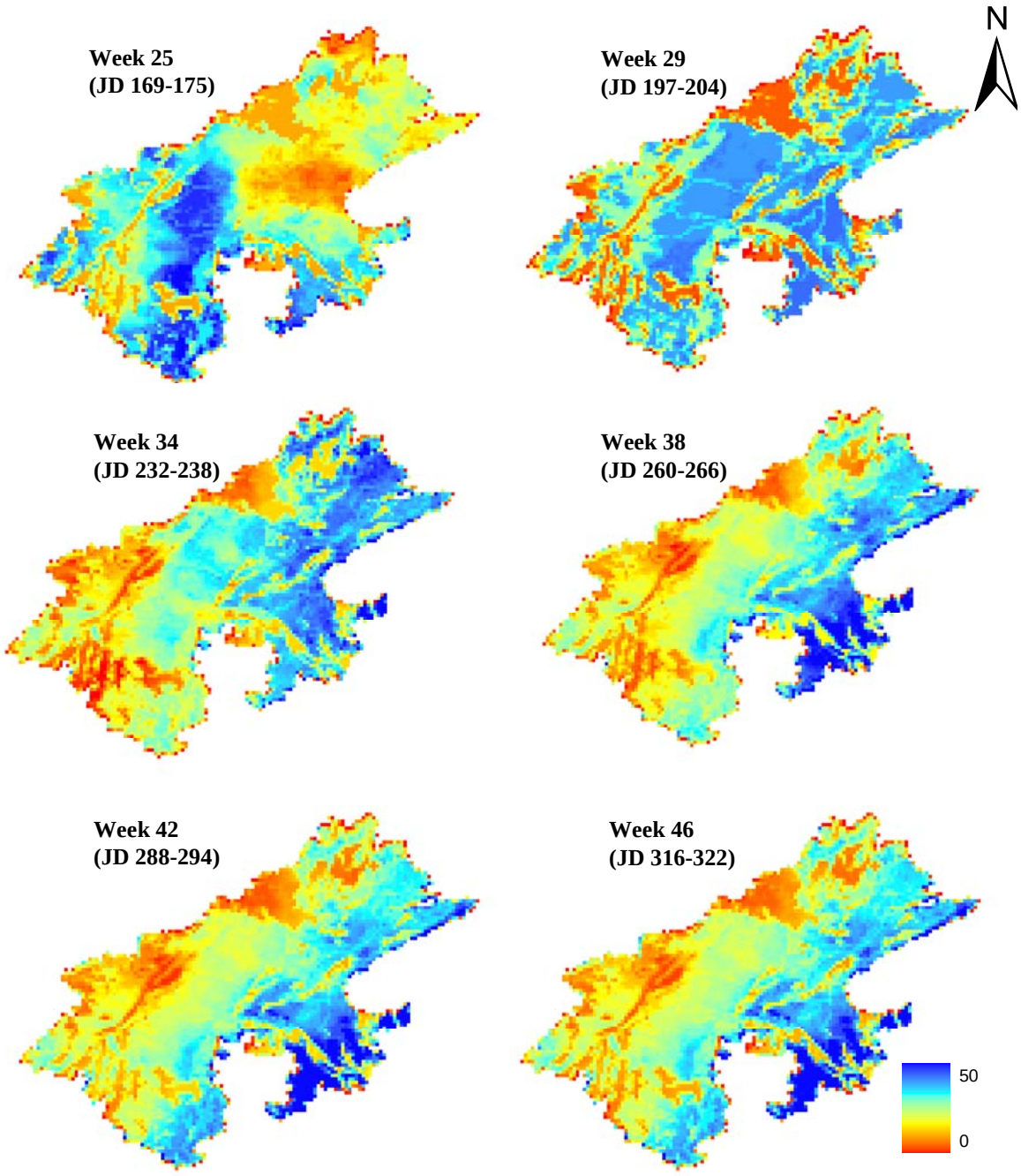

Figure 5-18: Spatio-temporal variation in volumetric soil moisture (% Vol) for the Khariff season, 2003

Likewise for potential evapotranspiration also, no correlation is evident, though the maximum crop evapotranspiration, because of the crop coefficient, does show an effect. The crop coefficients of the prominent crops were given as different inputs for the four phenological stages namely the initial season, crop development stage, mid season or reproductive stage and late season or maturity stage as shown in the graphs in Figure 5-18.

The graphs show the trends of soil moisture profile from the sowing date to the date of harvesting of Bajra, Jowar & Maize. Bajra is sown in the first week of July which is the 23rd meteorological week. Jowar or sorghum is usually sown in the last week of June and harvested by first week of November

and maize is sown in the second week of July and harvested by first week of November. For all the crops, the model has generated a similar trend. The profile does not fluctuate much in the initial germination stage. Once the second stage, the crop development starts, the profile starts receding. It gives a peak whenever there is rain. At the start of the mid season of the crops, it shows a tendency to decrease steadily. The decrease from the start of mid – season can be attributed to the higher rate of evapotranspiration in this season due to high Kc. The rate of decrease for each crop signifies the influence of Kc which was highest for Sorghum (1.24 in the mid-season) which shows the steepest slope while decreasing. Bajra which has the least Kc, 1.02 in the mid season can be seen to be having a gradual slope. Similar results were observed by Mandal et al (Mandal et al 2007). Incorporating irrigation data can give different results with soil moisture rising whenever irrigation is provided, similar to the peaks observed here during high rains.

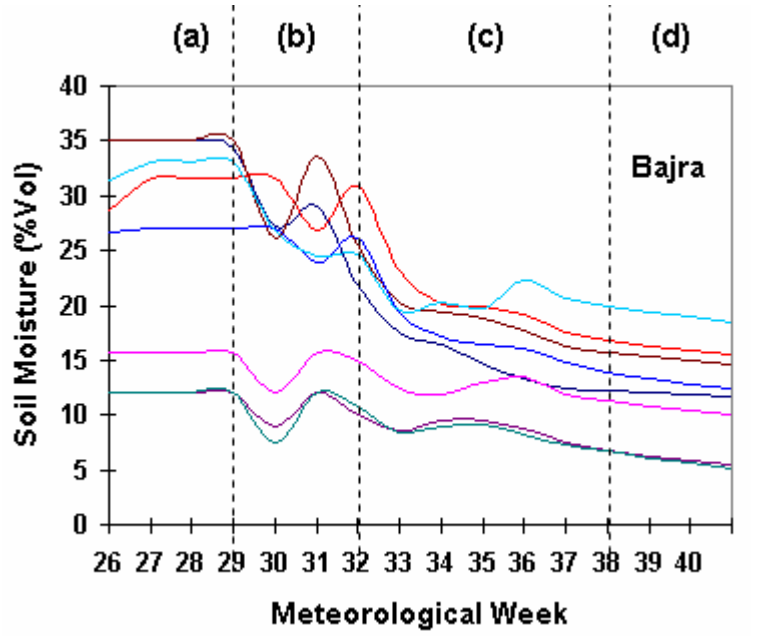

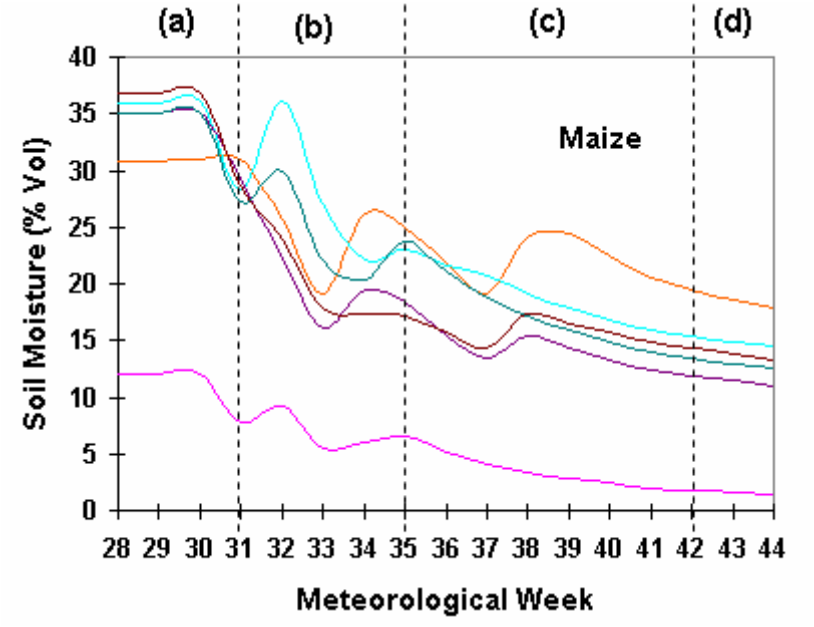

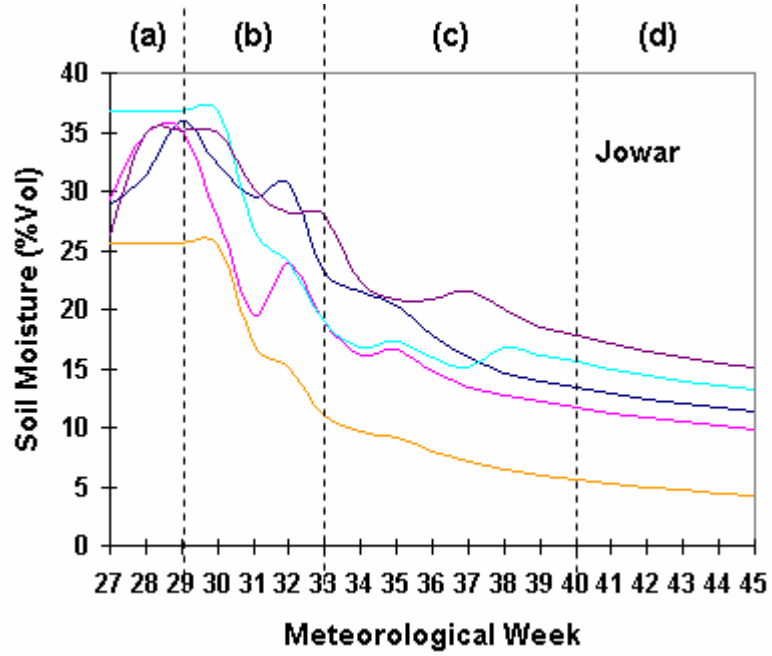

Figure 5-19: Variation in the soil Moisture profiles for Bajra, Maize and Jowar with the four crop phenological stages (a) Initial (b) Crop Development (c) Mid season and (d) Maturity

5.4. Statistical Comparison of Soil Moisture from Optical and Passive Microwave Remote Sensing Approaches with SWBM

Statistical Analysis was performed on soil moisture as inferred by the Optical Remote Sensing Approach and the parameters derived from Passive Microwave Remote Sensing Approach in relation to that simulated by the simple water balance model. The results obtained are discussed in the following sections.

5.4.1. Relationship of Vegetation Temperature Condition Index (VTCI) based Soil moisture with Simulated Soil Moisture from SWBM

Volumetric Soil moisture estimated from VTCI was analyzed with that simulated from the simple water balance model to assess its capability to infer soil moisture in the upper root zone. The 15 spatially variant grids in their 6 temporal periods were pooled for analysis. The relationships obtained were as given below in Figure 5-20. When grids of 5 * 5km, where the prominent crops dominate, were selected uniformly in the whole study area, the relation gave an RMSE of 7.04% with a correlation of 0.33 R^2. This relationship was further examined by regionalizing the grids. Seven grids in the semiarid region and seven grids in the sub humid region were plotted separately.

Better correlation & RMSE were obtained for the semi – arid region, where as it became worse for the sub –humid region. The higher RMSE observed can be attributed to the overall underestimation of soil moisture by the SWBM. The better value of the coefficient of determination (R^2) in the semi arid region shows that the ability of VTCI to estimate soil moisture beneath the surface is better in semi arid region than sub humid region. VTCI which is a drought monitoring index is generally found to indicate drought comparatively better in areas of moderate vegetation than in dense vegetation (Wang et al 2001). In our study area, the NDVI values in sub humid region are generally higher than in semi-arid region signifying the density of vegetation. So from the results obtained, it is clear that VTCI can indicate root zone soil moisture in semi arid area relatively better than in sub humid area.

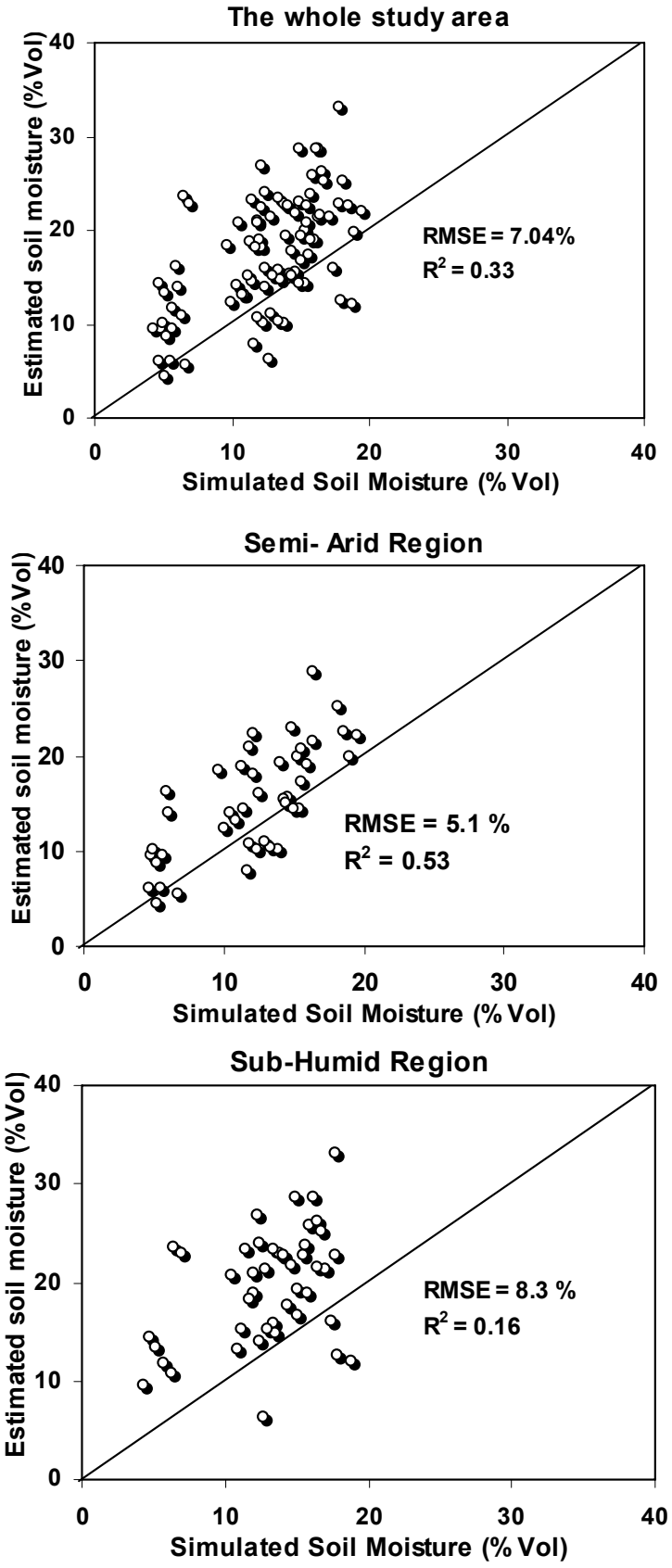

Figure 5-20: Relationship of Weekly Simulated soil moisture from SWBM and Estimated soil moisture from VTCI & In-situ Soil Moisture

The mean values of volumetric soil moisture content for the chosen samples simulated using the SWBM are 13.4% for semi arid region, 14.5% for the sub-humid region and 14.2% for the whole area. The resultant RMSE values convey that 62% in the semi-arid area and 44% in the sub-humid area have been correctly estimated. In the whole of the study area, 51% was estimated accurately.

5.4.2. Comparative Sensitivity of Horizontally Polarised Brightness Temperature (T_{BH}) with Simulated Soil Moisture from SWBM

The passive microwave horizontally polarized brightness temperature T_{BH} was regressed with the weekly simulated soil moisture (% vol.) to assess its ability to infer the spatio- temporal variation of soil moisture in the upper root zone. The analysis has been done separately for the climatic regions in the study area and for average values in 3 window sizes, one to one pixel, 3 * 3 pixel and 5 * 5 pixel windows. To compare the variation of T_{BH} with simulated soil moisture, both the datasets were subjected to generalization. Temporal aggregation was done for $T_{BH,}$ which is available for every alternate day. It was averaged on weekly basis from the third week of June to last week of November match with the temporal resolution of the weekly simulated soil moisture. The soil moisture was which simulated at a spatial resolution of 5 km was also aggregated to 25 km for the 24 weeks.

Prigent et al (Prigent et al 2005) have examined the relationship of T_{BH} as provided by the Special Sensor Microwave/Imager (SSM/I) and soil moisture at various locations on the globe. For India, they reported that T_{BH} provided by passive microwave remote sensed data gives inverse linear correlation with soil moisture when the vegetation density is minimal. As the vegetation density increase, the relationship turns positive. Our study, conducted for Eastern Rajasthan is seen to be yielding similar results for root zone soil moisture too. The results for the two climatic regions for the two frequencies in the different windows size adopted are summarized in the Table 5-6.

Climatic Region	***Frequency in GHz***	***Window Size for analysis***					
		1 pixel		***3*3 pixels***		***5 *5 pixels***	
		Slope	***R^2***	***Slope***	***R^2***	***Slope***	***R^2***
Semi - Arid	***6.9***	-0.293	0.75**	-2.501	0.71**	-1.428	0.43**
	36.5	-0.427	0.11	-0.047	0.003	0.165	0.04
Sub - Humid	***6.9***	-0.858	0.27**	-1.034	0.19*	0.223	0.02
	36.5	1.061	0.34	0.552	0.33*	0.632	0.536**

Table 5-6: Sensitivity of T_{BH} with simulated soil moisture from SWBM in different scenarios

** indicates Pearson's correlation coefficient is significant at 0.01 level (2-tailed)

* indicates Pearson's correlation coefficient is significant at 0.01 level (1-tailed)

The results indicate that the lower frequency, 6.9 GHz in semi arid climatic region gives the best correlation (Figure 5-22). It shows an inverse relation in all the window sizes considered, pixel by pixel, 3*3 and 5*5. This is in agreement with the results in previous work which showed sparse vegetation and low frequency can yield better relationship between microwave parameters and soil moisture (Prigent et al 2005). The sparse vegetation in the semi - arid and the inverse relationship of microwave frequencies with their sensing depths can be again presumed to be the reasons behind this result. At 6.9 GHz, the sub humid region also shows an inverse relation, but owing to the low R^2, the validation is doubtful. This lack of good relation shown by sub-humid region is due to the significant effect of denser vegetation present, compared to the semi-arid region. The mean NDVI for the semi

arid region is 0.3 for the season and 0.52 for the sub humid region. The variation of vegetation density as indicated by NDVI is shown in the spatial profile from sub-humid to semi-arid region given in Figure 5-21.

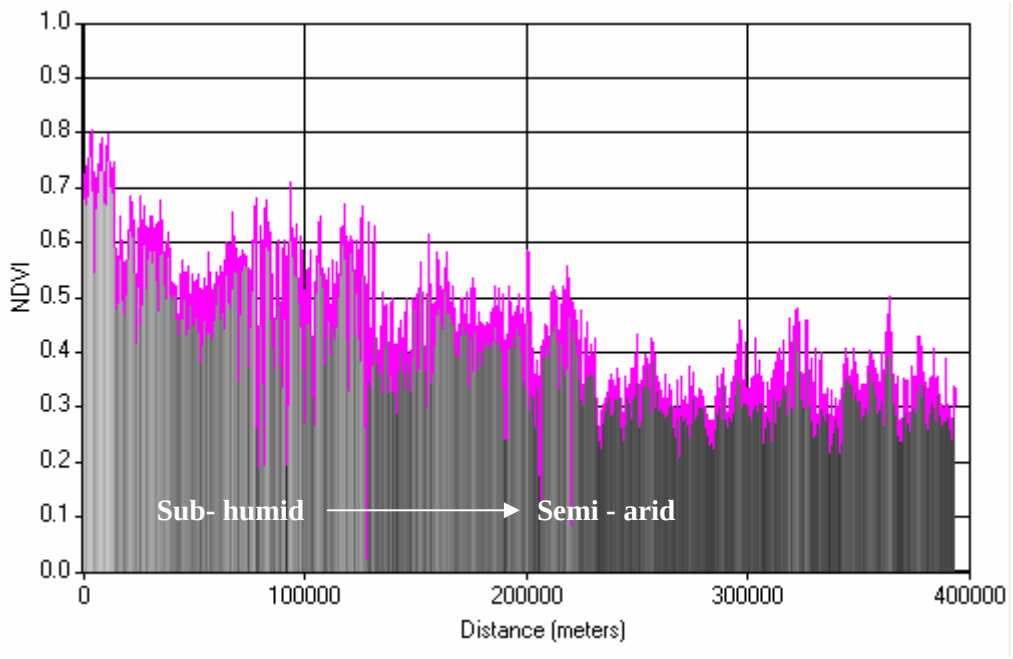

Figure 5-21 Spatial Variation in NDVI from Sub-humid (24^{o} 39' 60" N, 74^{o} 06' E) to Semi –arid (26^{o} 53' 04" N, 76^{o} 06' 02"E) region for JD 273

For 36.9 GHz in the semiarid region though having an inverse slope, does not qualify to be considered as the coefficient of determination is very low. The higher the frequency is, lower is the effect of root zone soil moisture. Also, when the frequency is higher, the influence of vegetation density also increases. The positive relations shown by 36.5 GHz in the sub humid region in all window sizes compared to the negative results given by 6.9 GHz for 1*1 pixel and 3*3 pixel sizes confirm this inference. The relationship for 6.9 GHz has turned positive in 5 * 5 window size which indicates the decrease in correlation when larger window average values are used. The rest of the plots too give the same trend in pixel by pixel, 3 * 3 and 5 * 5 window sizes, though the relations are relatively better when taken pixel by pixel.

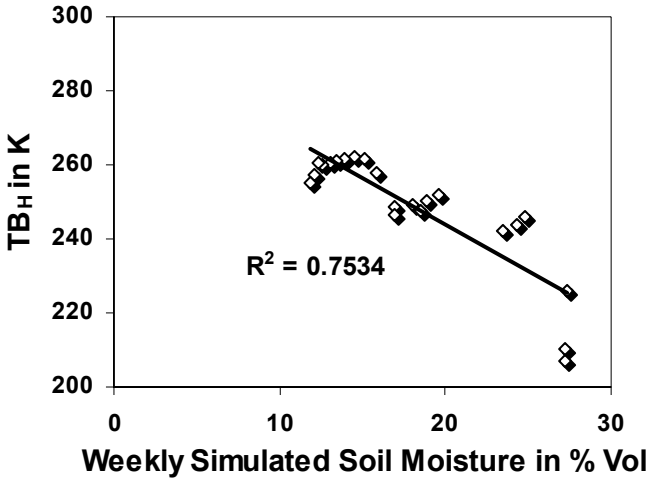

Figure 5-22: Plot showing relationship between T_{BH} and simulated soil moisture for semi-arid region (26^{o} 53' 04" N, 76^{o} 06' 02"E) at 6.9 GHz for 1*1 pixel window

5.4.3. Comparative Sensitivity of Polarisation Difference (PD) with Simulated Soil Moisture from SWBM

The passive microwave polarization difference (PD) was also regressed with the weekly simulated soil moisture (% vol.) to assess its ability to infer the variation of soil moisture in the upper root zone. In accordance with previous work (Prigent et al 2005), PD is seen to share a positive relationship with soil moisture. For India, it has been reported that PD provided by passive microwave remote sensed data gives positive linear correlation with soil moisture when the vegetation density is minimal. The results for the two climatic regions for the two frequencies in the different windows size adopted are summarized in table. Same trend in variation as T_{BH} can be observed.

In this case too, the best correlation was obtained in semi-arid region at 6.9 GHz frequency (Figure 5-23). The relationship obtained for semi-arid region for 6.9 GHz is presented in Figure 5-23. The relationship stays positive for 6.9 GHz in both the climatic regions but goes inverse for sub-humid at 36.5 GHz. The correlation and significance is less for sub- humid region as compared to the semi-arid region, the reason being the same as discussed in Section 5.4.2. The higher density of vegetation influences the relationship of soil moisture with PD also. The only noticeable difference from T_{BH} is that as the window size increased 36.5 GHz is observed to be giving better results in semi-arid region.

Climatic Region	Frequency in GHz	Window Size for analysis					
		1 pixel		3*3 pixels		5 *5 pixels	
		Slope	R^2	Slope	R^2	Slope	R^2
Semi - Arid	6.9	0.47	0.78**	2.038	0.71**	1.766	0.66**
	36.5	1.251	0.27	0.512	0.49**	0.625	0.65**
Sub - Humid	6.9	1.652	0.46**	0.701	0.26**	0.466	0.14
	36.5	1.873	0.11	-0.009	0.001	-0.056	0.03

Table 5-7: Sensitivity of PD with simulated soil moisture from SWBM in different scenarios

** indicates Pearson's correlation coefficient is significant at 0.01 level (2-tailed)

* indicates Pearson's correlation coefficient is significant at 0.01 level (1-tailed)

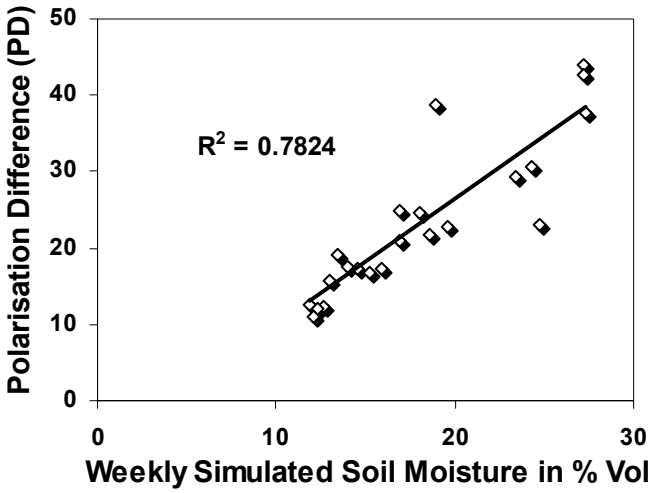

Figure 5-23: Plots showing relationship between PD and simulated soil moisture for semi-arid (26° 53' 04" N, 76° 06' 02"E) region at 6.9 GHz for 1*1 pixel window

The graphs presented in Figure 5-24 show the temporal variation of T_{BH} and PD with simulated soil moisture for 6.9 GHz. The negative relation of T_{BH} and positive relation of PD are evident from the profiles of semi-arid region. For the sub-humid region, the lack of correlation can also be seen. The significant use of passive microwave parameters in semi-arid environment, as indicators of soil moisture at the upper root zone is supported by the graphs. It is clear from the results presented that these parameters can depict only the temporal variability and not the spatial variability.

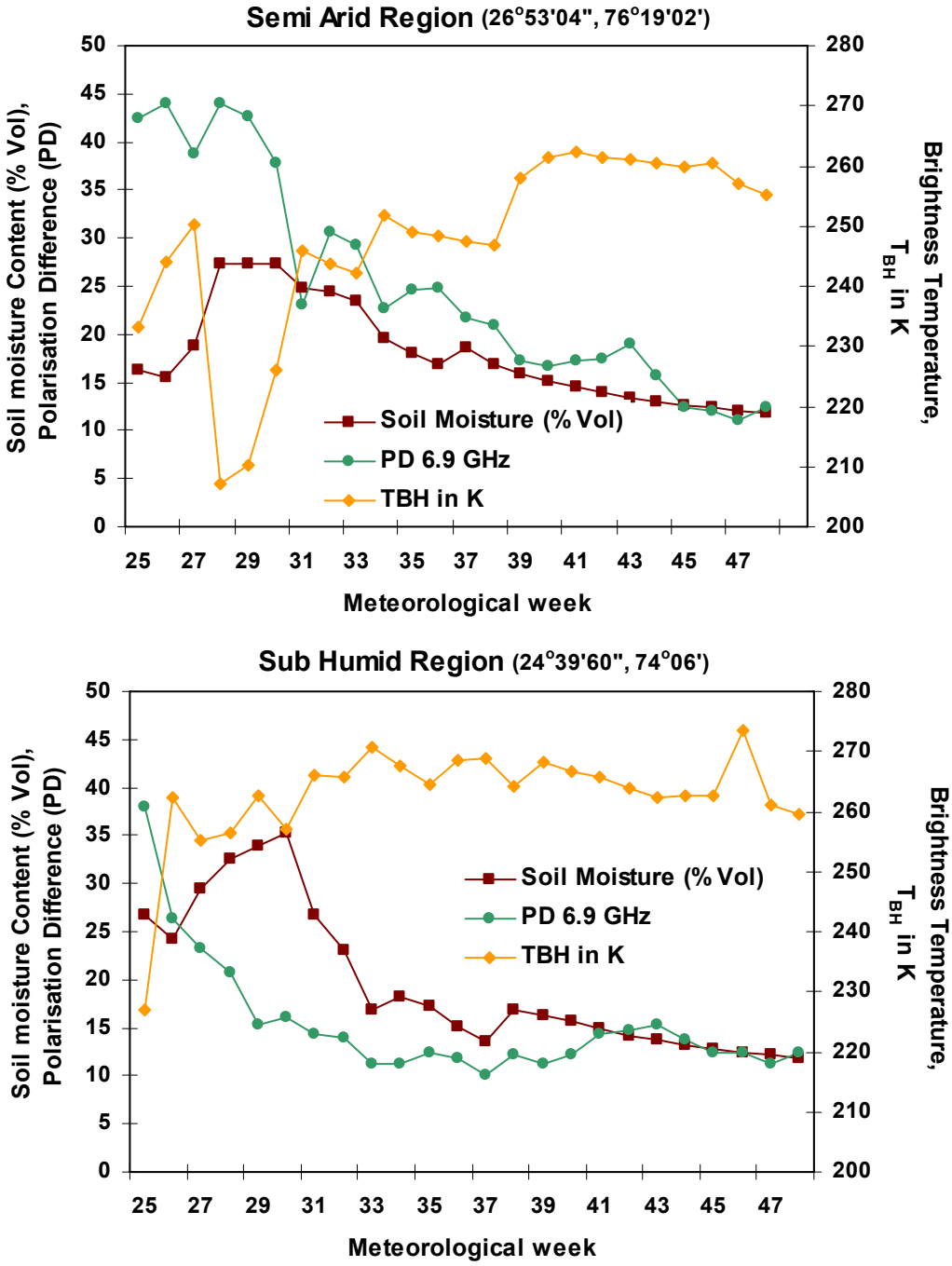

Figure 5-24: Temporal Variation of T_{BH} and PD with simulated soil moisture for different climatic region at 6.9 GHz

6. Conclusions and Scope for Further Research

This chapter discusses in detail conclusion arrived after examining the different methods and approaches adopted in the study for their utility in assessing soil- moisture in the upper root zone in the study area. It evaluates their effectiveness related to the study. The chapter ends with a note about the limitations of the research and recommendation for future studies in this topic.

6.1. Conclusion

The main objective of the study was to assess the performance of optical and passive microwave remote sensed data to infer soil moisture in the upper root zone for the prominent crops in Eastern Rajasthan. The spatio-temporal assessment by VTCI and the passive microwave parameters have been discussed in Sections 5.1.5 and 5.2.1 respectively. Because of lack of in –situ soil moisture measurements, the comparison of the estimate from optical data and the parameters derived from passive microwave data is done with weekly simulated soil moisture from a simple water balance model (SWBM). The SWBM gave its output at varying rooting depths for the crops according to their phenological stage. The comparison yielded relatively better results for semi – arid region where vegetation density is less, thereby leading to the overall conclusion that the use of VTCI and microwave parameters to infer soil moisture in the upper root zone, where maximum root activity of the prominent crops takes place is limited to sparse and moderately vegetative agricultural fields as found in semi-arid region.

Answers for the questions framed for the research and hypothesis validation are discussed below after careful interpretation of the results.

Question 1: Can VTCI be computed in a better method to correlate with the in –situ soil moisture in the upper root zone?
Answer: The optical remote sensed index, VTCI, was computed in two different ways other than the existing one desiring better results. But the methodology adopted confirmed the null hypothesis that VTCI estimated by method 1 gives the best correlation with soil moisture in the upper layer. The alternate hypothesis that VTCI can give better results when agriculture land-use is considered alone or that it can be obtained at a higher resolution by downscaling LST is rejected. If the downscaling was not done by DisTrad technique, which involves NDVI itself, the results may come different. With DisTrad technique, LST can not be downscaled to use for VTCI computation.

Question 2: Can Vegetation Temperature Condition Index from optical remote sensed data be used to infer the average soil moisture for the upper root zone?
Answer: The use of VTCI to estimate soil moisture in upper layer was examined using the weekly simulated measure from SWBM. The estimates from VTCI are relatively higher than that simulated measures. The underestimation by SWBM was not quantified and calibrated in this study. With the existing RMSE and Coefficient of Determination, the estimation is found to be better for semi –arid region than sub – humid region. The alternate hypothesis that optical remote sensed data can be used

to infer average soil moisture in the upper root zone is accepted only for semi-arid region. For sub humid region, the null hypothesis is accepted.

Question 3: Can parameters derived from passive microwave data be used to assess soil moisture for the upper root zone?
Answer: Horizontally polarised brightness temperature (T_{BH}) and Polarisation Difference (PD) were the parameters considered to answer this question. High correlation of T_{BH} and PD with simulated soil moisture from SWBM in the semi –arid region with low frequency micro wave data supports the usefulness of these parameters with low frequency microwave channels in semi –arid climatic region. For sub–humid areas, the efficiency is still questionable. So the null hypothesis that soil moisture in the upper root zone can not be inferred from passive micro wave data is rejected for semi –arid areas and at low frequency, but retained for elsewhere and with higher frequency.

6.2. Limitations of the study

The study undertaken is in the Khariff cropping season in India, which goes in rhythm with the southwest monsoons. The clouds cast by the monsoons caused unavailability of LST images which limited the proper use of VTCI for the season. So the study was done with the 6 images from the mid week of September to last week of October.

Lack of real time meteorological data required for the Simple Water Balance Model, hindered the calibration of the model for the study area thereby limiting the study to comparison between the estimates. If the model was calibrated for 2007, the estimation of soil moisture using VTCI could have been quantitatively validated. The model is also limited to rain fed crops as it irrigation data is not incorporated. Irrigation in Eastern Rajasthan is done using tube wells unlike the Indira Gandhi Canal in Western Rajasthan. So it cannot be expected to be available.

6.3. Scope for Further Research

The study evaluated the use of publicly available remote sensing data for assessing of soil moisture condition beneath the surface. The methodology successfully analyzed the questions framed for the research but in course of the study, ways to improve the methodology were recognized. They could not be incorporated because of the limitations given in section 6.1 and time constraints. Some of the recommendations to upgrade the methodology are listed below.

- This study was intended for the prominent crops in the Khariff season in Eastern Rajasthan. The field work was done in two stages, in an attempt to capture the variability of the relationship with VTCI and in-situ soil moisture with the different phenological stages. The cloud cover during the period limited the borders of the study. The soil moisture measurements taken from field during the initial stages gave a considerable correlation of 0.57 R^2, when tried with another optical index Shortwave Infrared Water Stress Index (SIWSI). This presents scope for further research by integrating short wave infrared and near infrared data for root zone soil moisture monitoring.

- The inherent cloud problem with VTCI will not be applicable if the research is done for the Rabi cropping season from November to April provided irrigation data is available.

- Antecedent Precipitation Index was tried to be computed solely from passive microwave parameters. This methodology could not be continued till the end because data of a single year has been considered. If yearly AMSRE data can be included in the methodology, it can be expected to yield better results for estimation of soil moisture.

- The simple water balance model can also provide Actual Evapotranspiration as output. This parameter along with soil moisture can be further used to assess the water deficit for the crops which can be linked to drought monitoring in the region.

7. References

Adegoke JO, Carleton AM. 2002. Relations between soil moisture and satellite vegetation indices in the U.S Corn Belt. *American Meteorological Society* 3: 395-405

Alemaw BF, Chaoka TR. 2003. A continental scale water balance model: a GIS approach for Southern Africa. *Physics and Chemistry of the Earth.* 28: 957-66

Allen RG, Pereira LS, Raes D, Smith M. 1998. *Crop evapotranspiration - Guidelines for computing crop water requirements - FAO Irrigation and drainage paper 56*, Fao and Agriculture Organisation of the United Nations, Rome, Italy

Arya LM, Richter JC, Paris JF. 1983. Estimating Profile Water Storage from Surface zone Soil Moisture Measurements Under Bare Field Conditions. *Water Resources Research* 19: 403-12

Boegh E, Soegaard H, Hanan N, Kabat P, Lesch L. 1998. A remote sensing study of the NDVI-Ts relationship and the transpration from sparse vegetation in the Sahel based on high resolution satellite data. *Remote Sensing of Environment* 69: 224-40

Boken VK. 2005. Agriculture Drought and Its Monitoring and Prediction: Some Concepts. In *Monitoring and Predicting Agricultural Drought*, ed. VK Boken, AP Cracknell, RL Heathcote, pp. 3-10. New York: Oxford University Press

Borg H, Grimes DW. 1986. Depth Development of roots with time: an empirical description. *Trans. ASAE* 29: 194-8

Brogaard S, Runnstrom M, Seaquist JW. 2005. Primary production of Inner Mongolia, China, between 1982 and 1999 estimated by a satellite data-driven light use efficiency model. *Global and Planetary Change* 45: 313-32

Carlson TN, Gillies RR, Perry E. 1994. A method to make use of thermal infrared temperature and NDVI measurements to infer surface soil water content and fractional vegetation cover. *Remote Sensing Reviews* 9: 161-73

Carlson TN, Gillies RR, Schmugge TJ. 1995. An interpretation of methodologies for indirect measurement of soil water content. *Agriculture for Meteorology* 77: 191-205

Carlson TN, Ripley DAJ, Schmugge TJ, eds. 2002. *Chapter 6: Rapid soil drying and its implications for remote sensing of soil moisture and the surface energy fluxes*. Florida: CRC Press

Ceballos A, Scipal K, Wagner W, Mertinez-fernandez J. 2005. Validation and downscaling of ERS Scatterometer derived soil moisture data over the central part of the Duero Basin, Spain. *Hydrological Processes* 19: 1549-66

Chauhan NS. 2003. Spaceborne soil moisture estimation at high resolution: a microwave optical/IR synergistic approach. *International Journal of Remote Sensing* 24: 459 - 622

Choudhury BJ, Blanchard BJ. 1983. Simulating soil water recession coefficients for agricultural watersheds. *Water Resources Bulletin* 19: 241 - 7

Choudhury BJ, Golus R, E. 1988. Estimating Soil Wetness using Satellite Data. *International Journal of Remote Sensing* 9:7: 1251-7

Choudhury BJ, Kerr YH, Njoku EG, Pampaloni P. 1995. *Passive Microwave Remote Sensing of Land - Atmosphere Interactions*. Presented at ESA/NASA International Workshop, St Lary, France

Choudhury BJ, Owe M, Goward SN, Golus R, E, Ormsby JP, et al. 1987. Quantifying Spatial and Temporal Variabilities of Microwave Brightness Temperature over the U.S Southern Great Plains. *International Journal of Remote Sensing* 8: 177 -91

Chow VT, Maidment DR, Mays LW. 1988. *Applied Hydrology*: McGraw-Hill. 572 pp.

Claps P, Laguardia G. 2004. *Assessing spatial variability of soil water content through Thermal Inertia and NDVI*. Presented at Remote Sensing for agriculture, ecosystems and hydrology V,Proceedings of SPIE, Bellingham

Dadhwal VK, Patel NR. 2007. *Remote Sensing and Soil Moisture Estimation, Lecture presented at Winter School on Micrometeorology on drought*, KHEDA, Rajasthan, India

de Troch FP, Troch PA, Su Z, Lin DS, eds. 1996. *Chapter 9: Application of Remote Sensing for Hydrological Modelling*. Dordrecht: Kluwer Academic Publishers

Dobson MC, Ulaby FT, Hallikainen MT, El-Rayes MA. 1985. Microwave dielectric behaviour of wet soil - part 2: dielectric mixing models. *IEEE Transactions for Geosciences and Remote Sensing* GE-23: 35-46

Doorenboos J, Pruitt WO. 1977. *Guidelines for predicting crop water requirements*, UN- FAO, Rome

Engman ET. 1990. Progress in Microwave Remote Sensing of Soil Moisture. *Canadian Journal of Remote Sensing* 16: 6-14

Engman ET, Chauhan N. 1995. Status of Microwave Soil Moisture Measurements with Remote Sensing. *Remote Sensing of Environment* 35: 213 - 26

Engman T. 1991. Application of remote sensing of soil moisture for water resources and agriculture. *Remote Sensing of Environment* 35: 213-26

Entekhabi D, Nakamura H, Njoku EG. 1994. Solving the Inverse Problem for Soil Moisture and Temperature Profiles by Sequential assimilation of Multifrequency Remotely Sensed Observations. *IEEE Transactions for Geosciences and Remote Sensing* 32: 438-48

Farrar TJ, Nicholson SE, Lare AR. 1994. The influence of soil type on the relationships between NDVI, rainfall and soil moisture in semiarid Botswana. 2. NDVI response to soil moisture. *Remote Sensing of Environment* 50: 121-33

Felde GW. 1998. The Effect of Soil Moisture on the 37 GHz Microwave Polarisation Difference Index (MPDI). *International Journal of Remote Sensing* 19: 1055-78

Friedl MA, Davis FW. 1994. Sources of variation in radiometric surface temperature over a tallgrass prairie. *Remote Sensing of Environment* 48: 1-17

Galantowicz JF, Entekhabi D, Jackson TJ. 1999. Efficient Models of Soil Heat and Water Flow and Emission for Moisture and Temperature Determination from Remote Sensing Observations. *IEEE Transactions for Geosciences and Remote Sensing*

Gillies RR, Carlson TN. 1995. Thermal Remote Sensing of Surface Soil Water Content with Partial Vegetation Cover for Incorporation into Climate Models. *Journal of Applied Meteorology* 34: 745-56

Gillies RR, Carlson TN, Kustas W, Humes K. 1997. A verification of the 'triangle' method for obtaining surface soil water content and energy fluxes from remote measurements of the Normalised Difference Vegetation Index (NDVI) and surface radiant temperature. *International Journal of Remote Sensing* 18: 3145-66

Goetz SJ. 1997. Multisensor analysis of NDVI, surface temperature and biophysical variables at a mixed grassland site. *International Journal of Remote Sensing* 18: 71-94

Goward SN, Xue Y, Czarjkowski KP. 2002. Evaluating land surface moisture conditions from the remotely sensed temperature/vegetation index measurement: An exploration with the simplified simple biosphere model. *Remote Sensing of Environment* 79: 225-42

Guariso G, Walker J. 2005. *A multi-sensor approach for surface soil estimation: A Field Study in Eastern Australia*, Polytechnic of Milan

Holmes T. 2003. *Measuring surface soil parameters using passive microwave remote sensing: The ELBARA Field Experiment*. Vrije Universiteit, Amsterdam

Jackson TJ, ed. 2005. *Passive Microwave Remote Sensing of Soil Moisture and Regional Drought Monitoring*. New York: Oxford University Press. 89-104 pp.

Jackson TJ, Hawley ME, O'Neill PE. 1987. Preplanting Soil Moisture Using Passive Microwave Sensors. *Water Resources Bulletin* 23: 11-9

Jackson TJ, Schmugge TJ. 1991. Vegetation Effects on the Microwave Emission of Soils. *Remote Sensing of Environment* 36: 203-12

Jackson TJ, Schmugge TJ, Engman ET. 1996. Remote Sensing Applications to Hydrology: Soil Moisture. *Hydrological Sciences Journal* 41: 517-30

Jackson TJ, Schmugge TJ, Nicks AD, Coleman GA, Engman ET. 1981. Soil Moisture Updating and Microwave Remote Sensing for Hydrological Simulation. *Hydrological Sciences Bulletin* 26: 305 -19

Jensen ME, Haise HR. 1963. Estimating evapotranspiration from solar radiation. *Journal of Irrigation and Drainage Division of The American Society of Civil Engineers* 89: 15-41

Jordan JD, DShih SF. 1993. Comparison of Thermal based Soil Moisture Estimation Techniques ona Histosol. *Soil and Crop Science Society of Florida Proceedings.* 52: 83

Jupp DLB, Guoliang T, McVicar TR, Yi Q, Fuqin L. 1998. *Soil Moisture and Drought Monitoring Using Remote Sensing 1: Theorotical Background and Methods*, CSIRO Australia

Khichar ML, Niwas R, Prakash O. 2003. Crop coefficients of pearl millet (Pennisetum Glaucum) under rainfed condition. *Annals of Agricultural Research New Series* 24: 838 - 41

Kramer PJ. 1969. *Chapter 4: Roots and Root Growth Development*. New Delhi: Tata McGraw Hill Publishing Company

Kustas WP, J.M N, Anderson MC, French AN. 2003. Estimating subpixel surface temperatures and energy fluxes from the vegetation index-radiometric temperature relationship. *Remote Sensing of Environment* 85: 429-40

Liang S. 2003. *Quantitative Remote Sensing of Land Surfaces*: John Wiley & Sons, INC.

Loew A. 2007. Impact of Surface Heterogeneity on Surface Soil Moisture Retreivals from Passive Microwave Data at the Regional Scale: The Upper Danube Case. *Remote Sensing of Environment* doi :10.1016/j.rse.2007.04.009

Magagi RD, Kerr YH. 2001. Estimating surface soil moisture and surface roughness over semiarid areas from the use of the copolaristaion ratio. *Remote Sensing of Environment* 75: 432-45

Mandal UK, K.S.S S, Victor US, Rao NH. 2002. Profile water balance model under irrigated and rainfed systems. *Agronomy Journal* 94: 1204-11

Mandal UK, Victor US, Srivastava NN, Sharma KL, Ramesh V, et al. 2007. Estimating yield of sorghum using root zone water balance model spectral characteristics of crop in a dryland Alfisol. *Agricultural Water Management* 87: 315-27

Masek CH. 2002. *Adapting the SCS Method for Estimating Runoff in Shallow Water Table Environments*. M.Sc thesis. University of South Florida, South Florida

McVicar TR, Bierwirth PN. 2001. Rapidly assessing the 1997 Drought in Papua New Guinea using composite AVHRR imagery. *International Journal of Remote Sensing* 22: 2109-28

McVicar TR, Jupp DLB. 1998. The current and potential operational uses of remote sensing to aid decisions on drought exceptional circumstances in Australia: a review. *Agricultural Systems* 57: 399-468

Ministry of Agriculture. 1972. *Handbook on Hydrology*. New Delhi: Govt of India

Mishra SK, Singh VP. 2003. *Soil Conservation Service Curve Number (SCS - CN) Methodology*: Springer

Mo T, Choudhury BJ, Schmugge TJ, Jackson TJ. 1982. A Model for Microwave Emission from Vegetation Covered Fields. *Journal of Geophysical Research* 87: 11229-37

Mohanty BP, Skaggs TH. 2001. Spatio-temporal evolution and time-stable characteristics of soil moisture within remote sensing footprints with varying soil, slope, and vegetation. *Advances in Water Resources* 24: 1051 - 67

Moran MS, Clarke TR, Inoue Y, Vidal A. 1994. Estimating crop water deficit using the relation between surface - air temperature and spectral vegetation index. *Remote Sensing of Environment* 49: 246-63

Mutreja KN. 1986. Applied Hydrology. pp. 290-339. New Delhi: Tata McGraw-Hill Publishing Company Ltd.

Njoku EG, Entekhabi D. 1996. Passive Microwave Remote Sensing of Soil Moistrue. *Journal of Hydrology* 184: 101-29

Njoku EG, Kong JA. 1977. Theory for passive microwave remote sensing of near-surface soil moisture. *Journal of Geophysical Research* 82: 3108-18

Ottle C, Vidal-Madjar D. 1994. Assimilation of soil moisture Inferred from Infrared Remote Sensing in a Hydrological Model over the HAPEX-MOBILHY Region. *Journal of Hydrology* 158

Parida BR. 2006. *Analysing the effect of severity and duration of Agricultural drought on crop performance using Terra/MODIS Satellite data and Meteorological data*. M.Sc thesis. International Institute for Geo-information Science and Earth Observation, Enschede. 104 pp.

Patel NR, Kumar S, Pande LM. 2006. Quantification of Water Limited Yield in Rainfed Crops using GIS based Modeling. *Journal of Applied Hydrology* XVII: 60 - 8

Peacock JM, Wilson GL, eds. 1984. *Chapter 7: Sorghum*. Chichester: John Wiley & Sons Ltd. 261 pp.
Pearson C, ed. 1984. *Chapter 8: Pennisetum Millet*. Chichester: John Wiley & Sons Ltd. 289 pp.
Pimenta MT. 2000. Water Balances Using GIS. *Physics and Chemistry of the Earth.* 25: 695 - 8
Price JC. 1980. The potential of remotely sensed thermal infrared data to infer surface soil moisture and evaporation. *Water Resources Research* 16: 787-95
Price JC. 1985. On the analysis of thermal infrared: the limited utility of Apparent thermal inertia. *Remote Sensing of Environment* 18: 59-73
Prigent C, Aires F, Rossow WB, Robock A. 2005. Sensitivity of Satellite Microwave & Infrared Observations to Soil Moisture at a Global Scale: Relationship of Satellite Observations to In-situ Soil Moisture Measurements. *Journal of Geophysical Research* 110
Prince SD, Goward SN. 1995. Global Primary Production: a remote sensing approach. *Journal of Biogeography* 22
Rajalakshmi TK. 2003. Drought: From bad to worse in Rajasthan. *Frontline* 20
Raju S, Chanzy A, Wigneron JP, Calvet JC, Kerr YH, Laguerre L. 1995. Soil moisture and temperature profile effects on microwave emission at low frequencies. *Remote Sensing of Environment* 54: 85-97
Rao NPV, Venkataratnam L, Rao KPV, Ramana KV, Singarao MN. 1993. Relation between root zone soil moisture and normalised diference vegetation index of vegetated fields. *International Journal of Remote Sensing* 14: 441-9
Rathore MS. 2005. *State level analysis of drought policies and impacts in Rajasthan, India.*, Colombo, Sri Lanka: IWMI. 40p. (Working paper 93 : Drought Series Paper No. 6)
Reichle R, Walker JP, Koster RD, Houser PR. 2002. Extended vs Ensemble Kalman Filtering for Land Data Asssimilation. *Journal of Hydrometeorology* 3: 728-40
Sadeghi AM, Hancock GD, Waite WP, Scott HD, Rand JA. 1984. Microwave Measurements of Moisture Distributions in the Upper Soil Profile. *Water Resources Research* 20: 927 - 34
Sahu D. 1990. *Land Forms hydrology and sedimentation*. Calcutta, India: Naya Prakash Publication
Sandholt I, Rasmussed K, Anderson J. 2002. A simple interpretation of the surface temperature/vegetation index space for assessment of the surface soil moisture status. *Remote Sensing of Environment* 79: 213-24
Saxton KE, Rawls W. 2006. Soil Water Characteristic Estimates by Texture and Organic Matter for Hydrologic Solutions.
Schmugge TJ, ed. 1985. *Chapter 5: Remote Sensing of Soil Moisture*. New York: John Wiley and Sons. 101 - 24 pp.
Schmugge TJ, Jackson TJ, McKim HL. 1980. Survey of Methods for soil moisture determination. *Water Resources Research* 16: 961 - 79
Shyampura RL, Sehgal J. 1995. Soils of Rajasthan for Optimising Land Use. In *NBSS Publications, Soils of India Series*. Nagpur, India: National Bureau of Soil Survey And Landuse Planning
Smith AM, Scipal K, Wagner W, eds. 2005. *Active Microwave Systems for Monitoring Drought Stress*. New York: Oxford University Press. 105-18 pp.
Smith RCG, Choudhury BJ. 1991. Analysis of normalised difference and surface temperature observations over southeastern Australia. *International Journal of Remote Sensing* 12: 2021-40
Song J, Weseley ML, Coulter RL, Brandes EA. 2000. Estimating watershed evapotranspiration with PASS. Part 1: Inferring rootzone soil moisture conditions using satellite data. *Journal of Hydrometeorology* 1: 447-60
Teng WL, Wang JR, Doraiswamy PC. 1993. Relationship between Satellite Microwave Radiometric Data, Antecedent Precipitation Index and Regional Soil Moisture. *International Journal of Remote Sensing* 14: 2483-500
Thornthwaite CW, Mather JR. 1955. *The Water Balance*, Drexel Institutional Laboratory for Climatology, Centeron, N.J, New Jersey
Tyagi NK, Sharma DK, Luthra SK. 2000. Evapotranspiration and Crop Coefficients of Wheat and Sorghum Climate in India. *Journal of Irrigation and Drainage Engineering* 126: 215-22
Tyagi NK, Sharma DK, Luthra SK. 2003. Determination of evapotranspiration for maize and berseem clover. *Irrigation Science* 21: 173-81

USDA. 1972. *National Engineering Handbook. Section 4. hydrology. USDA SCS*. Tolland, CT: USDA-NRCS

Van de Griend AA, Engman ET. 1985. Partial Area Hydrology and Remote Sensing. *Journal of Hydrology* 81: 211-51

Van Oevelen PJ. 2000. *Estimation of areal soil water content through microwave remote sensing*. Doctoral thesis. Wageningen University. 227 pp.

Verstraeten WW, Veroustraete F, van der Sande CJ, Grootaers I, Feyen J. 2006. Soil moisture retrieval using thermal inertia determined with visible and thermal spaceborne data, validated for European forests. *Remote Sensing of Environment* 101: 299 - 314

Volkmar KM, Woodbury W, eds. 1995. *Plant - Water Relationships*. New York: Maecel Dekker. 23 - 43 pp.

Walker JP, Houser PR. 2001. A Methodology for Initializing Soil Moisture in a Global Climate Model: Assimilation of Near-surface Soil Moisture Observations. *Journal of Geophysical Research* 106: 11 761 - 11 74

Wang JR, O'Neill PE, Jackson TJ, Engman ET. 1983. Multifrequency Measurements of the Effects of Soil Moisture, Soil Texture and Surface Roughness. *IEEE Transactions for Geosciences and Remote Sensing* GE-21: 44-51

Wang JR, Schmugge TJ. 1980. An empirical model for the complex dielectric permittivity of soils as a function of water content. *IEEE Transactions for Geosciences and Remote Sensing* GE -18: 28 - 295

Wang L, Qu JJ, Zhang S, Hao X, Dasgupta S. 2007a. Soil moisture estimation using MODIS and ground measurements in eastern China. *International Journal of Remote Sensing* 28: 1413 - 8

Wang PX, Li XW, Gong Jy, Song C. 2001. *Vegetation Temperature Condition Index and Its Application for Drought Monitoring*. Presented at Proceedings of InternationaI Geoscience and Remote Sensing Symposium, Sydney, Australia

Wang X, Xie H, Guan H, Zhou X. 2007b. Different responses of MODIS-derived NDVI to root-zone soil moisture in semi-arid and humid regions. *Journal of Hydrology* 340: 12-24

Watts G, ed. 1997. *Chapter 5: Hydrological Modelling in Practice*. West Sussex, England: John Wiley & Sons Ltd.

Wetzel PJ, Atlas D, Woodward RH. 1984. Determining soil moisture from geosynchronous satellite infrared data: A feasibility study. *Journal of Climatology and Applied Meteorology* 23: 375-91

Wigneron JP, Kerr Y, Chanzy A, Jin Y, Q. 1993. Inversion of Surface Parameters from Passive Microwave Measurements over a Soyabean Field. *Remote Sensing of Environment* 46: 61-72

Wigneron JP, Schmugge TJ, Chanzy A, Calvet JC, Kerr Y. 1998. Use of Passive Microwave Remote Sensing to Monitor Soil Moisture. *Agronomie* 18: 27-43

Wilheit TT. 1978. Radiative Transfer in a Plane Stratified Dielectric. *IEEE Transactions for Geosciences and Electronics* GE - 16: 138-43

Xue Y, Cracknell A. 1995. Advanced thermal inertia modeling. *International Journal of Remote Sensing* 16: 431

Yang X, Tian G. 1991. *A remote sensing model for wheat drought monitoring*. Presented at Proceedings of the 12th Asian Conference on Remote Sensing, SEAMEO, Singapore

Zegelin S. 1996. *Soil Moisture Measurement*. Presented at Field Measurement Techniques in Hydrology, Cooperative Research Centre for Catchment Hydrology, Corpus Christi College, Clayton

URLs

1. Department of Agriculture, Rajasthan.(www.rajasthankrishi.gov.in) Last Accessed Date: 21/12/07

8. Appendices

Appendix 1: Values of Crop Coeffcients and length of crop phenological stages

Crop	Initial Season		Crop Development Season		Mid Season (Reproductive)		Late Season (Maturity)	
	Length (in days)	Kc	Length (in days)	Kc	Length (in days)	Kc	Length (in days)	Kc
Pearl Millet[1]	15	0.45	25	0.82	40	1.02	25	0.43
Sorghum[2]	20	0.53	35	0.82	45	1.24	30	0.85
Maize[3]	20	0.55	35	1.0	40	1.23	30	0.64
Other Crops[4]	30	0.55	45	1.1	40	1.1	28	0.75
Scrubs[5]	10	0.85	20	1.05	-	0.85	-	0.85
Forest[6]	-	1.0	-	1.0	-	1.0	-	1.0
Barren[7]	-	0.4	-	0.4	-	0.4	-	0.4
Water[8]	-	1.05	-	1.05	-	1.05	-	1.05

[1]*Estimated for Hisar station in(Khichar et al 2003)*
[2]*Estimated for Karnal station in(Tyagi et al 2000)*
[3]*Estimated for Karnal station in(Tyagi et al 2003)*
[4]*Averaged values for Legumes & Vegetables given in the FAO database (Doorenboos & Pruitt 1977) which constitute the majority of the other crops.*
[5]*Assumed to be same as that of grass pasture provided in the FAO database (Allen et al 1998, Doorenboos & Pruitt 1977)*
[6]*Assumed to be same as that of Conifer trees provided in the FAO database (Doorenboos & Pruitt 1977)*
[7]*Assumed to be same as that of agricultural area in non growing times, provided in the FAO database (Doorenboos & Pruitt 1977)*
[8]*Taken from FAO database (Doorenboos & Pruitt 1977)*

Appendix 2: Rainfall Series Maps for third weeks of (a) June (b) July (c) August and (d) September

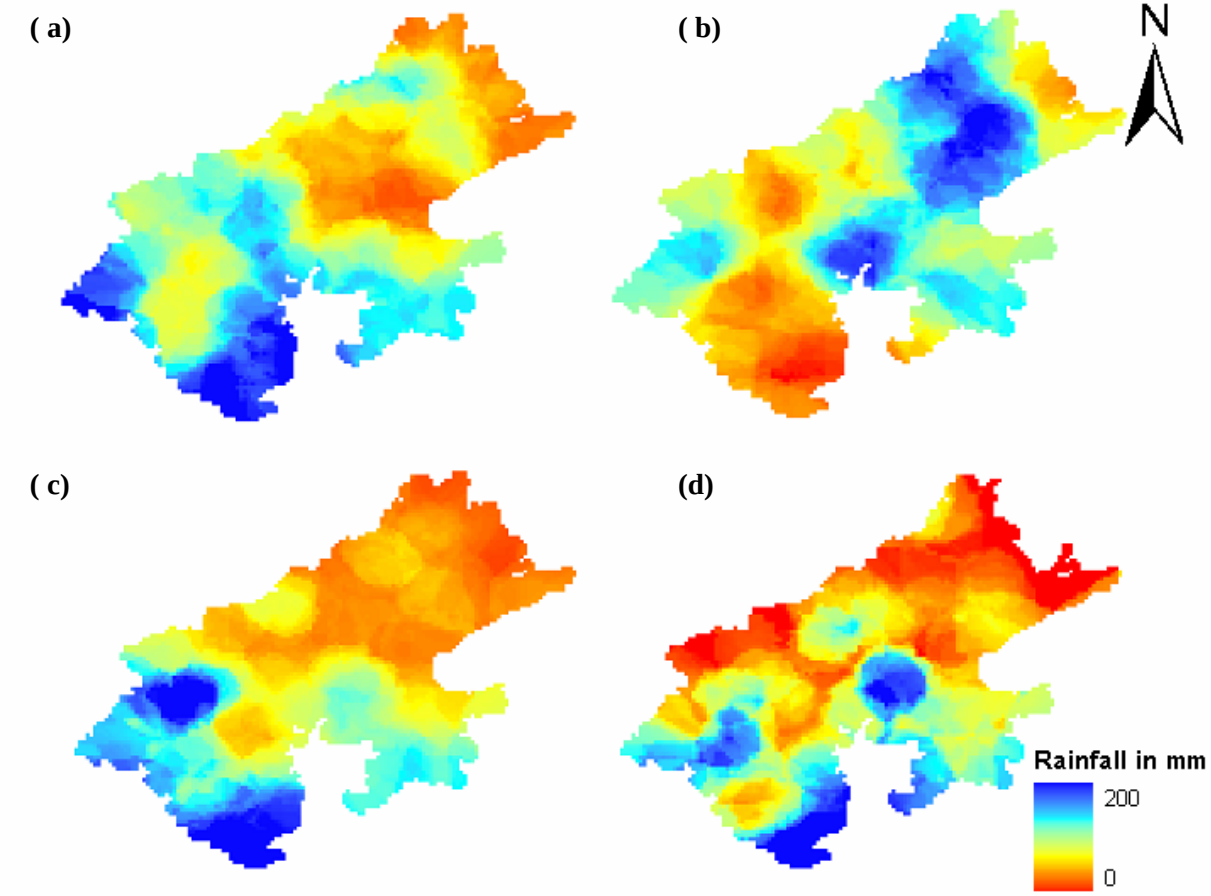

Appendix 3: Procedure for quantification of Runoff

The inputs considered to identify the Curve Number for a particular grid are

1. Landuse map: The NDVI image of the study area was classified based on their temporal profiles. The first level classes which include Agricultural land, Forest or thick natural vegetation, Scrubs or thin natural vegetation, Barren or Fallow land and Water were used (Ref Section 4.2.1).

2. Hydrologic Soil Group (HSG): This input integrates the soil properties, namely soil texture, depth and drainage. The four groups namely A, B, C and D are briefed below (Mishra & Singh 2003).

Group A
(Infiltration rate is between 0.002 & 0.003 mm/sec)
The soils in this group have high infiltration rates even when they are thoroughly wetted, high rate of water transmission and low runoff potential and low runoff potential. They include primarily deep, well to excessively drained sands or gravels.
Group B
(Infiltration rate is between 0.001 & 0.002 mm/sec)
These soils have moderate infiltration rates when thoroughly wetted and moderate rates of water transmission. They consist primarily of moderately deep to deep, moderately well to well drained soils with fine, moderately fine to moderately coarse texture like shallow loess & sandy loam.
Group C
(Infiltration rate is between 0.0003 & 0.001 mm/sec)
The soils that fall under this group have low rates of infiltration when thoroughly wetted and also a slow rate of water transmission. They are of moderately fine to fine texture as clay loams, shallow sandy loam and soils low in organic content.
Group D
(Infiltration rate between 0 & 0.0003 mm/sec)
Soils of this group exhibit very low rates of infiltration when they are thoroughly wetted and very slow rates of transmission. They include primarily clay soils of high swelling potential, soils with a permanent high water table, soils with a clay pan or clay layer at or near the surface, and shallow soils over nearly impervious material.
Using the soil properties maps prepared by NBSS, the HSG groups were classified. Given below are the classes for each parameter considered to categorise into HSGs.

3. Antecedent Moisture Condition (AMC) which is the index of the soil condition with respect to runoff potential before the storm. Both the original procedure of USDA and its Indian modification, defines three AMCs corresponding to dry, average and wet moisture conditions. These conditions are derived empirically using the cumulative rainfall in the previous 5 days. Daily rainfall was interpolated using Modified Inverse Distance Weighted Average Method and for every day, the precipitation for the previous five days is summed up.

Criteria for classification of HSG

Hydrologic Soil Group	Soil Texture	Soil Depth	Soil Drainage
Group A	Sandy	Deep, > 1000 mm	Excessive and Somewhat excessive
Group B	Coarse loamy	Moderately deep 750 – 1000 mm	Well and Moderately well
Group C	Loamy, Fine loamy, Fine	Moderately shallow and Shallow 250 – 750 mm	Imperfect and Poor
Group D	Clayey, Rock outcrops	Very shallow and Extremely shallow < 250 mm	Very poor and Extremely poor

Thresholds for AMC classes

AMC Class	AMC (mm)	Condition
I	< 35	Dry soil but not the wilting point
II	35 – 52.5	Average Conditions
III	> 52.5	Saturated soils, heavy rainfall or light rain

Curve Numbers adopted for each landuse

Land use	Adopted Literature and Corresponding description	Hydrologic Soil Group			
		A	B	C	D
Agricultural Land	Cultivated Land: Without conservation treatment (Chow et al 1988)	72	81	88	91
Scrub/ thin natural vegetation	Pasture or range land : poor condition (Chow et al 1988)	68	79	86	89
Forest/ Thick natural vegetation	Wood or forest land: good cover (Chow et al 1988)	25	55	70	71
Barren/ Fallow	Fallow: Bare soil (Mishra & Singh 2003)	77	86	91	94

Depending on these three inputs, the values of curve number for AMC II were adopted from the tables given in ((Chow et al 1988),(Mishra & Singh 2003)). For the landuse and HSGs in the study area, the CNs adopted under AMC II are tabulated above.From the CNs identified for AMCII, CNs for AMC I and AMC III are calculated using the following equations (Chow et al 1988).

$$CN1 = \frac{(4.2 * CN2)}{(10 - (0.058 * CN2))}$$ **Equation 8-1**

$$CN3 = \frac{(23 * CN2)}{(10 + (0.13 * CN2))}$$ **Equation 8-2**

Appendix 4: Field Capacity for different Soil Textures

Soil Texture	*Field Capacity*
Sand	***12.1***
Coarse Loamy	***26.7***
Loamy	***26.7***
Fine Loamy	***35.0***
Fine	***37.1***
Clay	***42.0***

Appendix 5: Effective Rainfall Series Maps of third weeks for (a) June (b) July (c) August and (d) September

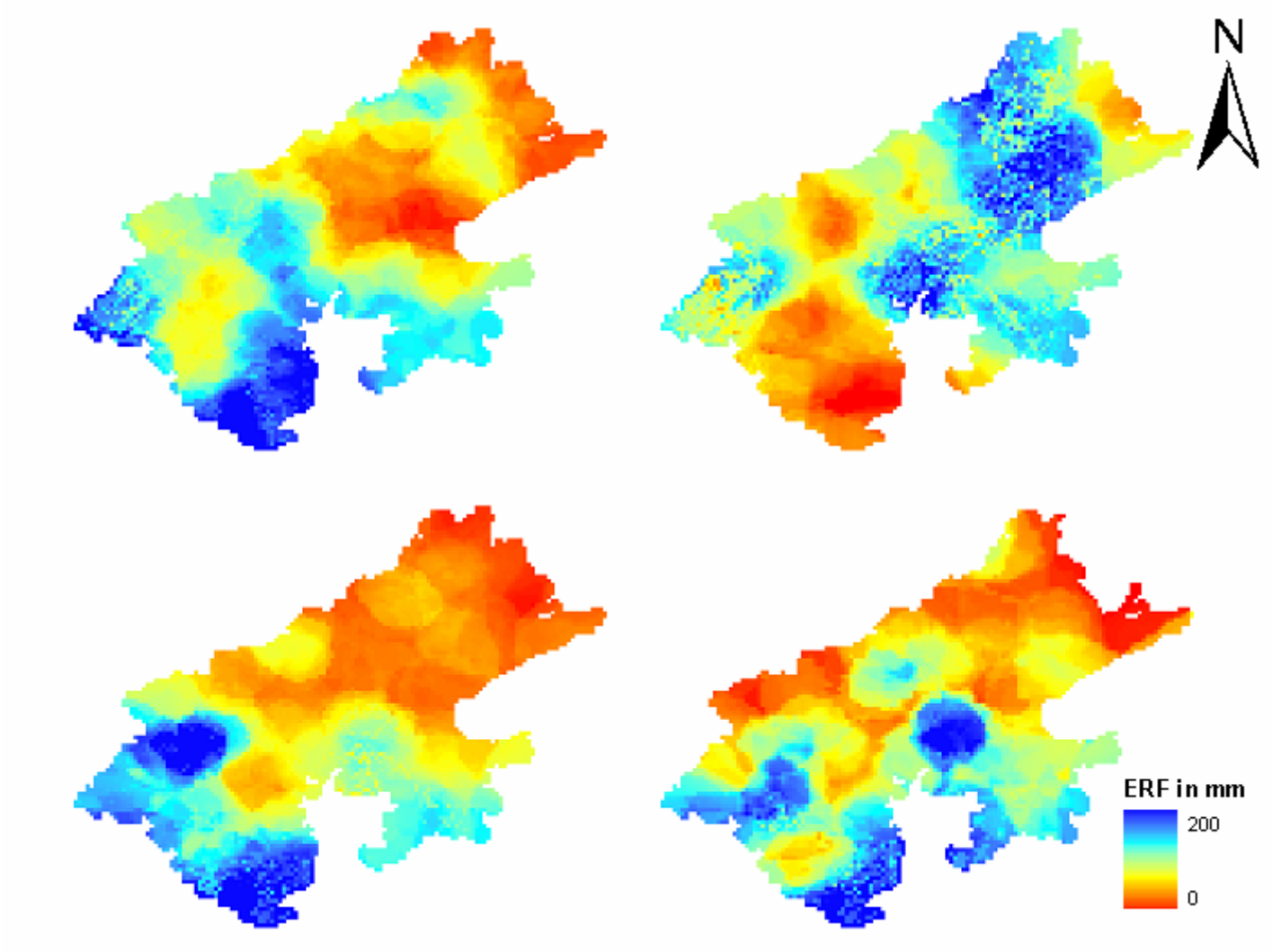

Appendix 6: Potential evapo-transpiration Series Maps for third weeks of (a) June (b) July (c) August and (d) September

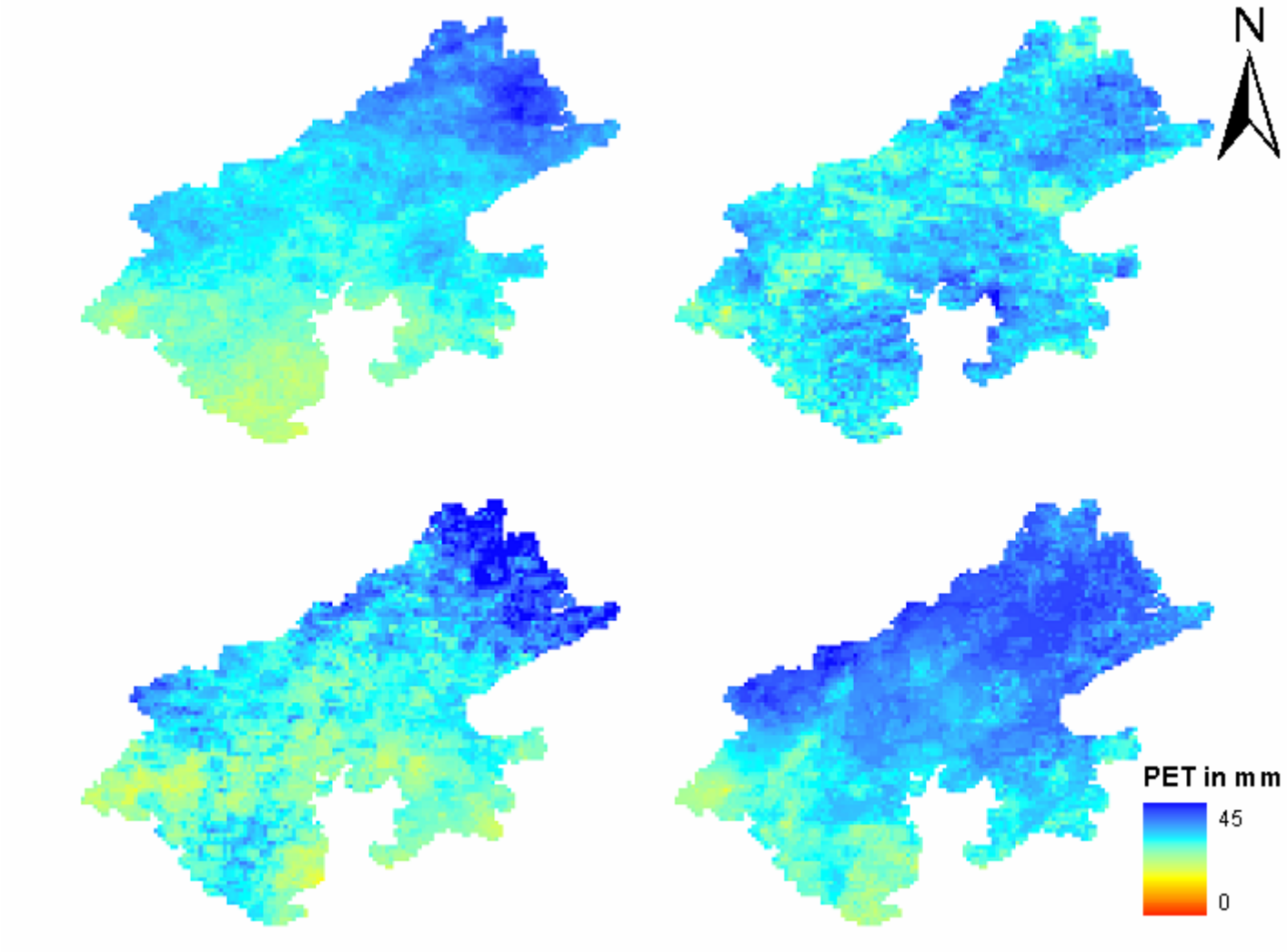

Appendix 7: In-situ soil moisture measurements (Sept 28th to Oct 8th, 2007)

	Place	*Crop Type*	*Surface*	*15cm*	*30cm*	*45cm*	SM_{avg}
1	Hirala	Bajra	9.85	25.55	24.25	26.75	16.76
2	Tholayi	Bajra	11.34	21.08	27.90	28.40	16.53
3	Dadhli	Bajra	1.70	7.50	12.17	15.27	6.67
4	Ruppura	Bajra	5.80	22.20	20.17	22.33	14.22
5	Manorpura	Bajra	4.03	12.53	16.03	16.40	9.64
6	Toda Bata	Bajra	5.20	23.37	24.90	19.33	16.20
7	Dudhli	Bajra	1.93	8.63	11.83	8.03	6.93
8	Bidhiani	Bajra	12.20	22.93	25.90	31.83	16.40
9	Bilwa	Bajra	4.73	13.83	18.83	20.73	11.01
10	Watika	Bajra	5.87	23.53	22.80	21.13	15.56
11	Lakhna	Bajra	1.10	11.33	16.00	27.73	9.21
12	Dhawas	Bajra	13.07	16.20	16.63	18.17	11.08
13	Sinwar	Bajra	1.63	5.77	7.73	8.57	4.61
14	Sanswati	Bajra	4.60	8.47	9.77	8.13	6.18
15	Govindpura	Bajra	0.83	6.23	8.43	9.97	5.01
16	Jaisinghpura	Bajra	1.58	9.38	10.98	13.48	6.89
17	Lohriya Bagru	Bajra	2.37	10.37	10.07	10.33	6.90
18	Udaipur	Bajra	15.55	26.83	33.53	31.40	20.29
19	Dharoli	Jowar	9.37	24.93	32.77	24.57	19.42
20	Bhateda	Maize	7.37	18.63	22.00	24.33	13.67
21	Gurha	Jowar	14.87	20.57	29.23	25.03	16.79
22	Debori	Jowar	13.67	22.50	23.90	20.70	15.64
23	Marta	Maize	14.40	27.30	28.93	31.90	18.90
24	Nandbela	Maize	20.03	36.87	41.07	38.13	26.22
25	Debori	Maize	6.80	10.70	15.60	20.50	8.94
26	Kanpur	Maize	17.57	27.70	32.20	30.90	20.14
27	Udaipur	Maize	10.63	18.87	20.23	17.07	13.21
28	Sakroda	Maize	26.27	34.63	44.03	42.20	26.47
29	Hariav	Maize	11.50	19.80	27.77	28.77	16.01
30	Khemli	Maize	13.40	27.10	34.93	37.80	21.06
31	Naharmarga	Maize	5.92	27.70	32.73	34.67	20.27

Appendix 8: Source for various data used

1. EOS Data Gateway: This interface provides access to all data publicly available from NASA satellites. It was used to download MODIS and AMSRE datasets for the study. (http://lpdaac.usgs.gov/main.asp).
2. Vienna University of Technology, Institute of Photogrammetry and Remote Sensing: The ERS Scatterometer soil moisture data was available from IPF, VUT. (http://www.ipf.tuwien.ac.at/radar).

3. University of Bonn: The AMSRE root zone soil moisture was available from University of Bonn . http://postel.mediasfrance.org/en/BIOGEOPHYSICAL-PRODUCTS/Soil-Moisture).
4. Space Application Centre (SAC), Ahmedabad: The solar radiation data produced from EUMETSAT bands were available from Dr B.K Bhattacharya, Crop Inventory & Modeling Division, Agricultural Resources Group, SAC.
5. Dept. of Revenue, Govt of Rajasthan: The Rainfall gauge station data and temperature data for 2003 were obtained from this institution.

Appendix 9: Field Photos

Maize Fields of Udaipur

With Rajasthani ladies in Bajra fields of Jaipur

With the Theta probe, measuring soil moisture in sandy soils in Jaipur

A farmer in his Maize field (Notice the rocky outcrops in Udaipur)

Measuring soil moisture Maize fields with clayey soil in Udaipur